

**A new approach to the polyaxial stress numerical analysis
of underground openings**

Dario Scussel



A thesis submitted to the School of Engineering, University of KwaZulu Natal,
in fulfillment of the requirements for the degree of Doctor of Philosophy

Durban, South Africa, November 2012

Supervisors:

Prof Sarvesh Chandra

Department of Civil Engineering, Indian Institute of Technology Kanpur

Prof Cristina Trois

Dean and Head of School, School of Engineering, University of kwaZulu-Natal

DECLARATION

As the candidate's Supervisor I agree to the submission of this thesis

Durban 09/03/2013,

I, Dario Scussel declare that

1. The research reported in this thesis, except where otherwise indicated, is my original research
2. This thesis has not been submitted for any degree or examination at any other university.
3. This thesis does not contain other persons' data, pictures, graphs or other information, unless specifically acknowledged as being sourced from other persons.
4. This thesis does not contain other persons' writing, unless specifically acknowledged as being sourced from other researchers. Where other written sources have been quoted, then:
 - a. Their words have been re-written but the general information attributed to them has been referenced
 - b. Where their exact words have been used, then their writing has been placed in italics and inside quotation marks, and referenced.
5. This thesis does not contain text, graphics or tables copied and pasted from the Internet, unless specifically acknowledged, and the source being detailed in the thesis and in the References sections.

DETAILS OF CONTRIBUTION TO PUBLICATIONS

This research project has produced three research papers, one of which is already published, one accepted with minor review and one waiting for review. These works correspond to the three main chapters of the present thesis.

I carried out these projects with critical feedback of the Professor Sarvesh Chandra.

Durban 09/03/2013 ,

ACKNOWLEDGMENTS

This study has been carried out at the School of Civil Engineering, University of KwaZulu Natal (UKZN) in Durban (South Africa).

These past three years have been a period of continuous personal growth, which has coincided with my first real independent experience away from Italy, away from all my certainties and beliefs. The help and guidance of Professor Sarvesh Chandra have been the key to the success of this research and to him goes all my gratitude. His vast knowledge and experience have led the way for the accomplishment of this work, which I will carry with me for the rest of my career.

I would like to thank Professor Cristina Trois, who strongly suggested this PhD and always made me feel her necessary contribution.

I would like to thank also my friends and colleagues Lohit, Gyan, Argaw, Sambit and Durgesh with whom I shared the present fears and the hopes for the future.

Finally my thanks go to Valentina, partner, colleague and friend in this experience, who never stopped encouraging me and making me feel her love even when everything went wrong.

ABSTRACT

The traditional design methodologies for tunnel and underground excavations are divided in to three categories: Empirical, Analytical, and Observational approaches, whereas in the last years the Numerical approach has strongly become popular both for the intrinsic simplicity of the software packages and their ability to manage problems unsolvable with the classic methods.

In this thesis, the underground openings have been analyzed using constitutive models other than the Mohr-Coulomb theory. FLAC is used for the analysis and the software has been implemented to include the Polyaxial Strength Criterion. The details of the modifications made in the software are presented and the results are compared with the Singh's elasto-plastic stress distribution in squeezing grounds.

The applicability of the Polyaxial Strength Criterion has been therefore extended to all the numerical suites designed for geo-mechanical purposes (FEM, FDM, ...) and the obtained results compared to the observations of deformation and radial squeezing pressure of the instrumented tunnels in the Chibro-Khodri underground power station.

This study will develop better comprehension of the behavior of the underground openings and also provide a useful tool to the designers in the planning stages.

INDEX OF CONTENTS

Declaration.....	ii
Acknowledgments.....	iii
Abstract.....	iv
Index of Contents.....	v
Index of Figures.....	viii
Index of Tables.....	x
1 Introduction.....	1
1.1 Framework.....	1
1.2 Problem Statement.....	2
1.3 Scope and Objectives of the Thesis.....	2
1.3 Organization of the Thesis.....	3
1.4 Bibliography.....	4
2 Literature Review.....	5
2.1 Introduction.....	5
2.2 Squeezing of Rocks.....	5
2.3 Empirical and Semi-Empirical methods.....	7
2.3.1 Classification of a Rock Mass.....	7
2.3.2 Terzaghi's Rock Load Theory and Deere's Rock Quality Designation (RQD).....	8
2.3.3 Bieniawki's Rock Mass Rating system (RMR).....	11
2.3.4 Norwegian Geotechnical Classification.....	14
2.3.5 Correlation between RMR and Q.....	17
2.3.6 Geotechnical Strength Index (GSI).....	18
2.4 Analytical Methods.....	19
2.4.1 Stress analysis of a tunnel immersed in an Elastic Continuum.....	19
2.4.2 Tensional analysis of a tunnel immersed in a strongly fractured rock mass.....	27
2.4.3 Stress field of a circular tunnel in an Elasto-Plastic medium.....	33
2.5 Observational Methods.....	39
2.6 Numerical Methods for underground openings.....	40

2.6.1	Finite Elements Methods (FEM).....	41
2.6.2	Finite Differences Methods (FDM).....	42
2.6.3	Boundary Elements Methods (BEM).....	42
2.6.4	Discrete Elements Methods (DEM).....	42
2.6.5	Hybrid methods.....	42
2.6.6	Recent improvements in numerical Methods in rock mechanics.....	43
2.7	References.....	43
3	Polyaxial Stress Analysis of Underground Openings using FLAC®	47
3.1	Abstract	47
3.2	Introduction	47
3.3	Elasto-Plastic Theory of Stress Distribution in Broken Zone using Polyaxial Strength Criterion in Squeezing Ground conditions	48
3.4	Numerical Analysis	50
3.4.1	Statement of the problem	50
3.4.2	Modifications to implement the Polyaxial Constitutive Model	50
3.4.3	Solution Scheme.....	52
3.4.4	Comparison of Numerical and Analytical Results	55
3.5	Conclusions	56
3.6	Acknowledgments.....	56
3.7	List of Symbols:	56
3.8	References.....	57
3.9	Appendix A: Spreadsheet for the implementation of the tunnel solution	59
3.10	Appendix B: FISH Code	60
4	A New Approach to obtain tunnel support pressure for Polyaxial state of Stress	66
4.1	Abstract	66
4.2	Introduction	67
4.3	Development of an Equivalent Mohr-Coulomb Failure Criterion.....	70
4.4	Determination of Equivalent Cohesion and Angle of Internal Friction.....	73
4.5	Comparison of analytical and numerical results.....	76
4.6	Conclusions	79
4.7	List of Symbols:	80
4.8	References.....	81

4.9	Appendix A: FLAC's code for the automatic determination of the equivalent Mohr-Coulomb parameters	82
4.10	Appendix B: Spreadsheet for the comparison of the tunnel solutions.....	84
5	A new approach to design of tunnels in squeezing ground.....	86
5.1	Abstract	86
5.2	Introduction	87
5.3	Case Study – The Chhibro Khodri Tunnel.....	93
5.4	Method of analysis.....	95
5.5	Conclusions	98
5.6	Acknowledgments.....	98
5.7	List of Symbols:	98
5.8	References.....	99
6	Conclusions	101
6.1	Summary	101
6.2	Conclusions	101
6.3	Recommendations for further developments	102

INDEX OF FIGURES

Figure 2-1 - Saint Martin La Porte access adit at chainage 1325 m before re-shaping the tunnel cross section (Barla, Bonini, Debernardi, (2010))	6
Figure 2-2 - Classification of Squeezing Behavior (Hoek, 2000).....	7
Figure 2-3 - Terzaghi's (1946) Rock Load Factor concept.....	10
Figure 2-4- Grimstad and Barton (1993) chart for the design of support	15
Figure 2-5 - Geological strength index for jointed rock masses (Hoek and Marinos, 2000).....	18
Figure 2-6 - representation of the problem and diagram of stresses	20
Figure 2-7 - maximum and minimum principal stresses around a circular tunnel in hydrostatic conditions in accord to Equations 2-38 and 2-39.....	20
Figure 2-8 – Circular tunnel in a non-hydrostatic stress field.....	22
Figure 2-9 - Vertical Stress Measurements (Underground excavation in rocks, Hoek and Brown (1990)).....	23
Figure 2-10 – Variation of the ratio of average horizontal stress to vertical stress with depth below surface (Underground excavation in rock, Hoek and Brown (1990)).....	23
Figure 2-11 - tangential and radial principal stress in horizontal direction for increasing values of λ	24
Figure 2-12 - tangential stress at the tunnel surface for increasing values of λ	25
Figure 2-13 – Geometrical configuration of an elliptic tunnel immersed in an anisotropic stress field	25
Figure 2-14 – Stress distribution at the surface of an elliptic tunnel with major axes in horizontal direction	26
Figure 2-15 - Stress distribution at the surface of an elliptic tunnel with major axes in vertical direction	26
Figure 2-16 – Ideal strain softening response of a rock mass	28
Figure 2-17 - Typical representation of the Mohr-Coulomb Criterion in terms of principal stresses (a) and shear and normal stresses (b)	29
Figure 2-18 - Typical representation of a non-linear failure criterion	30
Figure 2-19 - Relationships between major and minor principal stresses for Hoek-Brown and equivalent Mohr-Coulomb criteria (hoek, Carranza-Torres, Corkum (2002)).....	32

Figure 2-20- Typical representation of the Peak and Residual conditions of the Mohr-Coulomb Failure Criterion	33
Figure 2-21 - Plasticized tunnel under hydrostatic stress field	34
Figure 2-22 - Problem of a plasticized circular tunnel in hydrostatic stress conditions in accord to Ribacchi's hypotheses (1986)	36
Figure 2-23 - distribution of radial and tangential stresses under isotropic in-situ stress field.....	36
Figure 2-24- Problem of a plasticized circular tunnel in anisotropic state of stress (Singh, 2006)...	37
Figure 3-1 – Typical stress distribution around an underground opening	48
Figure 3-2 - Schematic boundary conditions of the problem.....	49
Figure 3-3 - Graphical Polyaxial Strength Criterion	51
Figure 3-4 - Domains for a specific σ_2 value	53
Figure 3-5 - Geometrical configuration of the model	55
Figure 3-6 - Comparison of analytical and numerical FLAC solution for the tunnel problem in figure 3-3.....	56
Figure 4-1 - Results of Polyaxial Tests on Dunham Dolomite (Mogi, 1967)	67
Figure 4-2 - Problem of a circular tunnel in elasto-plastic rock mass (Singh and Goel, 2006)	68
Figure 4-3- Stress field induced in the vicinity of a circular tunnel in hydrostatical stress conditions	70
Figure 4-4- Variation of the ratio of average horizontal stress to vertical stress with depth below surface (Underground excavation in rocks, Hoek and Brown (1990))	71
Figure 4-5- Bi-dimensional representation of PSC and MC in the σ_1 - σ_3 plane.....	72
Figure 4-6 - Bi-dimensional representation of PSC and MC in the τ - σ plane	73
Figure 4-7 - Graphical relation between ϕ and ϕ	74
Figure 4-8- Graphical relation between angle ϕ of internal friction and non-dimensional cohesion	75
Figure 4-9 - Relation between internal friction angle ϕ' and equivalent cohesion c' for $\sigma_2 = 0$	76
Figure 4-10– Geometrical configuration of the application example	77
Figure 4-11 - Comparison of the analytical solutions (stress distribution)	78
Figure 4-12 - Comparison of the numerical solutions (stress distribution).....	79
Figure 4-13 - Comparison of the analytical and numerical solutions	80
Figure 5-1 - Singh et al. (1992) approach for predicting squeezing conditions	87
Figure 5-2 - Problem of a circular tunnel in an elasto-plastic rock mass.....	91
Figure 5-3 - Geological section along the Chhibro Khodri Tunnel (Jain et al., 1975).....	93
Figure 5-4 - Regional geology of the Chhibro Khodri Tunnel	94

Figure 5-5 - Average errors in the determination of the squeezing pressure P_1 for different values of f_i	97
--	----

INDEX OF TABLES

Table 2-1- Definition of Terzaghi's Rock Classes and Rock Load Theory	9
Table 2-2 - Terzaghi's Rock Load System as modified by Deere's (1970).....	11
Table 2-3 - Qualitative description of a rock mass by means of the Rock Quality Designation	11
Table 2-4 – Classification of the jointed rocks as per Bieniawski (1993) and relative adjustment for joint orientation	12
Table 2-5- Rock Mass Classes for the RMR Classification.....	13
Table 2-6 – Meaning of the RMR classes of quality.....	13
Table 2-7 - Q Rock Mass Quality for Tunneling	14
Table 2-8 - Excavation Categories Determination.....	16
Table 3-1 - Values proposed for peak and residual state	52
Table 3-2 - Data of the numerical problem.....	55
Table 3-3- Results of the different approach.....	59
Table 4-1 - Relation between angle ϕ and equivalent angle ϕ' of internal friction	74
Table 4-2 - Estimation of A and B for increasing values of internal angle of friction.....	75
Table 4-3 - Rock mass data of a typical problem.....	76
Table 4-4 - Comparison of the tunnel solutions.....	84
Table 5-1 - Relation between angle ϕ and equivalent angle ϕ' of internal friction	90
Table 5-2 - Estimation of A and B for increasing values of internal angle of friction.....	90
Table 5-3 - Geometrical dimensions and rock mass characteristics	94
Table 5-4 - Peak resistance parameters for the different approaches.....	95
Table 5-5 - Computed Squeezing Pressures.....	96
Table 5-6 - Variation of the internal pressure P_1 for different values of the factor f_1	97
Table 5-7 - Variation of the internal pressure P_1 for different values of the factor f_2	97

Chapter 1

1 INTRODUCTION

1.1 FRAMEWORK

The unceasing development that characterizes the modern economy is directly linked to the quality, capacity and efficiency of the infrastructure, connecting the strategic nodes of each nation. The famous mountain (San Gottardo, Frejus..) or undersea (Euro Tunnel) road or railway tunnels are not the only underground excavations today as there is a consolidated trend of moving all the facilities underground such as power stations, metro stations, parking and storage space for dangerous and nuclear waste to reduce the impact that they could induce to the narrow space and environment.

In mixed structures, with superstructure and underground infrastructure, the excavated part is always the most important and determinant for the success of the entire realization. The possibility to excavate always in safe and competent soils or rock masses is rare and a deviation from the original alignments is not possible, the engineers have to take the challenge of facing these conditions.

The excavation of tunnels in non-competent ground, in particular in Squeezing Conditions, is one of the most challenging experiences in geotechnical engineering for the difficulties and uncertainties involved both in the design and in the execution of works. The Squeezing ground conditions occur when the modification of the stress field in a rock mass, due to the opening of a void, induces an overstress such that the rock fails. The rock mass failures are often consequence of a large time dependent deformations at the excavation boundaries. The choice of the most appropriate excavation-support system is the key to avoid loss of functionality or stability in the excavation works.

Nowadays, despite of considerable amount of studies in this field, a universally accepted theory valid for prediction of support pressures and design of underground caverns in squeezing ground conditions does not exist. The designing approaches adopted in tunnel engineering are commonly subdivided in to three main categories:

- Empirical In the empirical approaches, the geotechnical design parameters are determined by expressions exclusively founded on the empirical analysis of the data collected by the observation of the behavior of a large number of underground excavations. The long experience accumulated in the worldwide tunnel practice over many years permitted development of several empirical relations, which are commonly used in tunneling engineering.

- Analytical The analytical methods predict the behavior of a soil or rock mass by means of the application of theoretical laws. These can be subdivided in Elastic and Elasto-Plastic Theories. A rock mass can be represented as a homogeneous mass of resistance lower than the resistance of undisturbed rock material, or as blocks of undisturbed rock material but naturally spaced out by joints and fractures, depending on the ratio between spaces of the discontinuities and excavation dimension. The analytical resolution of complex geotechnical problems entails the introduction of a high number of parameters, which cannot be easily determined and may distort the final results obtained from analytical approach.

The use of analytical approaches, by the resolution of easy problems, is strongly suggested for didactic purposes. The theoretical understanding of how a rock mass behaves below the surface is necessary for proper planning of excavation or any application of support technique.

Observational In this category, are placed those methodologies that produce suggestions for the final design of an underground excavation based on the observation and subsequent comparison of the behavior of an underground opening with the corresponding performance predicted at the designing stage. Specific provisional inspection galleries are also excavated before the final design of an underground work to determine the quality index of a complex rock mass system and finally design and calibrate the correct retaining system.

The design of underground excavations cannot just rely on only one technique chosen among the traditional methods. The recommended procedure is based on the use of a rational combination of more than only one approach for an initial comparison of the consistency of the results and an ongoing work of refinement of the applied approach based on an observational technique. This iterative procedure leads to the best possible results for difficult situations.

1.2 PROBLEM STATEMENT

About 30 years ago, for the first time, numerical methodologies were applied to real geo-mechanical problems, with a considerable delay with respect to other engineering disciplines. The numerical solutions, although not complex from a theoretical point of view, overcome the difficulty of resolving complex geometries which cause complexities in analytical closed Equations. The presently available techniques allow a detailed analysis of any engineering problem and simplify the realization any complex problem and allows comparison of different design approaches for the problem. Numerical and traditional methodologies are indissolubly interconnected; any numerical model to be implemented needs a set of physical laws describing the overall behavior of the selected ground, while the empirical approaches help in determination of the indexes of quality and resistance for the surrounding ground.

Among the high number of analytical models suggested in literature, only a small number has been converted to numerical models suitable for commercial applications. The small choice of failure criterion in geotechnical software commonly available is directly related to the fact that tradition is to use only a few established relations. The absence of periodic upgrades of the available software is a complex problem that, combined with difficulty in the implementation of user defined failure criteria, discourages many from promoting the application of their innovative theories into real practical applications.

1.3 SCOPE AND OBJECTIVES OF THE THESIS

In this thesis, motivated by the above considerations, an innovative numerical failure criterion, able to model deep underground excavation in squeezing rock conditions, is developed and converted to a form such that it can be easily implemented in any numerical application software. The Polyaxial Constitutive model, introduced by Singh et al. in 1998 has been modified and applied in this thesis.

The present constitutive model has been, specifically fitted for describing the behavior of very weak rock masses. This model has the merit of incorporating the effect caused by the intermediate principal stress on shear resistance of the rock mass. The applicability of this failure criterion has the main difficulty in its application into numerical approaches, discouraging its extensive use in practice although the good feedbacks of its applications in the field problems are shown.

In the present work, the Polyaxial Strength Criterion has been converted into a more convenient form and has been expressed in the format of Mohr-Coulomb criterion by using equivalent shear strength parameters. The relationship between these equivalent shear strength parameters and the strength

parameters used in Mohr-Coulomb criterion has been established. This allows the Polyaxial Strength Criterion to be implemented in any numerical code that uses Mohr-Coulomb criterion. This has been implemented in two stages. In the first stage, a specific programming code in FISH, has been incorporated in FLAC (two dimensional explicit finite differences program for engineering mechanics computation) strictly following the Singh's Polyaxial Strength Criterion and laid the foundations for the second stage. In second stage, the Polyaxial Strength Criterion relationship has been suitably modified to be expressed in the form similar to Mohr-Coulomb criterion and obtain equivalent parameters, which can be used without any modification in the geotechnical numerical suites and this approach is more elegant, and convenient to use. This approach, in fact, brings out the similarities between Singh's Theory and Mohr-Coulomb failure criterion by introducing new equivalent shear strength parameters.

The results obtained from both the numerical approaches suggested in this work are examined and compared to the analytical solution suggested by Singh for analyzing the polyaxial state of stress around a circular tunnel in squeezing conditions. The suggested constitutive models give results, which are in very close agreement with the analytical solution.

In the final part of this research, to demonstrate the potential of the failure model proposed, the Squeezing pressures observed in three instrumented sections of a tunnel section in case of severe squeezing is compared to the results obtained by numerical model suggested in this study as well as with the Mohr-Coulomb criterion. It is observed that for Squeezing conditions the suggested approach using Polyaxial Strength Criterion and using uniaxial compressive strength obtained by Barton's relation gives better results.

1.3 ORGANIZATION OF THE THESIS

This thesis is subdivided into 6 Chapters. The three main Chapters of this research are written as set of already published research papers or ready for a future publication. The present Chapter is intended to provide a general introduction of this research and explains the organization of the following Chapters.

The second Chapter presents an exhaustive description of the squeezing phenomenon and a review of the designing techniques currently available in squeezing conditions. A separate section of this Chapter is exclusively dedicated to introduce the Polyaxial Strength Criterion and its analytical applications.

Chapter 3, initially written for the international conference INDOROCK 2011 organized by the Indian Society of Rock Mechanics and Tunneling Technology (ISRMTT) at IIT Roorkee (India), has been successively updated and published at the beginning of 2012 in the Volume 18 of the Journal of Rock Mechanics and Tunneling Technology (ISSN 0971-9059).

It describes the first successful effort to implement a programming code for the numerical application of the Polyaxial Strength Criterion in FLAC and includes all the verification of its complete functionality.

In Chapter 4, already accepted for publication by the Journal of Tunneling and Space Technology (ISSN: 0886-7798), it is presented the proposed modification of the Polyaxial Strength Criterion to achieve the Equivalent Mohr-Coulomb Theory. The relative Equivalent parameters of shear resistance are also described and determined. As for the numerical model for FLAC the present methodology is verified in a specific numerical application.

In Chapter 5, already accepted for publication by the International Journal of Geomechanics (ISSN: 1532-3641 eISSN: 1943-5622), the Equivalent Mohr-Coulomb constitutive model, as described in Chapter 4 and subsequently modified, is applied to a real case of tunnel subjected to severe squeezing conditions, the inspection gallery of Chhibro Khodri, India. All the stages of the implementation are clearly explained and the outcomes compared to the observation executed during the excavations execution.

Finally, in Chapter 6, the conclusions of this work and some suggestions for further studies are given.

1.4 BIBLIOGRAPHY

- [1] Barla, G. (1995). Squeezing rocks in tunnels. *ISRM News Journal*, 2(3&4), 44-49.
- [2] Barla, G. (2004). *Tunnelling Under Squeezing Rock Conditions*.
www.polito.it/ricerca/rockmech/publcazioni/art-rivista.
- [3] Itasca (2006), Reference Manual, *FLAC 5.0*, Itasca Consulting Group Inc, Minneapolis (2006).
- [4] Jethwa, J. L. (1981). Evaluation of Rock Pressures in Tunnels through Squeezing Ground in Lower Himalayas. PhD thesis, Department of Civil Engineering, University of Roorkee, India, 272.
- [5] Singh, M, Singh, B, Choudhari, J. Critical strain and squeezing of rock mass in tunnels, *Tunnelling and Underground Space Technology* 22 (2007) 343 - 350.
- [6] Ribacchi, R., (1986). Stato di sforzo e deformazione intorno ad una galleria, *L'ingegnere*, LXI, 135-184.
- [7] Scussel, D., Chandra, S. (2012). Polyaxial Stress Analysis of Underground Openings using *FLAC*; *Journal of Rock Mechanics and Tunnel Technologies*, Volume 18, Number 1, 41 – 54.
- [8] Singh, B, Goel, R. K., Mehrotra, V. K., Garg, S. K. and Allu, M. R. (1998). Effect of intermediate principal stress on strength of anisotropic rock mass. *J. Tunnelling & Underground Space Technology*, Pergamon, 13(1), 71-79.
- [9] Singh, Bhawani, Jethwa, J. L., Dube, A. K. and Singh, B. (1992). Correlation between observed support pressure and rock mass quality. *Tunnelling & Underground Space Technology*, Pergamon, 7(1), 59-74.
- [10] Singh, B.; Goel, R.K. (2006). *Tunnelling in Weak Rocks*. *Geo-Engineering*. 5. Elsevier Science. p. 512.
- [11] Tanzini, M. (2001). *Gallerie: aspetti geotecnici della progettazione e costruzione*. Dario Flaccovio Editore S.r.l.

Chapter 2

2 LITERATURE REVIEW

2.1 INTRODUCTION

The behavior of the rock mass has been studied extensively in the recent decades in order to define a reliable law for predicting the advent of squeezing phenomena in underground excavations. In this Chapter, the main characteristics and recent improvements of empirical, analytical, observational and numerical methods, the universally recognized approaches in rock mechanics, are explained in detail.

Because the exclusive use of one of these techniques is not sufficient for a correct analysis of squeezing of rocks, the knowledge of the largest number of them is the fundament for its satisfactory investigation.

This review of literature is the foundation for the development of a new approach for the analytical and numerical application in tunneling engineering of the polyaxial constitutive model based on objective in situ observations.

2.2 SQUEEZING OF ROCKS

One of the biggest challenges of the Rock Mechanics, and specifically of Underground Engineering, is to develop a reliable theory for predicting support pressures for the Squeezing ground conditions in order to prevent any adverse situations. According to an official definition suggested by the International Society for Rock Mechanics (ISRM), Barla (1995), the Squeezing of Rock can be described as “the time dependent large deformation which occurs around the tunnel and is essentially associated with creep caused by exceeding a limiting shear stress. Deformation may terminate during construction or continue over a long time period”.

In an undisturbed rock mass, any natural or artificial alteration of the initial spatial configuration, in fact, induces an immediate re-distribution of the state of stress with the final intent of reaching a new stable condition. The stress redistribution following the opening of an underground excavation produces a generalized increment of the difference between maximum and minimum principal stresses (deviatoric stress $\sigma_d = \sigma_1 - \sigma_3$) in the surrounding rock mass and maximum at the internal surfaces of the void. If the new stress configuration does not exceed the resistance of the rock mass, stable / non-squeezing conditions are maintained, otherwise unstable / squeezing conditions may be observed.

The overcoming of the material resistance may produce localized or diffused failures. The plasticization of the rock mass always starts at the surface of the excavation, where the stress conditions are more critical, and, successively, moves in the outwards direction. The installation of an internal support system is usually necessary in case of failure to increase the possibility of achieving a new safe state.

The convergence of the faces of an excavation in squeezing conditions can be so pronounced that, in complex cases, may even exceed the 10% of the radius of the cavity. Excessive deformations may create unpleasant aesthetic effects as well as affect the functionality and even the stability of underground works, causing big delays in their final accomplishments.

The magnitude of the deformations and the time needed for the complete stabilization are a complex

function of the tectonic, geological and hydrogeological characteristics of the formations affected by the excavations as well as of the petrographic and geotechnical properties of the rock mass. The technologies of excavation and the rapidity of the installation of a support system have also a strong influence and their choice plays a central role in the reduction of squeezing.



FIGURE 2-1 - SAINT MARTIN LA PORTE ACCESS ADIT AT CHAINAGE 1325 M BEFORE RE-SHAPING THE TUNNEL CROSS SECTION (BARLA, BONINI, DEBERNARDI, (2010))

For these reasons, a careful preliminary study of the geological and geo-mechanical properties of the rock mass allows the preventive estimation of possible conditions of instability, in order to implement without delays the appropriate methodologies for the squeezing control. A late identification of an unstable condition results in slow and hazardous excavation, due to the use of inappropriate construction techniques, and can even entail the necessity of modifying the tunnel alignment during the realization of the works.

The degree of Squeezing is quantified by the strain measured at the surface of an excavation and is commonly subdivided in to 5 classes of magnitude as indicated in Figure 2-2. Such classification was introduced by Hoek (2000) with reference to his approximate relationship for the tunnel radial strain ε_r estimation as given by Equation 2-1.

$$\varepsilon_r = 0.15 \frac{P_i}{P_0} \left(1 - \frac{P_i}{P_0} \right) \sigma_{cr}^{-\left(\frac{3P_i}{P_0} - 1 \right) / \left(3.8 \frac{P_i}{P_0} - 0.54 \right)} \quad (2-1)$$

where P_0 is the hydrostatic in situ stress, P_i the internal reaction of the lining and σ_{cr} the uniaxial compressive strength of the rock mass.

According to the observations reported by Hoek (2000), Squeezing conditions occur when the minimum strain, expressed as normalized closure at the internal surface of the lining, reaches the minimum amount of 1 %. The chart of strain versus non-dimensional stress is plotted in Figure 2-2, which is used to classify squeezing rock conditions.

According to Dube and Singh (1986), Squeezing is a phenomenon generally related to low resistance overstressed grounds, whereas hard rocks may undergo rock burst conditions.

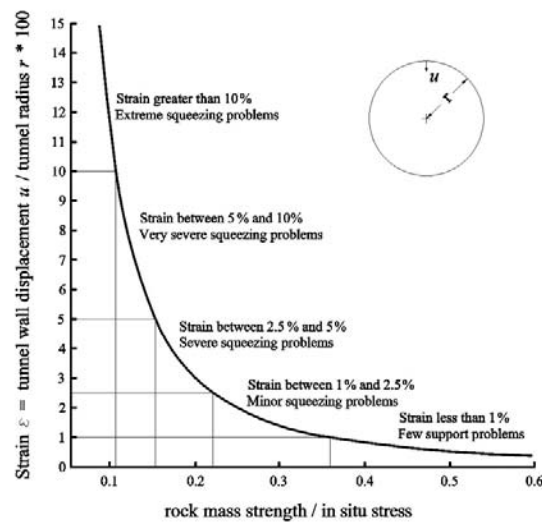


FIGURE 2-2 - CLASSIFICATION OF SQUEEZING BEHAVIOR (HOEK, 2000)

In the following sections of this Chapter, the most common techniques available for the rock mass characterization and the solutions for a proper design of underground excavations have been described. The organization of this Chapter has been conceived with a special focus on the squeezing problems in tunneling engineering.

2.3 EMPIRICAL AND SEMI-EMPIRICAL METHODS

2.3.1 CLASSIFICATION OF A ROCK MASS

A rock mass is hardly a continuous, homogeneous and isotropic volume, but is more often affected by discontinuities, faults, joints and could have been subjected to various actions of alteration and degradation in its geological history. Only the combination of the information coming from the petrographic and geotechnical conditions of the rock matrix with those relative to the physical and geometrical characteristics of the sets of discontinuities distinguishing the volume considered returns an appropriate description of the overall rock mass state.

To describe a rock mass an extensive use of the engineering geo-mechanical classifications is made these days. The modern geo-mechanical engineering classifications rank a rock mass assigning simple indexes of quality to the different components of the material and combine them in a global index, function of their bigger or smaller contribution to the overall resistance. By means of a coherent system of ranking any parameter that could negatively influence the stability of an underground excavation can be identified, providing the basis for the stability analysis.

The rock masses were, in the course of time, classified on the basis of their origin, mineralogical composition, void index, fracture/joint intensity, joint inclination, flow rate of water, velocity of propagation of shock waves, weatherability, colour, grain size or surface properties. A complete geological and geotechnical characterization of a rock mass primarily includes the recognition of the local main lithotypes, followed by the description of the geomechanical characteristics, such as:

- mechanical conditions of the rock matrix, including degree of alteration, structure, color, texture and compressive strength of intact rock matrix;

- geo-structural and geo-mechanical conditions of the natural discontinuities comprising of, for each family of joints, orientation, persistence, spacing, aperture, filling composition and mechanical properties.

The evaluation of the effects produced by the presence of an aquifer completes the description of the factors that affects the stability of an underground excavation. The parameters part of the first group can be easily determined in laboratory or with easy in situ tests, while those of the second group need specific in situ characterization.

The rating system on the basis of a geo-mechanical classification system must rely on clear guidelines regarding the methods of monitoring and following subdivision into classes of quality. A classification, based on objective considerations, easily reproducible and consistent in different scenarios, encourages the sharing of results and their comparison in view of a constant evolution of the methodologies of design and construction.

The vast amount of case studies existing in literature allowed the development of several classification systems and relating to important geotechnical properties. Angle of Friction ϕ , Cohesion c , Elastic Modulus E and Uniaxial Compressive Strength σ_{cr} are some of the important parameters deducible by means of empirical or semi-empirical relations.

The most used classifications are currently three, the RMR introduced by Bieniawski (1973) for the South African Council for Scientific and Industrial Research (CSIR), the Q System by Barton (1974) and the more recent GSI by Hoek and Brown (1997), classification specifically made in support of the homonym non-linear constitutive model.

2.3.2 TERZAGHI'S ROCK LOAD THEORY AND DEERE'S ROCK QUALITY DESIGNATION (RQD)

The geo-mechanical classification introduced by Terzaghi in 1946 is the first organized attempt to predict the load applied to the support of a deep tunnel by the observation of the characteristics of the surrounding rock mass. His theory is based on his long professional experience in alpine railway tunnels excavation and differs from the preceding techniques in considering the strength of a rock mass as the complex combination of several geological and geotechnical parameters.

According to Terzaghi's approach, a rock mass is, in fact, classified on the basis of the uniaxial compressive strength, frequency and spatial distribution of the discontinuities, geological origin of the rock mass, presence of water and swelling materials, chemical alteration suffered and in situ stress conditions.

Based on these factors, Terzaghi describes the rock mass and defines nine homogeneous classes of rock as shown in Table 2-1. For each class, he gave a certain range of values of the load applied to the lining and included suggestions for its proper installation.

The load P_v , vertically applied on the lining as shown in Figure 2-3, is derived indirectly through the Rock Load Factor H_p (the height of the fractured rock above the excavation) in accordance with the Equation 2-2:

$$P_v = \gamma \cdot H_p \quad (2-2)$$

<i>Rock Class</i>	<i>Definition</i>	<i>Rock Load Factor Hp (feet) (B and Ht in feet)</i>	<i>Remark</i>
I. Hard and intact	Hard and intact rock contains no joints and fractures. After excavation the rock may have popping and spalling at excavated face.	0	Light lining required only if spalling or popping occurs.
II. Hard stratified and schistose	Hard rock consists of thick strata and layers. Interface between strata is cemented. Popping and spalling at excavated face is common.	0 to 0.5 B	Light support for protection against spalling. Load may change between layers.
III. Massive, moderately jointed	Massive rock contains widely spaced joints and fractures. Block size is large. Joints are interlocked. Vertical walls do not require support. Spalling may occur.	0 to 0.25 B	Light support for protection against spalling.
IV. Moderately blocky and seamy	Rock contains moderately spaced joints. Rock is not chemically weathered and altered. Joints are not well interlocked and have small apertures. Vertical walls do not require support. Spalling may occur.	0.25 B to 0.35 (B + Ht)	No side pressure.
V. Very blocky and seamy	Rock is not chemically weathered, and contains closely spaced joints. Joints have large apertures and appear separated. Vertical walls need support.	(0.35 to 1.1) (B + Ht)	Little or no side pressure.
VI. Completely crushed but chemically intact	Rock is not chemically weathered, and highly fractured with small fragments. The fragments are loose and not interlocked. Excavation face in this material needs considerable support.	1.1 (B + Ht)	Considerable side pressure. Softening effects by water at tunnel base. Use circular ribs or support rib lower end.
VII. Squeezing rock at moderate depth	Rock slowly advances into the tunnel without perceptible increase in volume. Moderate depth is considered as 150 ~ 1000 m.	(1.1 to 2.1) (B + Ht)	Heavy side pressure. Invert struts required. Circular ribs recommended.
VIII. Squeezing rock at great depth	Rock slowly advances into the tunnel without perceptible increase in volume. Great depth is considered as more than 1000 m.	(2.1 to 4.5) (B + Ht)	Heavy side pressure. Invert struts required. Circular ribs recommended. Circular ribs required. In extreme cases use yielding support.
IX. Swelling rock	Rock volume expands (and advances into the tunnel) due to swelling of clay minerals in the rock at the presence of moisture.	up to 250 feet, irrespective of B and Ht	

TABLE 2-1- DEFINITION OF TERZAGHI'S ROCK CLASSES AND ROCK LOAD THEORY

Notes: The tunnel is assumed to be below groundwater table. For tunnel above water tunnel, Hp for Classes IV to VI reduces 50%. The tunnel is assumed excavated by blasting. For tunnel boring machine and roadheader excavated tunnel, Hp for Classes II to VI reduces 20-25.

Terzaghi's methodology has found wide application in North America, where the drill and blast and steel arches techniques were very common. Such methodologies essentially correspond to those used during his alpine experience. Unfortunately the method is not particularly suited to excavation methods different from the traditional ones and has a tendency to overestimate the squeezing pressure in tunnel of large diameter (Singh and Goel, 1999).

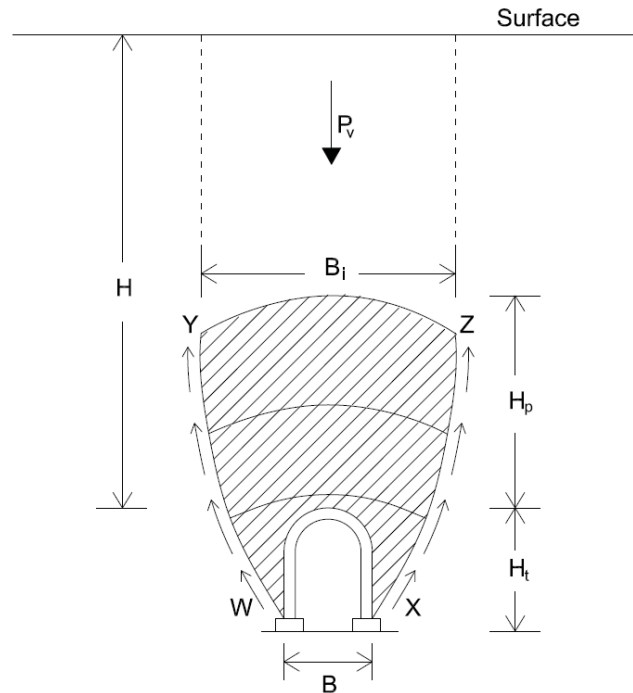


FIGURE 2-3 - TERZAGHI'S (1946) ROCK LOAD FACTOR CONCEPT

The opening of a tunnel causes the relaxation of the rock mass surrounding the void, allowing its partial closure. According to the Rock Load Theory, this movement is contrasted by the friction generated at the border of the plasticized area and by the pressure borne by the internal support system installed at the surface of the excavation.

In 1970, Deere slightly modified the classification suggested by Terzaghi as shown in Table 2-3, correlating it to his index RQD (Rock Quality Designation, 1964). The RQD index classifies a rock mass on the basis of the observed degree of jointing of a core sample recovered from a borehole. It is calculated as the percentage of the drill core recovery of the pieces of rock having lengths of 10 cm or more, Expressed as in Equation 2-3.

$$RQD = \frac{\sum \text{Length of core} > 10 \text{ cm}}{\text{Total length of core run}} \times 100 \quad (2-3)$$

In Table 2-3, in accordance with the classification RQD, is shown the subdivision into classes of rock mass quality as suggested by Deere.

The major disadvantage of the RQD approach is that, problem which obviously also affects the modified version of the Rock Load System, the knowledge of just the degree of rock mass fracturing does not allow a complete description of the rock mass in complexity. RQD is, however, an excellent indicator of fracturing rock and it is basic element in some of the most used rock mass classification systems: Rock Mass Rating system (RMR) and Q-system.

Rock class and condition	RQD (%)	Rock load (Hp)	Remarks
I. Hard and intact	95–100	Zero	Same as Table 2-1
II. Hard stratified or schistose	90–99	0–0.5 B	Same as Table 2-1
III. Massive moderately jointed	85–95	0–0.25 B	Same as Table 2-1
IV. Moderately blocky and seamy	75–85	0.25 B–0.35 (B + Ht)	Types IV, V, and VI reduced by about 50% from Terzaghi values because water table has little effect on rock load (Terzaghi, 1946; Brekke, 1968)
V. Very blocky and seamy	30–75	(0.2–0.6) (B + Ht)	Same as above
VI. Completely crushed	3–30	(0.6–1.10) (B + Ht)	Same as above
VIa. Sand and gravel	0–3	(1.1–1.4) (B + Ht)	Same as above
VII. Squeezing rock at moderate depth	NA	(1.10–2.10) (B + Ht)	Same as Table 2-1
VIII. Squeezing rock at great depth	NA	(2.10–4.50) (B + Ht)	Same as Table 2-1
IX. Swelling rock	NA	Up to 80 m irrespective of the value of B, Ht	Same as Table 2-1

TABLE 2-2 - TERZAGHI'S ROCK LOAD SYSTEM AS MODIFIED BY DEERE'S (1970)

RQD	>90%	75 - 90 %	50 - 75 %	25 - 50 %	0 - 25 %
Rock mass Quality	Very Good	Good	Fair	Poor	Very Poor

TABLE 2-3 - QUALITATIVE DESCRIPTION OF A ROCK MASS BY MEANS OF THE ROCK QUALITY DESIGNATION

2.3.3 BIENIAWKI'S ROCK MASS RATING SYSTEM (RMR)

The RMR classification was developed by Bieniawski (1973) for the South African Council for Scientific and Industrial Research (CSIR). Prior to appearing in the present form, the RMR classification has been updated 7 times, both in the allocation of points to different parameters and in the inclusion of correction factors to refine the results and facilitate its use in special conditions. The last update is dated 1993; to avoid misunderstanding it is really important to always define if the version used is different.

In order to apply a rock mass classification, it is essential that the rock mass is divided into homogeneous geo-mechanical regions. The RMR index, then, will be determined in each region making use of the following 6 parameters:

- RMR₁ - Rock Quality Designation (RQD)
- RMR₂ - Uniaxial Compressive Strength of the Intact Material
- RMR₃ - Joints Spacing
- RMR₄ - Joints Condition
- RMR₅ - Groundwater condition
- RMR₆ - Joints Orientation

(a) Five basic rock mass classification parameters and their ratings										
1	Strength of intact rock material	Point load strength index (MPa)		> 10	4 - 10	2 - 4	1 - 2			
		Uniaxial compressive strength (MPa)		> 250	100 - 250	50 - 100	25 - 50	5 - 25	1 - 5	< 1
	Rating			15	12	7	4	2	1	0
2	RQD (%)	90 – 100	75 – 90	50 – 75	25 – 50			< 25		
	Rating	20	17	13	8			3		
3	Joint spacing (m)	> 2	0.6 – 2	0.2 – 0.6	0.06 – 0.2			< 0.06		
	Rating	20	15	10	8			5		
4	Condition of joints	not continuous, very rough surfaces, unweathered, no separation	slightly rough surfaces, slightly weathered, separation <1 mm	slightly rough surfaces highly weathered, separation <1 mm	continuous, slickensided surfaces, or gouge <5 mm thick, or separation 1–5 mm			continuous joints, soft gouge >5 mm thick, or separation >5 mm		
	Rating	30	25	20	10			0		
5	Groundwater	inflow per 10 m tunnel length (l/min), or		none	< 10	10 – 25	25 – 125	> 125		
		joint water pressure/major in situ stress, or		0	0 – 0.1	0.1 – 0.2	0.2 – 0.5	> 0.5		
		general conditions at excavation surface		Compl. Dry	Damp	Wet	Dripping	Flowing		
	Rating			15	10	7	4	0		
(b) Rating adjustment for joint orientations										
Strike and dip orientation of joints		very favourable	favourable	fair	unfavourable	very unfavourable				
Rating	tunnels	0	– 2	– 5	– 10	– 12				
	foundations	0	– 2	– 7	– 15	– 25				
	slopes	0	– 5	– 25	– 50	– 60				
(c) Effects of joint orientation in tunnelling										
Strike perpendicular to tunnel axis				Strike parallel to tunnel axis			Dip 0° – 20°			
Drive with dip		Drive against dip								
Dip 45° – 90°	Dip 20° – 45°	45° – 90°	Dip 20° – 45°	Dip 45° – 90°	Dip 20° – 45°	irrespective of strike				
very favourable	favourable	fair	unfavourable	very unfavourable	fair	fair				

TABLE 2-4 – CLASSIFICATION OF THE JOINTED ROCKS AS PER BIENIAWSKI (1993) AND RELATIVE ADJUSTMENT FOR JOINT ORIENTATION

Bieniawski clearly defined the procedure for the evaluation of these six factors. The process for the determination of the first five is summarized in Table 2-4.a, while the procedure for the evaluation of the remaining one, which considers the effect of the joints on the excavation in numbers, is split up in Tables 2-4.b and 2-4.c.

The system of ranking is based on the attribution of a value that describes the status of each one of the six parameters. The sum of the results of each characterization returns the RMR index.

$$RMR = \sum_{i=1}^6 RMR_i \quad (2-4)$$

The sum of the first 5 indices lies between 0 and 100, while the, always negative, sixth is an adjustment parameter which is a function of the angle formed between the excavation and discontinuities. Only after having applied the necessary corrections, a rock mass can be classified in accordance to Table 2-5.

RMR Rating	100 - 81	80 - 61	60 - 41	40 - 21	20 - 0
Class Number	I	II	III	IV	V
Description	Very Good	Good	Fair	Poor	Very Poor

TABLE 2-5- ROCK MASS CLASSES FOR THE RMR CLASSIFICATION

The observation of the behavior of 168 tunnels excavated in hard rock is the basis of the proposed approach. For this reason it is reasonable to expect a better degree of correlation when applied to this kind of rock. However, this classification has been widely spread in various fields, both mining and in civil engineering, from tunneling to slope stability and foundations, in any condition of rock.

As shown in Table 2-6, Bieniawski correlated each RMR class of rock to appropriate values of rock mass cohesion and internal friction angle, unsupported tunnel span and its self-support time. The knowledge of these values is fundamental in any geotechnical design approach.

Class Number	I	II	III	IV	V
Average stand-up time	10 year for 15 m span	6 months for 8 m span	1 week for 5 m span	10 hours for 2.5 m span	30 minutes for 0.5 m span
Rock mass cohesion (kPa)	> 400	300 – 400	200 – 300	100 – 200	< 100
Rock mass friction angle	> 45°	35° – 45°	25° – 35°	15° – 25°	< 15°

TABLE 2-6 – MEANING OF THE RMR CLASSES OF QUALITY

2.3.3.1 CORRELATIONS IN TERMS OF RMR

The results of RMR classification can be related to the value of modulus of deformation and unconfined compressive strength by means of several empirical formulations. Bieniawski (1978) proposed the following relation for determining the modulus of deformation E_d , which is recommended for hard rocks ($RMR > 50$).

Bieniawski
$$E_d [GPa] = 2 \cdot RMR - 100 \quad (2-5)$$

Different other approaches have been proposed for the empirical evaluation of E_d in weak rock masses:

Stille (1986)
$$E_d [GPa] = 0.05 \cdot RMR \quad (RMR < 52) \quad (2-6)$$

Serafim & Pereira (1983)
$$E_d [GPa] = 10^{\frac{RMR-10}{40}} \quad (RMR < 50) \quad (2-7)$$

$$\text{Mehrotra, Mitra \& Agrawal (1991)} \quad E_d [GPa] = 10^{\frac{RMR-30}{50}} \quad (2-8)$$

$$\text{Hoek and Brown (1997)} \quad E_d [GPa] = \left(\frac{\sqrt{\sigma_{ci}}}{10} \right)^{\frac{RMR-32}{38}} (\sigma_{ci} < 100) \quad (2-9)$$

The uniaxial resistance of the rock mass σ_{cr} can be indirectly estimated using the formulation produced by Mohr-Coulomb with the values of cohesion and internal angle of friction suggested in Table 2-5 by Bieniawski.

$$\text{Mohr-Coulomb} \quad \sigma_{cr} = \frac{2c \cos \phi}{1 - \sin \phi} \quad (2-10)$$

2.3.4 NORWEGIAN GEOTECHNICAL CLASSIFICATION

This classification system was developed by Barton, Lien and Lunde, all members of the Norwegian Geotechnical Institute (NGI), in 1974. Usually it is called Barton's system or, more simply, Q system. The Barton's approach, as the classification proposed by Bieniawski, is based on the attribution of indices of quality to six important parameters characterizing the rock mass that put together define the global index of quality. The characterizing factors must be individually evaluated accordingly to the accurate guideline produced by Barton for their consistent calculations are:

- RQD (Rock Quality Designation)
- J_n (joint set number)
- J_r (joint roughness number)
- J_a (joint alteration number)
- J_w (joint water parameter)
- SRF (stress reduction factor)

Q - value	Rock mass quality
400 - 1000	Exceptionally Good
100 - 400	Extremely Good
40 - 100	Very Good
10 - 40	Good
4 - 10	Fair
1 - 4	Poor
0.1 - 1	Very Poor
0.01 - 0.1	Extremely Poor
0.001 - 0.01	Exceptionally Poor

TABLE 2-7 - Q ROCK MASS QUALITY FOR TUNNELING

The 6 indices are grouped into 3 quotients, multiplied together to obtain the value of the global index of Q (from which the name of the classification) as expressed by the Equation 2-11:

$$Q = \frac{RQD}{J_n} \frac{J_r}{J_a} \frac{J_w}{SRF} \quad (2-11)$$

The first ratio, RQD/J_n , is proportional to the size of the blocks constituting the rock mass. The second, J_r/J_a , is an approximation of the shear strength that we can expect from at the surface of the discontinuities, which is, of course, influenced by roughness and degree of alteration. The third quotient, J_w/SRF , is an indication of the stress condition borne by the rock mass, the in situ stress and the pore water pressure, which significantly reduces the shear strength of the joints of rock.

Barton, in contrast to the Bieniawski's approach, does not consider relevant the effect of orientation of joints with respect to the six factors included in the index Q.

As shown by Table 2-7, the range of admissible Q is very large. An exceptionally poor rock mass can present a Q value equal to 0.001 and one exceptionally good up to 1000. The accuracy in its determination is particularly useful for weak rocks, the condition where the classification has shown better correlation.

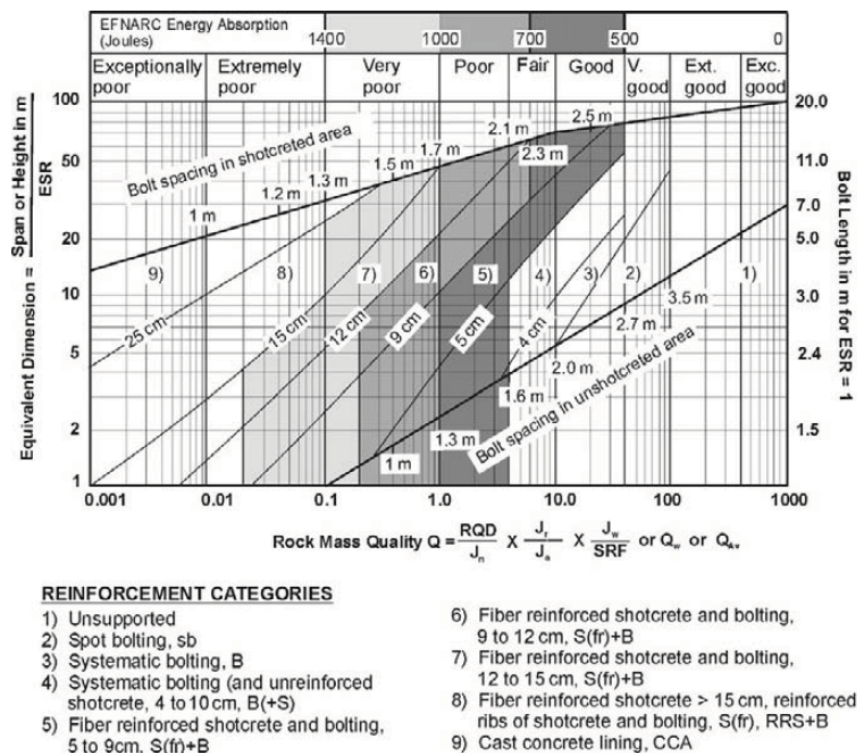


FIGURE 2-4- GRIMSTAD AND BARTON (1993) CHART FOR THE DESIGN OF SUPPORT

The optimum choice of tunnel support requirements can be deduced by the value of Q. The chart in Figure 2-4, introduced by Grimstad and Barton in 1993, suggests the appropriate support as a function of the Equivalent Dimension (of the excavation) and Q value, making use of all the latest available techniques of confinement.

The values of the Equivalent Support Ratio (ESR), necessary for the determination of the Equivalent Dimension, are tabulated in Table 2-8.

By means of Equivalent Support Ratio ESR and Q, Barton also proposed an estimation of the maximum length of unsupported tunnel D_{max} .

$$D_{max} = 2 \cdot ESR \cdot Q^{0.4} \quad (2-12)$$

A	Temporary mine openings	3 - 5
B	Permanent mine openings, water tunnels for hydro-electric projects, pilot tunnels, drifts and headings for large excavations.	1.6
C	Storage rooms, water treatment plants, minor road and railway tunnels, surge chambers and access tunnels in hydro-electric project	1.3
D	Underground power station caverns, major road and railway tunnels, civil defense chamber, tunnel portals and intersections.	1.0
E	Underground nuclear power stations, railway stations, sports and public facilities, underground factories.	0.8

TABLE 2-8 - EXCAVATION CATEGORIES DETERMINATION

2.3.4.1 CORRELATIONS IN TERMS OF Q

As for the RMR classification, based on the index Q, many useful empirical relationships have been proposed.

A mean value of the Modulus of Deformation E_d can be evaluated by means of the relation suggested by Barton (2002).

$$E_d = 10 \cdot Q_c^{1/3} \quad (2-13)$$

Where Q_c , Modified Tunnel Quality Index, can be expressed as follows

$$Q_c = Q \frac{\sigma_{cr}}{100} \quad (2-14)$$

Singh (1997) observed that, on the basis of the observation of the 35 instrumented tunnels, the magnitude of the Modulus of Deformation is also influenced by the in situ stress confinement in accordance to the following correlation

$$E_d = H^{0.2} Q^{0.36} \quad H > 50 \text{ m} \quad (2-15)$$

While the Modulus of Elasticity E_e can be expressed as follows

$$E_e = 1.5 Q^{0.6} E_r^{0.14} \quad (2-16)$$

where E_r is the Modulus of Elasticity for the intact rock.

To ensure the feasibility of the Mohr-Coulomb failure criterion, Barton, making use of the same indices, introduced the definition of Q, and derived two simple relations for the determination of angle of internal friction ϕ and cohesion c.

$$\phi = \tan^{-1} \left(\frac{J_r}{J_a} J_w \right) \quad (2-17)$$

$$c = \frac{RQD}{J_n} \frac{1}{SRF} \frac{\sigma_{ci}}{100} \quad (2-18)$$

Goel and Singh (2006) modified the formulation of the internal angle of friction given by Equation 2-17, incorporating the effect of the rock blocks interlocking, as follows

$$\phi = \tan^{-1} \left(\frac{J_r}{J_a} J_w + 0.1 \right) \quad (2-19)$$

2.3.5 CORRELATION BETWEEN RMR AND Q

Numerous attempts have been made to relate the results of the Q and RMR classifications. The determination of a certain law, valid in any condition of rock mass, which links these two approaches, creates objective difficulties. Some methods, in fact, have shown good results only in the soft rocks range, while others only in the hard rocks field.

$$\text{Bieniawski (1989)} \quad RMR = 9 \ln Q + 44 \quad (2-20)$$

$$\text{Rutledge and Preston (1978)} \quad RMR = 5.9 \ln Q + 43 \quad (2-21)$$

$$\text{Moreno (1980)} \quad RMR = 5.4 \ln Q + 55.2 \quad (2-22)$$

$$\text{Cameron-Clarke and Budavari (1981)} \quad RMR = 5 \ln Q + 60.8 \quad (2-23)$$

$$\text{Abad et al. (1984)} \quad RMR = 10.5 \ln Q + 41.8 \quad (2-24)$$

And the approach suggested by Barton in 1995, the only relation based on a natural logarithm:

$$\text{Barton (1995)} \quad RMR = 15 \log Q + 50 \quad (2-25)$$

The variety of solutions proposed, is a clear indication of the difficulty of finding a direct relationship between the two classifications. Goel (1995) ascribes this difficulty to the complex determination of some factors of RMR and Q and, on the basis of this hypothesis, he suggests the use of the indexes RCR (Rock Condition Rating) and N (Rock Mass Number).

The RCR is the RMR index unconstrained by the effect of the crushing strength of the rock mass q_c (A in the Equation 2-26) and of the adjustment of joints orientation (B).

$$RCR = RMR - (A + B) \quad (2-26)$$

The Rock Mass Number N is, instead, a stress free Q index:

$$N = Q \cdot SRF \quad (2-27)$$

Goel proposes to use modified versions of the indices suggested by Barton and Bieniawski for an indirect determination of their relationship. The advantage of using N and RCR instead of Q and RMR is that there are no concerns in their determination and, therefore, their comparison cannot be influenced by errors of personal evaluation.

Based on the observation of 63 case studies he proposed the following correlation between RCR and N:

$$RCR = 8 \ln N + 30 \quad (2-28)$$

which, valid for $q_c > 5$ MPa has shown a significant correlation coefficient of 0.92.

2.3.6 GEOTECHNICAL STRENGTH INDEX (GSI)

The Geological Strength Index was introduced for the first time by Hoek in 1994 and was subsequently modified in collaboration with other authors. The latest version of the classification is dated 2000.

The GSI, even though has all the necessary features, was not born as geo-mechanical classification, but it was ideated by Hoek as support for the prediction of the parameters m_b , s and a of the Hoek and Brown failure criterion.

The methodology of rock mass classification is founded upon the visual observation of rock mass degree of jointing and surface alteration of rock. The combination of these two parameters, making use of the chart in Figure 2-5, returns the value of GSI.







		SURFACE CONDITIONS				
		VERY GOOD	GOOD	FAIR	POOR	VERY POOR
STRUCTURE		DECREASING SURFACE QUALITY →				
	INTACT OR MASSIVE - intact rock specimens or massive in situ rock with few widely spaced discontinuities	90			N/A	N/A
	BLOCKY - well interlocked undisturbed rock mass consisting of cubical blocks formed by three intersecting discontinuity sets	80	70			
	VERY BLOCKY - interlocked, partially disturbed mass with multi-faceted angular blocks formed by 4 or more joint sets		60	50		
	BLOCKY/DISTURBED/SEAMY - folded with angular blocks formed by many intersecting discontinuity sets. Persistence of bedding planes or schistosity			40	30	
	DISINTEGRATED - poorly interlocked, heavily broken rock mass with mixture of angular and rounded rock pieces				20	
	LAMINATED/SHEARED - Lack of blockiness due to close spacing of weak schistosity or shear planes					10
		↑ DECREASING INTERLOCKING OF ROCK PIECES ↓				

FIGURE 2-5 - GEOLOGICAL STRENGTH INDEX FOR JOINTED ROCK MASSES (HOEK AND MARINOS, 2000)

The Hoek and Brown non-linear failure criterion, introduced for the first time in 1980, presents the formulation suggested in 2002, as:

$$\sigma'_1 = \sigma'_3 + \sigma_{ci} \left(m_b \frac{\sigma'_3}{\sigma_{ci}} + s \right)^a \quad (2-29)$$

The parameters m_b , s and a can be directly computed knowing the entity of the resulting GSI of the rock mass making use of the following correlations:

$$m_b = m_i \exp\left(\frac{GSI - 100}{28 - 14D}\right) \quad (2-30)$$

$$s = \exp\left(\frac{GSI - 100}{9 - 3D}\right) \quad (2-31)$$

$$a = \frac{1}{2} + \frac{1}{6} \left(e^{-GSI/15} - e^{20/3} \right) \quad (2-32)$$

Where m_i is a constant of the material that can be determined by laboratory testing or estimated by specific tables, and D represents the degree of disturbance associated to the method of excavation used.

The values of the Q and RMR indexes can be related to the GSI . In particular, it is recommended to convert the GSI to Q index for weak rock mass ($GSI < 18$) and to RMR for harder materials ($GSI > 18$) in accordance to the following relations:

$$GSI = RMR_{89} - 5 \quad (2-33)$$

$$GSI = 9 \ln Q' + 44 \quad (2-34)$$

Where the Q' is a modified version of the Barton's index which contains only the first four factors of the original form:

$$Q' = \frac{RQD}{J_n} \frac{J_r}{J_a} \quad (2-35)$$

2.4 ANALYTICAL METHODS

During the construction of an underground excavation, the initial state of equilibrium of the adjacent rock mass is disturbed. Consequently, the volume affected would be subject to a redistribution of stresses, which is followed by deformations in the direction of the opening.

As already mentioned, if the induced state of stress overcomes the characteristic resistance of the material, the installation of an internal support is necessary for the obtainment of equilibrium and reducing excessive deformations. The opportunity of installing supports to reach the equilibrium and reduce deformations basically depends on:

- Ratio between excavation dimensions and discontinuities spacing
- Number of discontinuity sets
- Rock mass resistance characteristics
- Original state of stress
- Shapes of void and excavation techniques applied

2.4.1 STRESS ANALYSIS OF A TUNNEL IMMERSSED IN AN ELASTIC CONTINUUM

If the spacing among the discontinuities characterizing a rock mass is much bigger than the excavation dimensions, it would be admissible to consider that as a massive hard rock. Since the resistance of a rock material is usually sufficient to support very intensive stresses, avoiding the beginning of the plasticization, it will behave as an "elastic continuum". In elastic conditions, an analytical description of the stress field modification can be made for any stress field and for several shapes of voids. It is not common to experience truly elastic conditions in tunneling engineering but a preliminary analytical solution by an elastic model allows a first important determination of dangerous stress concentrations.

2.4.1.1 STRESS FIELD OF A CIRCULAR TUNNEL IN AN ELASTIC MEDIUM

The prediction of stresses and deformations induced in an isotropic elastic rock mass by opening of a circular tunnel can be easily made by means of analytical approaches. In the following paragraphs the case of circular tunnels in hydrostatic and anisotropic original stress field is described through analytical

solutions. The proposed procedures will be subsequently extended to the case of elliptic and non-circular tunnels.

2.4.1.2 CIRCULAR TUNNELS - HYDROSTATIC IN SITU STRESS FIELD

The analytical determination of the stress field surrounding a circular tunnel in hydrostatic in situ conditions is based on the four important hypotheses:

1. Circular tunnel of infinite length;
2. Homogeneous, Isotropic rock mass of infinite extension;
3. Hydrostatic virgin in situ stress P_0
4. Constant radial pressure P_i applied to the internal surface of the tunnel;

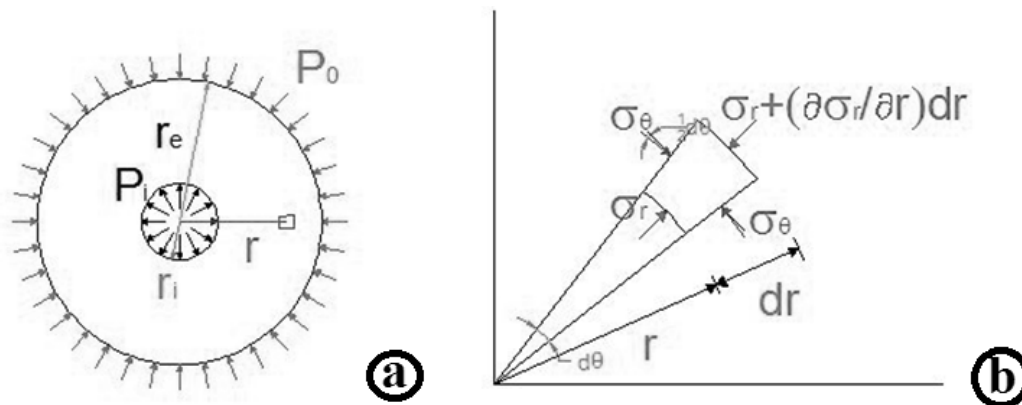


FIGURE 2-6 - REPRESENTATION OF THE PROBLEM AND DIAGRAM OF STRESSES

Due to the radial symmetry of all the elements characterizing the problem, a circular tunnel subjected to a hydrostatic stress field can be considered as an axial symmetrical plane strain problem, which entails that the stresses induced by the excavation are only function of the distance from the tunnel axes.

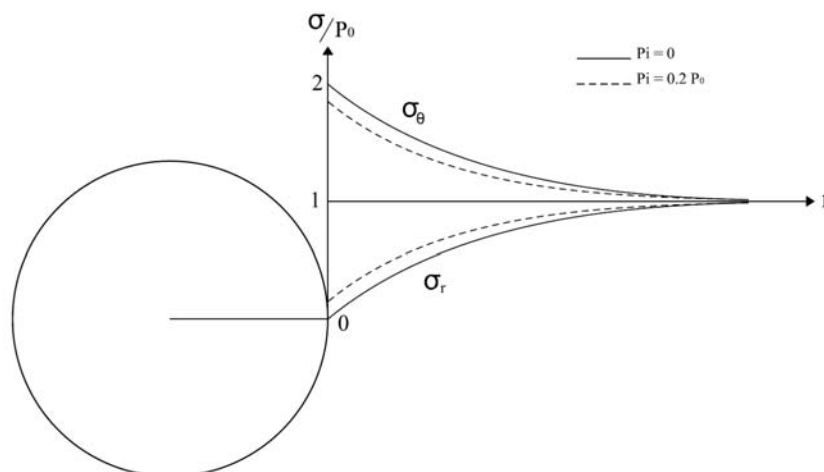


FIGURE 2-7 - MAXIMUM AND MINIMUM PRINCIPAL STRESSES AROUND A CIRCULAR TUNNEL IN HYDROSTATIC CONDITIONS IN ACCORD TO EQUATIONS 2-38 AND 2-39

A lined circular tunnel surrounded by an isotropic mass can be modeled as a cylinder of infinite length and infinite thickness ($r_e - r_i$). The effect of an internal lining is simulated by means of the constant radial stress P_i at the internal face, proportional to its structural stiffness, while the hydrostatic stress field through a stress P_0 , equal to the geostatic vertical pressure, is radially applied to the external face of the cylinder. The simplified section of the cylinder is shown in Figure 6a. Considering the plane perpendicular to the tunnel direction in Figure 2-6a, the stresses observed in tangential σ_θ and radial σ_r directions illustrated in Figure 2-6b are principal stresses, in the specific case, maximum σ_1 and minimum σ_3 .

The equilibrium of the small portion of rock mass shown in Figure 2-6b, occurs when the resultant of all the forces applied on it is null. The equation of equilibrium in cylindrical coordinates can be expressed as follow:

$$\frac{\partial \sigma_r}{\partial r} + \frac{\sigma_r - \sigma_\theta}{r} = 0 \quad (2-35)$$

For the integration of this differential Equation, which shows the modified state of stress, the introduction of the two following constitutive relations valid in elastic field is necessary:

$$\text{Poisson's ratio} \quad d\varepsilon_{rr} = \nu d\varepsilon_{ax} \quad (2-36)$$

$$\text{Hooke's law} \quad d\sigma = E d\varepsilon \quad (2-37)$$

For an infinite, lined, tunnel, the boundary conditions are summarized as follow:

$$r = r_i \quad \sigma_r = P_i$$

$$r = r_e \quad \sigma_r = \sigma_\theta = P_0$$

The analytical solution formulation of radial and tangential stresses

$$\sigma_r = P_0 - \frac{(P_0 - P_i)r_i^2}{r^2} \quad (2-38)$$

$$\sigma_\theta = P_0 + \frac{(P_0 - P_i)r_i^2}{r^2} \quad (2-39)$$

Some consideration comes out by the observation of the relations 2-38 and 2-39. The Mohr's circles representing the stress configuration are concentric, with center equal to the original hydrostatic pressure P_0 . The size of the circles proportionally decreases moving away from the tunnel centerline and reduces to the point P_0 at the infinite. For the same reason, the sum of σ_r and σ_θ , as expressed by the Equation 2-40, is constant and equal to twice the original in situ stress in presence of any confinement at the surface of the tunnel.

$$\sigma_r + \sigma_\theta = P_0 - \frac{(P_0 - P_i)r_i^2}{r^2} + P_0 + \frac{(P_0 - P_i)r_i^2}{r^2} = 2P_0 \quad (2-40)$$

Figure 2-7 illustrates how the most severe state of stress is concentrated at the surface of the tunnel, where the deviatoric stress ($\sigma_\theta - \sigma_r$), in absence of lining reaction, reaches the value of two times P_0 .

The deviatoric stress decreases rapidly moving away from the tunnel centerline, at the distance of two diameters behind the tunnel surface, the difference between the original stress P_0 and the principal stresses is only 4%. The pressure P_i applied to the internal surface of the tunnel has the effect to reduce the difference between the principal stresses but, considering its small entity with respect to the high pressures produced, it cannot induce sensible decrement in the stress conditions.

2.4.1.3 CIRCULAR TUNNELS – NON-HYDROSTATIC IN SITU STRESS FIELD

In order to make easier the treatment of a tunnel under non-hydrostatic stress conditions, it is assumed that the in situ original stresses P_h and P_v are coincident with the horizontal and vertical directions as shown in Figure 2-8. The principal stresses are interrelated through the horizontal stress ratio λ as in Equation 2-41:

$$P_h = \lambda P_v \quad (2-41)$$

The determination of the vertical component of the in situ stress does not present particular complications and can be estimated by means of the following easy relation:

$$P_v = \gamma h \quad (2-42)$$

where γ is the unit weight of the overlying rock mass and h is the depth below the surface.

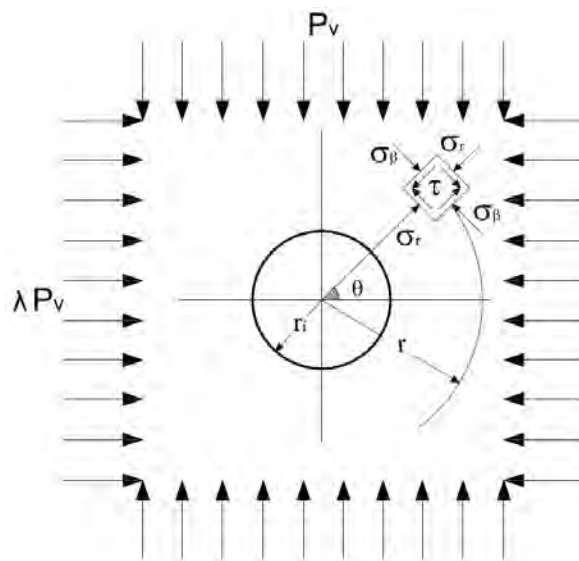
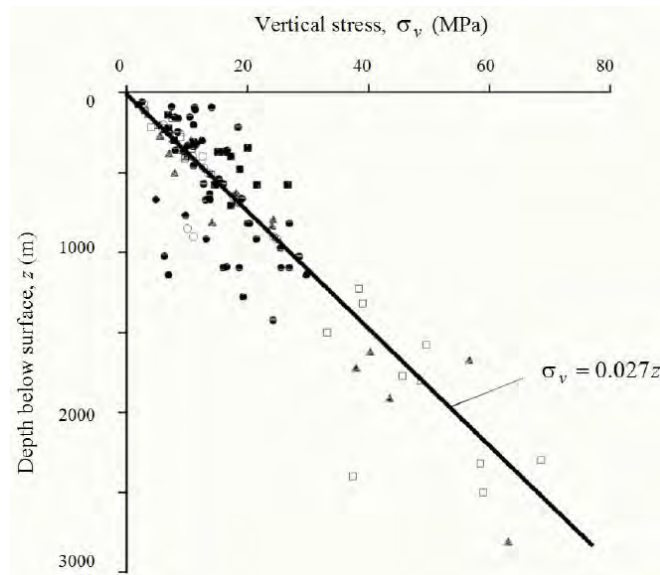


FIGURE 2-8 – CIRCULAR TUNNEL
IN A NON-HYDROSTATIC STRESS FIELD

Measurements of vertical stress at various mining and civil engineering sites around the world as reported by Hoek and Brown (1990) estimate the average unit weight of the earth's crust equal to 27 kN/m^3 . As illustrated in Figure 2-9, the measurements can vary from the expected geostatic pressure, but they can be improved by means of specific geological surveys.

The horizontal component of the in situ stress, instead, is a function of many parameters not always easy to determine. P_h can be either bigger or smaller than the vertical component P_v because λ (sometimes K or K_0), can show a large range of values ranging between 0 and 4.

At low depths, up to 1000 meters below the ground level, the gravitational effect of the rock mass is not preponderant and λ is a complex combination of the effects of gravity, superficial morphology, subsidence phenomena and, for the most part, intra-crustal tectonic stresses. For this reason in the vicinity of the ground surface λ can manifest that wide range of values.



**FIGURE 2-9 - VERTICAL STRESS MEASUREMENTS
(UNDERGROUND EXCAVATION IN ROCKS, HOEK AND BROWN (1990))**

Beyond that point the difference between vertical and horizontal components of the in situ stress reduces, showing the tendency to hydrostatic conditions.

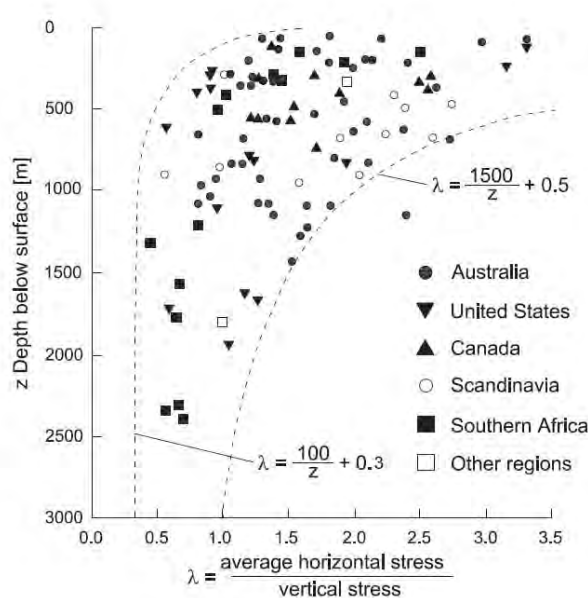


FIGURE 2-10 – VARIATION OF THE RATIO OF AVERAGE HORIZONTAL STRESS TO VERTICAL STRESS WITH DEPTH BELOW SURFACE (UNDERGROUND EXCAVATION IN ROCK, HOEK AND BROWN (1990))

Again the 116 measurements of in situ stress, shown in Figure 2-10, collected in various parts of the world and published by Hoek and Brown (1990) confirm that, for low depths, it is not possible to get an estimation of the original stress field, while the range of values for λ becomes narrow when the depth of 1000 meters is exceeded.

The state of stress induced by the opening of a circular tunnel in an anisotropic stress condition is well described by the Kirsch's equations (1898). The Kirsch's equations are based on the linear theory of elasticity and assume isotropic rock properties. They reduce to Equations 2-38 and 2-39 when the horizontal stress ratio is equal to one.

$$\sigma_r = \frac{1}{2} P_v \left((1 + \lambda) \left(1 - \frac{r_i^2}{r^2} \right) - (1 - \lambda) \left(1 - \frac{4r_i^2}{r^2} + \frac{3r_i^4}{r^4} \right) \cos 2\theta \right) \quad (2-43)$$

$$\sigma_\theta = \frac{1}{2} P_v \left((1 + \lambda) \left(1 + \frac{r_i^2}{r^2} \right) + (1 - \lambda) \left(1 + \frac{3r_i^4}{r^4} \right) \cos 2\theta \right) \quad (2-44)$$

$$\tau_{r\theta} = \frac{1}{2} P_v \left(- (1 - \lambda) \left(1 + \frac{2r_i^2}{r^2} - \frac{3r_i^4}{r^4} \right) \sin 2\theta \right) \quad (2-45)$$

Differently from the isotropic case, the radial σ_r and normal σ_θ tensions are not always principal stresses; this condition is achieved only along the principal directions and at the tunnel surface, where the expression of shear stress in Equation 2-45 becomes null. In an anisotropic stress field, the induced modifications of the stress field are not only sensitive to the distance from the centerline r , but are mostly a function of θ , measured with the horizontal plane passing through the center of excavation. In Figure 2-11 is presented the distribution of the principal stresses in radial and tangential direction for different values of horizontal ratio.

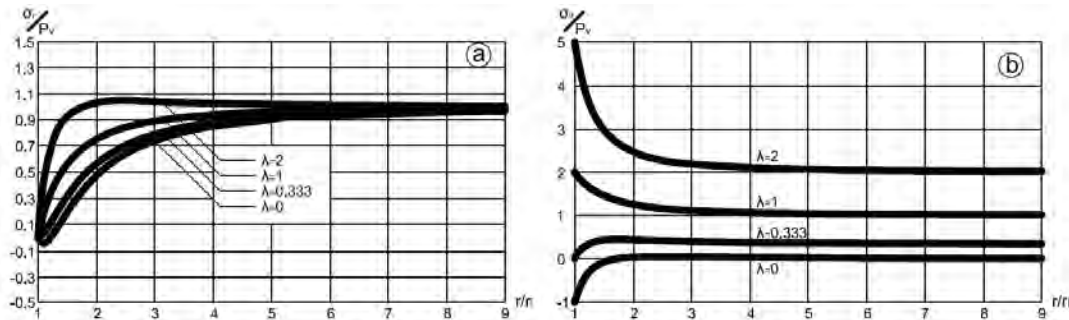


FIGURE 2-11 - TANGENTIAL AND RADIAL PRINCIPAL STRESS IN HORIZONTAL DIRECTION FOR INCREASING VALUES OF λ

In absence of internal confinement, the tangential stress at the tunnel contour ($r/r_i=1$), which is shown in Figure 2-12, can be expressed by means of Equation 2-46. The radial and shear stresses expressed by the relations 2-43 and 2-45 are, instead, null.

$$\frac{\sigma_\theta}{P_v} = \left((1 + \lambda) + 2(1 - \lambda) \cos 2\theta \right) \quad (2-46) \quad \begin{array}{l} \text{when } \theta = 90^\circ, 270^\circ \quad \sigma_\theta / P_v = (3\lambda - 1) \\ \text{when } \theta = 0^\circ, 180^\circ \quad \sigma_\theta / P_v = (3 - \lambda) \end{array}$$

The maximum tangential stress observed at the tunnel surface is always larger with respect to that registered in a hydrostatic stress field and located in the portion of tunnel. It is in normal direction to the minimum in situ principal stress direction. This difference is more evident when the vertical principal in situ stress is predominant (λ is bigger than 1). In the direction of the maximum in situ stress, instead, the tangential stress is smaller than the constant, hydrostatic, $2 \cdot P_0$.

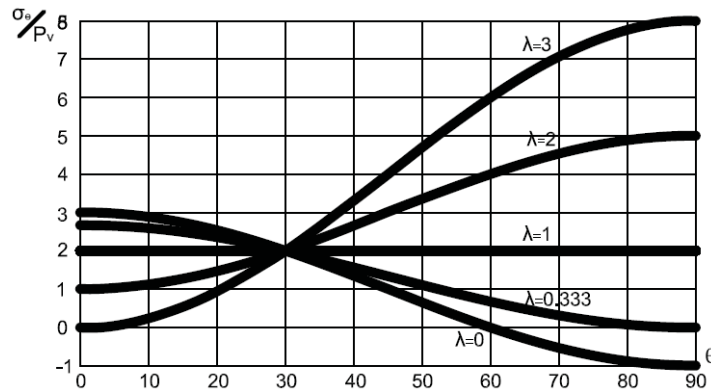


FIGURE 2-12 - TANGENTIAL STRESS AT THE TUNNEL SURFACE FOR INCREASING VALUES OF λ

When the horizontal stress ratio is smaller than 1/3 or bigger than 3, concentration of tensile stresses are also recognizable. These kinds of stresses are particularly dangerous in tunneling engineering because of the low resistance of the rock masses, which is approximately only half the rock mass cohesion.

2.4.1.4 NON CIRCULAR TUNNELS IN NON-HYDROSTATIC IN SITU STRESS FIELD

The analytical resolution of the stress distribution induced by the excavation of a tunnel different from the typical circular shape presents objective difficulties of implementation and a numerical approach for its analysis would be certainly more appropriate. The analytical solution of two specific cases is, however, possible and it is of great importance to extend the acquired knowledge of several underground excavations of different shapes.

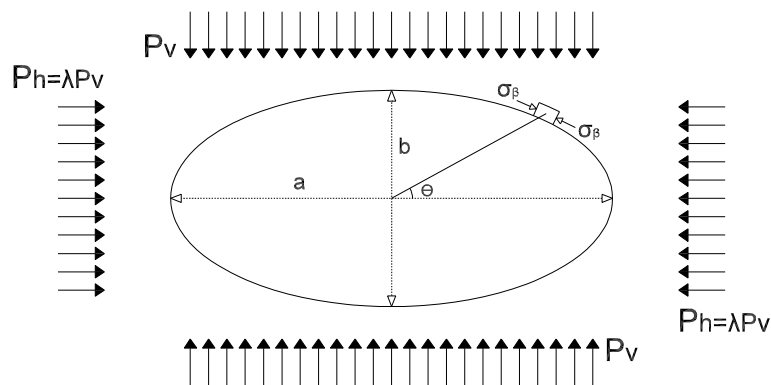


FIGURE 2-13 – GEOMETRICAL CONFIGURATION OF AN ELLIPTIC TUNNEL IMMERSSED IN AN ANISOTROPIC STRESS FIELD

The first example presented in this section, as shown in Figure 2-13, is the case of an elliptic tunnel. For the elliptic example, assuming the principal stresses coincident with the major and minor axes, a and b

of the ellipse, the pressure σ_β , perpendicular point by point to the surface of the void, as suggested by Ribacchi (1986), is expressed by the following relation:

$$\sigma_\beta = \frac{P_v \left\{ (\lambda - 1) \left[\left(\frac{a}{b} + 1 \right)^2 \sin^2 \theta - 1 \right] + 2 \frac{a}{b} \right\}}{\left(\frac{a^2}{b^2} - 1 \right) \sin^2 \theta + 1} \quad (2-47)$$

The geometrical characteristics of an ellipse can be described by means of the non-dimensional ratio a/b between maximum and minimum lengths of the principal axis. In particular, when a/b is equal to 1, the ellipse reduces to a circle and the relation 2-47 is coincident with the Equation 2-44.

Some considerations come out from the study of the Equation 2-47. As already mentioned, for the analysis of a circular tunnel, the most problematic stress configuration is observed when λ is external to the range 1/3 to 3 which corresponds to the generation of tensile stresses. The tensile stress observed and the extension of the interested tunnel surface is a function of the distance λ from the boundaries of the compressive stresses range.

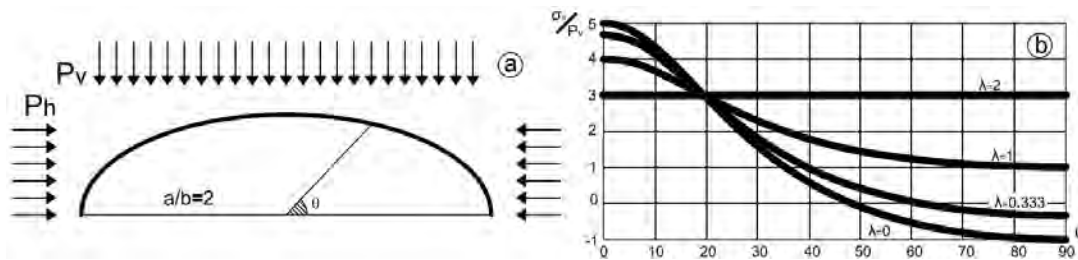


FIGURE 2-14 – STRESS DISTRIBUTION AT THE SURFACE OF AN ELLIPTIC TUNNEL WITH MAJOR AXES IN HORIZONTAL DIRECTION

Now the case of a circular tunnel subjected to an anisotropic stress field is compared to the elliptic tunnel with horizontal major axes ($a/b>1$) shown in Figure 2-14a. If the tangential stress at the tunnel surface is evaluated for different values of the horizontal ratio, the following outcomes can be deduced from the comparison with the circular case:

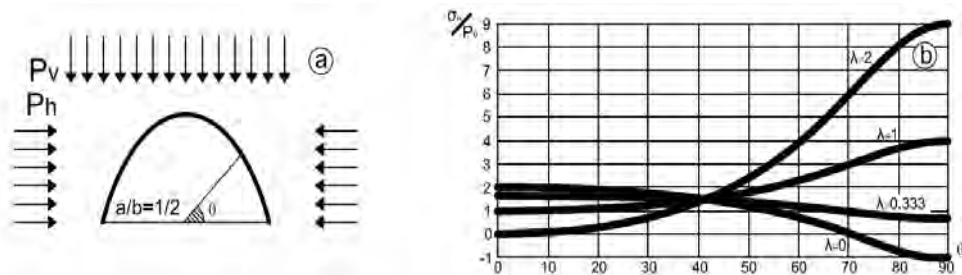


FIGURE 2-15 - STRESS DISTRIBUTION AT THE SURFACE OF AN ELLIPTIC TUNNEL WITH MAJOR AXES IN VERTICAL DIRECTION

- The development of tensile stress conditions is anticipated when the maximum in situ stress is directed vertically and delayed when it is directed horizontally;
- In hydrostatic conditions, the maximum tangential stress is considerably larger;

- If the horizontal ratio is bigger than 1, the maximum compressive tension, which is located at crown $\theta = 90^\circ$, is smaller.

The same comparison is now performed to an elliptic tunnel with the maximum axes horizontally oriented as shown in Figure 2-15.

- The development of tensile stress conditions is anticipated when the maximum in situ stress is directed horizontally and delayed when is directed vertically;
- The maximum entity of the compressive stress in hydrostatic conditions is larger than that observed in a circular tunnel;
- If the maximum principal stress is oriented in the direction of the minimum tunnel axes, the tangential stress produced by an elliptic excavation is considerably larger.

Throughout the analysis of the three above presented cases of circular and elliptic tunnels subjected to anisotropic stress field, it is observed that the state of stress at the internal surface of an underground excavation can be manipulated to achieve a less critical condition just modifying the shape of the tunnel section.

For anisotropic stress conditions, an elliptic tunnel section oriented with the major axes parallel to the maximum principal in situ stress direction is an efficient choice. This configuration allows reducing the portion of tunnel subjected to tensile stresses and the magnitude of the compressive stresses. In hydrostatic stress conditions, instead, the best option is always the circular shape.

A rectangular shaped tunnel can be considered in place of an elliptic shape. The stress distribution is similar to that obtained for an elliptical option but, in the proximity of the four corners, a severe increment of the tangential stress is observed. The entity of this increment, which is present for any value of λ , is direct function of the curvature of the corners and is so large that the resistance of the material may be locally overcome. The local failure of rock has the positive effect of mitigating the state of stress produced without compromising the global stability of the excavation. Its advent can be, however, minimized by increasing the original radius of curvature.

2.4.1.5 EFFECT OF THE ROCK MASS ANISOTROPY ON THE STRESS FIELD

According to Lekhnitskii, 1973, the state of stress at the contour of a tunnel immersed in an anisotropic rock mass, which presents directionally dependent properties, is strongly influenced by the orientation of the maximum and minimum components of the modulus of elasticity E . The maximum stress at the tunnel surface, in fact, tends to increase in the direction of the maximum.

Nevertheless, the response of an isotropic rock mass is noticeably different only in cases of pronounced anisotropy as, for instance, sedimentary rock or rock masses provided with explicitly oriented discontinuities (Martino and Ribacchi. 1972).

2.4.2 TENSIONAL ANALYSIS OF A TUNNEL IMMERSSED IN A STRONGLY FRACTURED ROCK MASS

The choice of the best location for the realization of an underground infrastructure is hardly based on a rational investigation of the geological and geotechnical structures present in the local area. More frequently the engineers must make the best of the geo-structural conditions imposed by other than engineering motivations.

When the degree of fracturing present in the rock mass is such that the ratio of excavation dimension / joint spacing is very large, the rock volume behaves as a granular soil and its original resistance drastically decreases. This condition can be modeled by means of an equivalent rock of weaker characteristics than those of the rock matrix. The drop in resistance is a direct function of the degree of

the physical and chemical alteration undergone by the rock mass and can be evaluated by means of any geo-mechanical classification. In these conditions the probability of facing difficulties during the excavation is very high even in presence of ordinary in situ stress fields.

The analytical determination the state of stress inducted by excavation of a tunnel is possible in respect of a relatively high number of initial conditions. The large number of geometrical or physical restrictions corresponds to a poor flexibility of the present approach, in particular when used for complex designing. In spite of these limitations, it is still widely applied and carved out an important preparatory role in the understanding of Tunneling Engineering. In fact, with the success of the numerical methods applied to geo-mechanical problems, almost every engineering problem can be easily reproduced and solved without any particular knowledge of tunneling engineering, but a strong analytical background is, however, still necessary to verify the accuracy of the numerical outcomes.

2.4.2.1 STRENGTH OF ROCK MASSES

The knowledge of the strength of a rock mass is fundamental for the design of underground infrastructures. The boundary between admissible and non-admissible states of stress in the three-dimensional principal stress space σ_1 - σ_2 - σ_3 is represented by a convex surface. This surface is called failure criterion or yield function and its general formulation is expressed as follow:

$$\Phi(\sigma_1, \sigma_2, \sigma_3) = 0 \quad (2-48)$$

When the stress applied to an element of the rock mass lies on the failure surface it fails and the plastic deformations start.

Depending on the characteristics of the rock mass, the limit surface will expand (hardening behavior) or, more commonly in rock masses, will contract (model softening behavior) when overlaid. The velocity of this contraction is different for different types of rocks. The modeling of the different behaviors at failure of the yield criteria can be represented in one-dimension as a function of the single principal stress and related strain as shown in Figure 2-16.

Considering the real resistance of a rock mass, it cannot support an unlimited amount of stress. The maximum limit that it can handle is given by the pressure of failure. Beyond that point it cannot withstand any further stress.

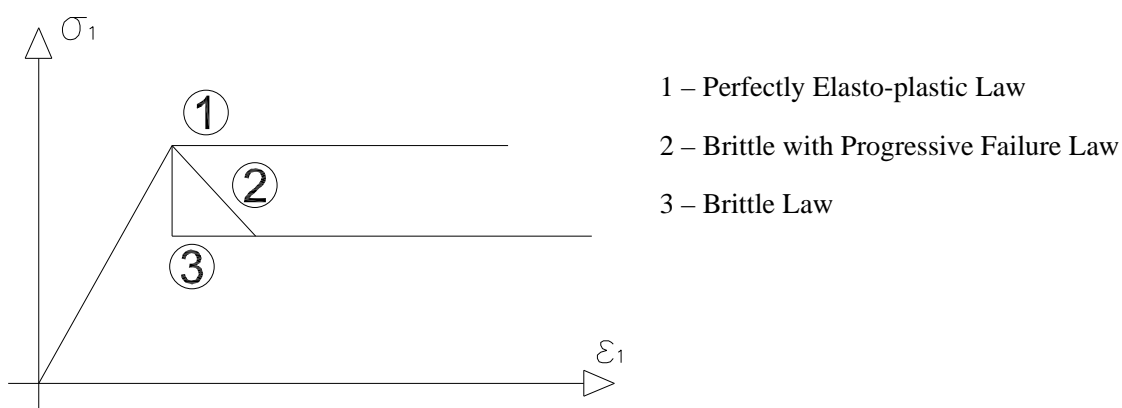


FIGURE 2-16 – IDEAL STRAIN SOFTENING RESPONSE OF A ROCK MASS

Depending on the post failure behavior, it is possible to represent a rock mass through three simple models. A rock mass will follow a perfectly elasto-plastic law (line 1 in Figure 2-16) if the stress supported by the material after the failure remains constant for increasing plastic deformation while brittle (line 3) or brittle with progressive failure laws (line 2) will be observed when a sudden or gradual decay of the supported pressure (and, therefore, the contraction of the yield criterion). In the presence of a brittle material, it is essential to know the values of resistance before (peak condition) and after (residual conditions) the contraction failure criterion surface.

2.4.2.1.1 FAILURE CRITERIA FOR ROCK MASSES

Several studies in the past have shown that because of the small difference between the intermediate principal stress σ_2 and the corresponding minimum principal stress σ_3 , encountered in most geotechnical problems, the behavior at failure of a rock mass is not substantially affected by intermediate principal stress. For this reason, generally, the constitutive models are expressed as a function of the minimum and maximum principal pressures σ_1 and σ_3 only, with a consequent simplification of their spatial representation. The failure criteria are usually drawn on three standard bi-dimensional planes, the σ_1 - σ_3 , the $(\sigma_1 - \sigma_3) / 2 - (\sigma_1 + \sigma_3) / 2$ and, finally, the τ - σ plane, as the failure envelope of the Mohr's circles limit the conditions of shear resistance. These representations are equivalent and conversions from one to another are controlled by simple geometric relations.

The easiest and most applied failure criterion is that suggested by Mohr-Coulomb. According to this approach, the failure of a soil or a rock is due to a combination of shear and normal stress, and is formulated, as shown in Equation 2-49. The shear stress is a linear function of the angle of internal friction ϕ and cohesion c of the material considered. The extensive use of this method is primarily due to its intrinsic simplicity of use and determination of the two parameters characterizing the shear strength. The Mohr-Coulomb failure criterion can be also expressed in terms of principal stresses as described in Equation 2-50:

$$\tau = c + \sigma \tan \phi \quad (2-49)$$

or

$$\sigma_1 = N_\phi \sigma_3 + \sigma_{cr} \quad (2-50)$$

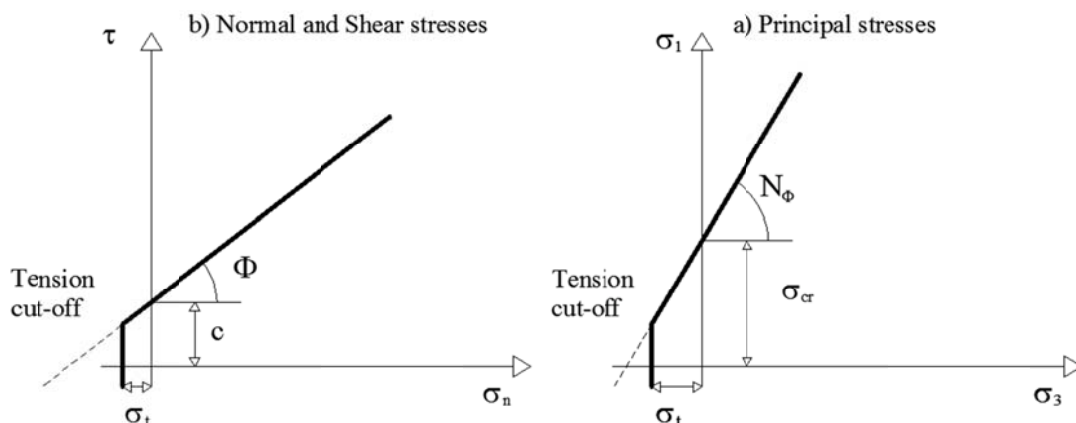


FIGURE 2-17 - TYPICAL REPRESENTATION OF THE MOHR-COULOMB CRITERION IN TERMS OF PRINCIPAL STRESSES (A) AND SHEAR AND NORMAL STRESSES (B)

In Equation 2-49, ϕ and c respectively describe the slope and the intercept of the failure envelope in the Mohr's plane. The parameter N_ϕ of the Equation 2-50, instead, quantifies the increment of resistance with increasing confining pressure σ_3 , while σ_{cr} defines the uniaxial compressive strength of the rock mass. The graphical representations of the Equation 2-49 and 2-50 are shown in Figures 2-17a and 2-17b.

The main limitation of the Mohr-Coulomb failure criterion is overestimation of the rock mass strength in tensile stress region or in low confining pressure. To partially reduce this problem it is introduced a tensile cut-off σ_t in tensile region, as shown in Figure 2-17.

A more realistic rock mass behavior can be obtained by using non-linear failure criteria. The characteristic concavity downwards of these constitutive models results in a smaller tensile strength and in instantaneous cohesion and angle of friction that increase and decrease respectively, with increasing confining pressure σ_3 .

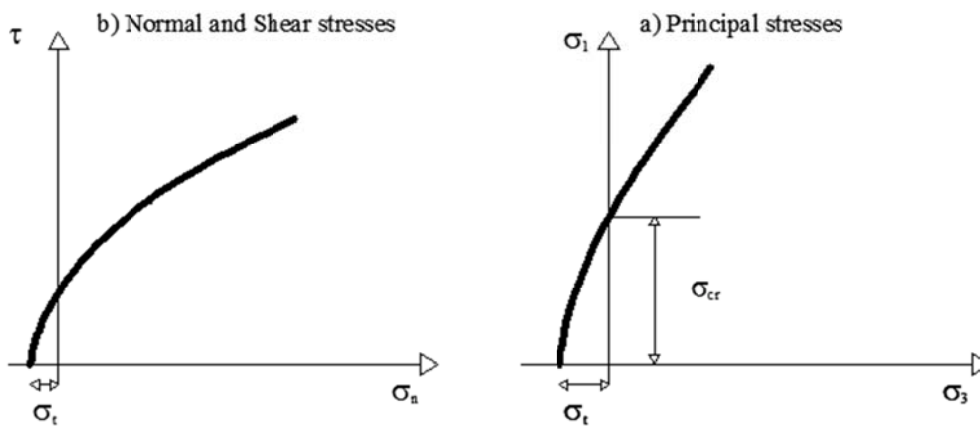


FIGURE 2-18 - TYPICAL REPRESENTATION OF A NON-LINEAR FAILURE CRITERION

In Figure 2-18 a typical representation of the non-linear failure criterion is shown. Among them, the criterion proposed by Hoek and Brown, which was already discussed in the rock mass classifications section, is the most used. Unlike any other existing two-dimensional non-linear constitutive models it can, in fact, rely on the reproducibility and repeatability typical of the Mohr-Coulomb strength criterion and on the complete and consistent theoretical and practical background based on specific numerical, analytical and empirical solutions developed by the authors of the present theory.

For the Hoek-Brown criterion it is possible, for the resolution of geomechanical problems, making use of Phase2, software package written by Rocscience, implementing the finite element method. Unlike the Mohr-Coulomb failure criterion, the Hoek and Brown criterion is hardly used on other geo-mechanical numerical suites. Hoek et al. (2002), for this reason, introduced the generalized Hoek-Brown failure criterion, by making use of the equivalent parameters of resistance c' and ϕ' as shown in Figure 2-19, which allows its application through the best fitting linear Mohr-Coulomb failure criterion.

The suggested equivalent cohesion and angle of friction are a function of the parameters characterizing the Hoek and Brown failure criterion as expressed by the following relations:

$$\phi' = \sin^{-1} \left(\frac{6am_b (s + m_b \sigma'_{3n})^{a-1}}{2(1+a)(2+a) + (s + m_b \sigma'_{3n})^{a-1}} \right) \quad (2-51)$$

$$c' = \frac{\sigma_{ci} \left[(1+2a)s + (1-a)m_b \sigma'_{3n} (s + m_b \sigma'_{3n})^{a-1} \right]}{(1+a)(2+a) \sqrt{1 + \frac{6am_b (s + m_b \sigma'_{3n})^{a\alpha-1}}{(1+a)(2+a)}}} \quad (2-52)$$

where $\sigma'_{3n} = \sigma'_{3\max} / \sigma_{ci}$ and σ_{ci} is the uniaxial compressive strength of rock material.

$\sigma'_{3\max}$ is the upper limit of the confining stress over which the relation between the criteria is considered. For underground excavation Hoek et al (2002) proposed the following relation for its determination:

$$\sigma'_{3\max} = 0.43 \sigma'_{cm} \left(\frac{\sigma'_{cm}}{\sigma_{in-situ}} \right)^{-0.94} \quad (2-53)$$

where $\sigma_{in-situ}$ is the maximum in situ stress registered in the direction perpendicular to the tunnel direction and σ'_{cm} is the rock mass uniaxial strength.

2.4.2.1.2 POLYAXIAL STRENGTH CRITERIA

Conditions of triaxial state of stress ($\sigma_2 = \sigma_3$), on which most of the geo-mechanical constitutive models are normally based, are accomplished only occasionally. In field, when the intermediate principal stress does not coincide with the minimum principal stress, these conditions are called polyaxial state of stress. Very pronounced polyaxial conditions are observed in the proximity of the surface of an underground excavation. For example, the stress oriented in the direction of a tunnel, which is intermediate principal stress, is two times the vertical in situ stress, and much greater than the minimum principal stress (radial), which is only equal to the resistance opposed by the lining system.

Several authors have tried to propose strength criteria that take into account the effect of the intermediate principal stress at failure to describe the behavior of a rock mass. The first author who conducted specific laboratory experiments to verify the effect of intermediate principal stress on the rock strength was Mogi (1967). Nadai (1950) and Drucker and Prager (1952) previously grasped the importance of the intermediate principal stress to explain the behavior of a rock mass under polyaxial stress, but were able to produce constitutive models based only on theoretical considerations as the suitable equipment for polyaxial testing were not available. From the analysis of numerous polyaxial tests carried out on specimens of fractured rocks Mogi (1967) suggested the following empirical failure criterion:

$$\frac{\sigma_1 - \sigma_3}{2} = f_1 \left(\frac{\sigma_1 + \beta \sigma_2 + \sigma_3}{2} \right) \quad (2-54)$$

The intermediate principal stress therefore physically improves the characteristic resistance of a fractured rock. In accordance with the relation proposed by Mogi its impact, compared to that of the minimum principal pressure, is modulated by a coefficient β smaller than 1.

The constitutive model suggested by Mogi was subsequently modified by Al-Ajmi in 2006, which produced the following Mogi-Coulomb strength criterion:

$$\tau_{oct} = a + b \sigma_{m,2} \quad (2-55)$$

where τ_{oct} is the octahedral shear stress and $\sigma_{m,2}$ is expressed as follows:

$$\sigma_{m,2} = \frac{\sigma_1 + \sigma_3}{2} \quad (2-56)$$

In Equation 2-55 the coefficients a and b are equivalent to cohesion and tangent of the angle of internal friction in the Mohr-Coulomb plane.

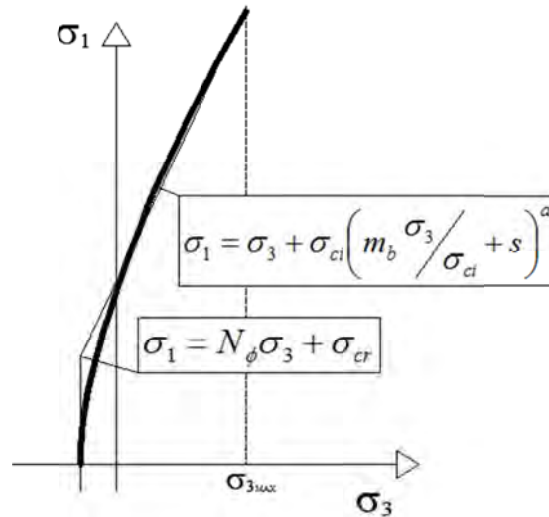


FIGURE 2-19 - RELATIONSHIPS BETWEEN MAJOR AND MINOR PRINCIPAL STRESSES FOR HOEK-BROWN AND EQUIVALENT MOHR-COULOMB CRITERIA (HOEK, CARRANZA-TORRES, CORKUM (2002))

In 1995, on the basis of several polyaxial laboratory lab tests performed on hollow cylinders, Wang and Kemeny proposed the following criterion:

$$\frac{\sigma_1}{q_c} = 1 + A \left[e^{\sigma_3/\sigma_2} \right] \cdot \left[\frac{\sigma_2}{q_c} \right]^{1-f e^{\sigma_3/\sigma_2}} \quad (2-57)$$

Where f (0.10-0.20) and A (0.75-200) are constants of the material and q_c the average uniaxial compressive strength of the rock material for various orientations of the planes of weakness. When the minimum principal stress is much smaller than the intermediate principal stress ($\sigma_3 \ll \sigma_2$), the relation 57 reduces to the following form:

$$\sigma_1 \approx q_c + (A + f) \cdot (\sigma_2 + \sigma_3) \quad (2-58)$$

In 1998, starting from the observation in laboratory and in field of an overestimation of the shear stress of a rock mass by the classical theory of elasto-plasticity, Singh et al. (1998) suggested a semi empirical approach that incorporates the effect of the intermediate principal stress σ_2 in the conventional formulation of the Mohr-Coulomb failure criterion by replacing σ_3 with the average value of σ_2 and σ_3 in the second term of the Mohr-Coulomb formulation:

$$\sigma_1 - \sigma_3 = \sigma_{cr} + \frac{\sigma_2 + \sigma_3}{2} A \quad (2-59)$$

where $A = \frac{2 \sin \phi}{1 - \sin \phi}$

The Polyaxial Strength Criterion, as suggested by Singh in Equation 2-59, has shown great reliability in weak rocks underground practical applications in northern India. It will be extensively treated in subsequent sections of this thesis.

2.4.3 STRESS FIELD OF A CIRCULAR TUNNEL IN AN ELASTO-PLASTIC MEDIUM

At the opening of an underground excavation a redistribution of the original stress field occurs and elasto-plastic deformations, in the surrounding rock mass, can be observed. Exceeded the limit of 1% of the tunnel radius (Hoek, 2000), the new conditions of stress overcome the rock mass resistance and the plasticization of the material starts. The plasticized area around the excavation (plastic zone) presents characteristic of residual resistance (Goguel, 1947) smaller than those of the original rock mass. The development of the rock mass failure may end either with the collapse of the underground structure or with the achievement of a new equilibrium, usually facilitated by the installation of support. The predicted magnitude of the plasticized zone for different support systems at the internal surface of the excavation is of significant importance in rock mechanics.

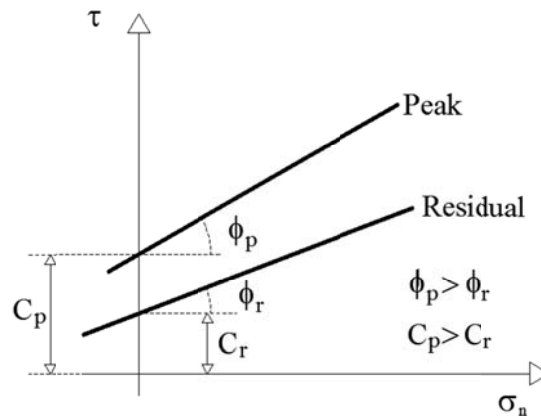


FIGURE 2-20- TYPICAL REPRESENTATION OF THE PEAK AND RESIDUAL CONDITIONS OF THE MOHR-COULOMB FAILURE CRITERION

Based on the Mohr-Coulomb failure criterion, for a circular tunnel of infinite length subjected to a radial internal pressure P_i and an hydrostatic pressure P_0 equal to the overburden stress (plane strain conditions), surrounded by a perfectly elasto-plastic or brittle rock mass, an exact closed-form solution for determining the radius of the plastic zone can be obtained. In this paragraph, this analytical solution is developed as suggested by Ribacchi (1986) on the hypothesis that the behavior of the rock mass can be described by a peak failure envelope and a residual failure envelope, as shown in Figure 2-20. The result can however be extended to the case of perfectly elasto-plastic rock mass exchanging the residual strength parameters with those of peak.

The symmetry of the geometry of excavation and applied forces allows considering the radial σ_r and tangential σ_θ stresses as minimum σ_3 and maximum σ_1 principal stresses respectively. In the plastic zone the state of stress is governed by the equation of equilibrium and by the failure criterion in terms of residual parameters:

$$\frac{\partial \sigma_r}{\partial r} = \frac{\sigma_\theta - \sigma_r}{r} \quad (2-60)$$

$$\sigma_{\theta} = \frac{1 + \sin \phi_r}{1 - \sin \phi_r} \sigma_r + \frac{2c_r \cos \phi_r}{1 - \sin \phi_r} \quad (2-61)$$

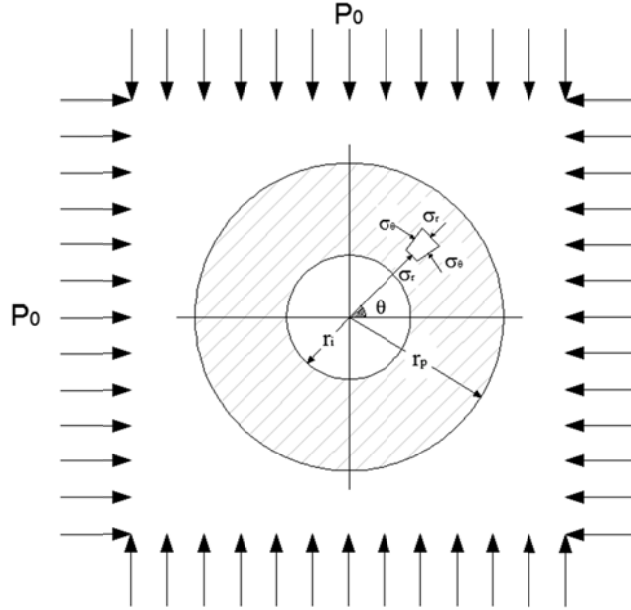


FIGURE 2-21 - PLASTICIZED TUNNEL UNDER HYDROSTATIC STRESS FIELD

Substituting the relation 2-61 in Equation 2-60, the equation of equilibrium can be rewritten as follows:

$$\frac{\partial \sigma_r}{\partial r} = \frac{k_2 \sigma_r + k_1}{r} \quad (2-62)$$

Because k_1 and k_2 are only constant functions of residual cohesion and angle of internal friction and the previous relation can be solved taking in to account the following boundary condition:

$$\sigma_r = P_i \quad \text{at} \quad r = r_i$$

where P_i is the reaction of the lining installed on the surface of the excavation ($r = r_i$). The resulting differential equation has the solution of the following form:

$$\frac{1}{k_2} \ln \left(\frac{k_2 \sigma_r + k_1}{k_2 P_i + k_1} \right) = \ln \left(\frac{r}{r_i} \right) \quad (2-63)$$

By means of the above Equation, the distribution of the radial pressure within the plasticized zone can be predicted. The Equation 2-65 describes the tangential stress in the broken zone and is obtained by substituting the Equation 2-64 in the chosen failure criterion in terms of residual parameters (Equation 2-61).

$$\sigma_r = \left(P_i + c_r \cot \phi_r \right) \left(\frac{r}{r_i} \right)^{\frac{2 \sin \phi_r}{1 - \sin \phi_r}} - c_r \cot \phi_r \quad (2-64)$$

$$\sigma_{\theta} = \frac{1 + \sin \phi_r}{1 - \sin \phi_r} (P_i + c_r \cot \phi_r) \left(\frac{r}{r_i} \right)^{2 \sin \phi_r / (1 - \sin \phi_r)} - c_r \cot \phi_r \quad (2-65)$$

The state of stress within the plasticized ring is, therefore, exclusively a function of applied pressure P_i on the internal surface of the excavation and the parameters of residual resistance chosen.

Equations 2-64 and 2-65 do not allow, however, to define the external limit of the plastic zone. Radial pressure P_b at the plastic radius and its extension r_p are obtained by assuming that at this distance are reached the peak failure conditions as expressed by the Equation 2-65:

$$\sigma_{\theta} = \frac{1 + \sin \phi_p}{1 - \sin \phi_p} P_b + \frac{2c_p \cos \theta_p}{1 - \sin \phi_p} \quad (2-66)$$

In addition to this, as shown in Figure 2-22, at the contour of the elastic zone is also valid the relation 2-40 existing between the principal stresses P_b and σ_{θ} .

$$\sigma_{\theta} = 2P_0 + P_b \quad (2-67)$$

The equivalence of the two previous relationships returns the value of the radial stress P_b in r_p .

$$P_b = \frac{2P_0 - \frac{2c_p \cos \phi_p}{1 - \sin \phi_p}}{1 + \frac{1 + \sin \phi_p}{1 - \sin \phi_p}} = P_0 (1 - \sin \phi_p) - c_p \cos \phi_p \quad (2-68)$$

In the elastic zone, the minimum and maximum principal stresses, determined using Equations 2-38 and 2-39, are expressed respectively as:

$$\sigma_r = P_0 - (P_0 - P_b) \left(\frac{r_p}{r} \right)^2 \quad (2-69)$$

$$\sigma_{\theta} = P_0 + (P_0 - P_b) \left(\frac{r_p}{r} \right)^2 \quad (2-70)$$

For the hypothesis of continuity, at the plastic radius r_p , the radial load P_b computed using Equation 2-64 for the plastic zone and using Equation 2-69 for the elastic zone must be equivalent. Accordingly to this, equating the different Equations 2-64 and 2-69 of the radial pressure σ_r , the magnitude of the plastic radius is determined as:

$$(P_i + c_r \cot \phi_r) \left(\frac{r_p}{r_i} \right)^{2 \sin \phi_r / (1 - \sin \phi_r)} - c_r \cot \phi_r = P_0 (1 - \sin \phi_p) - c_p \cos \phi_p$$

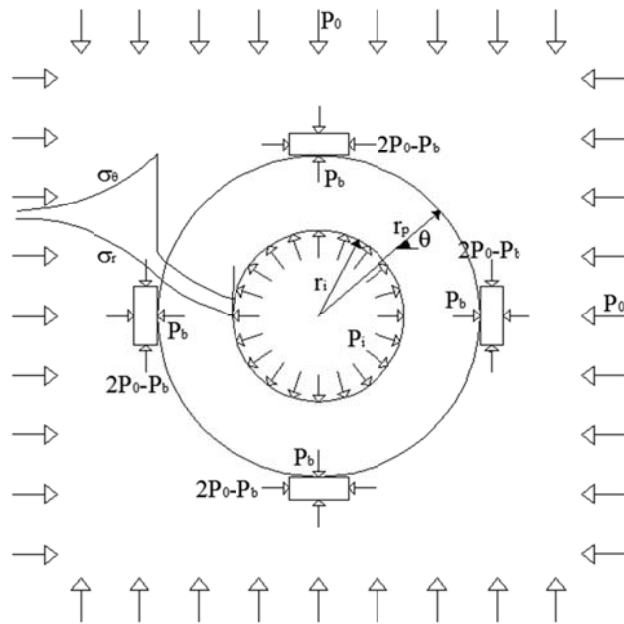


FIGURE 2-22 - PROBLEM OF A PLASTICIZED CIRCULAR TUNNEL IN HYDROSTATIC STRESS CONDITIONS IN ACCORD TO RIBACCHI'S HYPOTHESES (1986)

$$r_p = r_i \left(\frac{(P_0 + c_r \cot \phi_r) - (P_0 + c_p \cot \phi_p) \sin \phi_p}{(P_i + c_r \cot \phi_r)} \right)^{\frac{1 - \sin \phi_r}{2 \sin \phi_r}} \quad (2-71)$$

The typical distribution of radial and tangential stresses under isotropic in-situ stress field is shown in Figure 2-23.

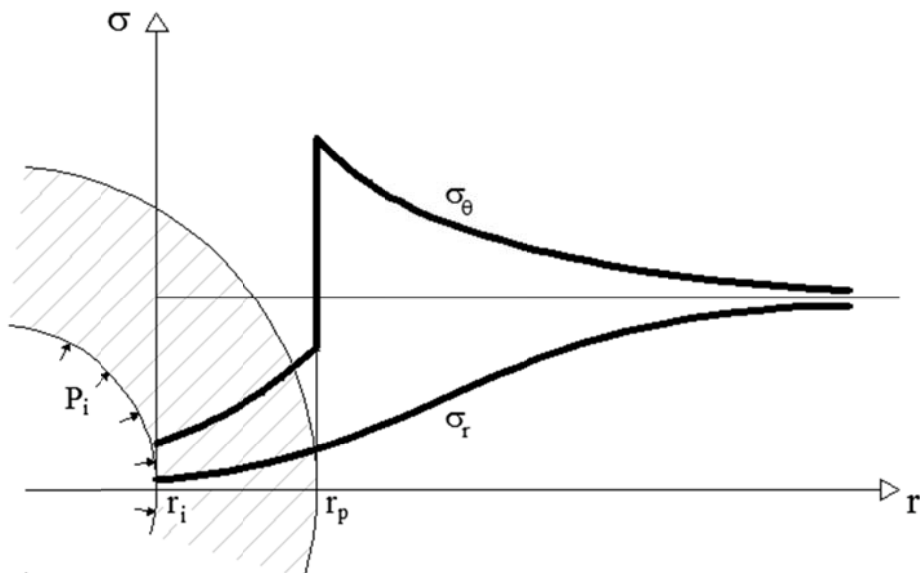


FIGURE 2-23 - DISTRIBUTION OF RADIAL AND TANGENTIAL STRESSES UNDER ISOTROPIC IN-SITU STRESS FIELD

In 1975, Daemen proposed a similar relation for the determination of the state of stress within the plastic zone. He replaced the boundary conditions introduced to solve the differential Equation 2-60 assuming a known extent of the plasticized zone. The reaction of the lining P_i is determined as follows:

$$P_i = \left(P_0 (1 - \sin \phi_p) - c_p \cos \phi_p + c_r \cot \phi_r \right) \left(\frac{r_i}{r_p} \right)^{2 \sin \phi_r / (1 - \sin \phi_r)} - c_r \cot \phi_r \quad (2-72)$$

Daemen in his analysis also included the contribution of the gravitational weight of the plasticized ring to the load applied to the containment system P_i :

$$\Delta P_i = \pm \gamma r_i \frac{1 - \sin \phi_r}{1 - 3 \sin \phi_r} \left[\left(\frac{r_i}{r_p} \right)^{2 \sin \phi_r / (1 - \sin \phi_r)} - 1 \right] \quad (2-73)$$

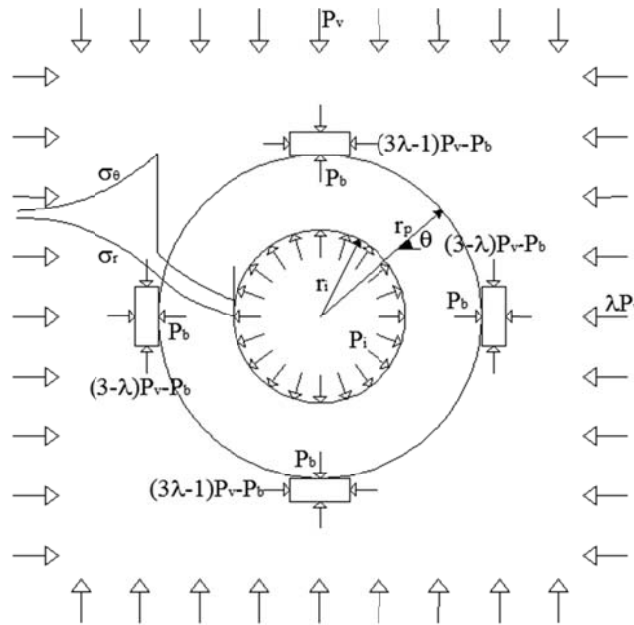


FIGURE 2-24- PROBLEM OF A PLASTICIZED CIRCULAR TUNNEL IN ANISOTROPIC STATE OF STRESS (SINGH, 2006)

Singh and Goel (2006) extended the approach suggested by Daemen to the case of anisotropic in-situ stress ($\lambda \neq 1$). Assuming a circular plastic zone for any original state of stress and using the relation 2-46, directly derived from Kirsch's Equations, to replace $2P_0$ in Equation 2-67, the formulation of the internal pressure P_i in horizontal ($\theta = 0^\circ$) and vertical directions ($\theta = 90^\circ$) becomes:

$$P_i = \left(\frac{P_v [(1 + \lambda) + 2(1 - \lambda) \cos 2\theta] - \frac{2c_p \cos \phi_p}{1 - \sin \phi_p} + c_r \cot \phi_r}{2(1 - \sin \phi_p)} \right) \left(\frac{r_i}{r_p} \right)^{2 \sin \phi_r / (1 - \sin \phi_r)} - c_r \cot \phi_r \quad (2-74)$$

which is coincident with the Daemen's approach when $\lambda = 1$.

Based on the experience gained in the study of tunnels in the north of India, Singh and Goel (2006) suggest the use of two different constitutive models, the Polyaxial Strength Criterion at peak condition that reduces to Mohr-Coulomb in residual state, in his theory of stress distribution. According to these hypotheses, the Equation 2-74 is transformed as:

$$P_i = \left(\frac{P_v [(1 + \lambda) + 2(1 - \lambda) \cos 2\theta] - \sigma_{cr} - AP_0 / 2}{2 + A/2} + c_r \cot \phi_r \right) \left(\frac{r_i}{r_p} \right)^{2 \sin \phi_r / (1 - \sin \phi_r)} - c_r \cot \phi_r \quad (2-75)$$

The generalized procedures presented above can be applied, making use of any failure criteria to most of the practical situations with only slight differences due to the different formulations.

Many other different approaches were suggested for the prediction of the plastic zone and determination of the plastic radius. The approach proposed by Duncan-Fama (1993), which uses the Mohr-Coulomb failure criterion, and that suggested by Carranza-Torres and Fairhurst (2000), which uses the Hoek-Brown failure criterion, are of great importance.

According to Duncan-Fama the pressure applied to the wall of the excavation P_i^{cr} below which the development of the plasticized zone is observed, can be expressed as:

$$P_i^{cr} = \frac{2P_0 - \sigma_{cr}}{N_\phi - 1} \quad (2-76)$$

where σ_{cr} is the UCS of the rock mass and $N_\phi = (1 + \sin \phi) / (1 - \sin \phi)$. The above formulation coincides with the relations 2-64 and 2-72 when the radius of the gallery is equal to the plastic radius ($r_i = r_p$).

If P_i is a pressure applied to the surface of the excavation lower than the critical pressure P_i^{cr} , the extension of the plastic radius of the associated plasticized region is expressed by the following relation:

$$r_p = r_i \left[\frac{2(\sigma_0 (N_\phi - 1) + \sigma_{cr})}{(N_\phi + 1)(N_\phi - 1)P_i + \sigma_{cr}} \right] \quad (2-77)$$

According to the approach suggested by Carranza-Torres and Fairhurst (2000) the internal critical pressure was defined as follows:

$$P_i^{cr} = \left[P_i^{cr} - \frac{s}{m_b} \right] m_b \sigma_{ci} \quad (2-78)$$

where P_i^{cr} is the scaled critical pressure, while m_b and s are parameters of the Hoek-Brown failure criterion. The extension of the plastic radius can be, instead, calculated with the following Equation:

$$r_p = r_i \cdot e^{\left[2 \left(\sqrt{P_i^{cr}} - \sqrt{P_i} \right) \right]} \quad (2-79)$$

p_i is the internal pressure applied and P_i is the relative scaled internal pressure. The scaled internal pressure can be expressed as follows:

$$P_i = \frac{p_i}{m_b \sigma_{ci}} + \frac{s}{m_b^2} \quad (2-80)$$

2.5 OBSERVATIONAL METHODS

The observational methods are based on the continuous monitoring of the deformations recorded on the surfaces of a geotechnical work, which are the basis for the analysis, interpretation and the potential revision of the initial design proposal. The major developments observed in recent years are in the excavation techniques with a widespread use of monitoring techniques which results in better understanding of the rock masses. .

Also with regard to the observational methods, great contribution to their development has been made by Karl Terzaghi that in the same period of the Rock Load System introduction, has given them the first organic treatment. In an unpublished introduction to the book "Theoretical Soil Mechanics" (1945) reported by Peck in 1969 he opposed a third way, the "experimental method", to the two most popular approaches in geotechnical engineering at that time, the abuse of (1) "wasteful" excessive factors of safety and the (2) "dangerous" practice of making rigid assumptions in accordance with general, average experience.

"[...] Soil Mechanics, as we understand it today, provides a third method which could be called the experimental method. The procedure is as follows: Base the design on whatever information can be secured. Make a detailed inventory of all the possible differences between reality and the assumptions. Then compute, on the basis of the original assumptions, various quantities that can be measured in the field. For instance, if assumptions have been made regarding pressure in the water beneath a structure, compute the pressure at various easily accessible points, measure it, and compare the results with the forecast. Or, if assumptions have been made regarding stress deformation properties, compute displacements, measure them, and make similar comparison. On the basis of the results of such measurements, gradually close the gap in knowledge and, if necessary, modify the design during construction.

Soil mechanics provides us with the knowledge required for practical application of this 'learn as you go' method [...]."

In 1945 were, therefore, already known the basic principles of the observational method, but its implementation was obstructed by the difficulty in determining the constitutive parameters of a rock mass and by the absence of appropriate technologies for the proper monitoring of the application of a design.

Peck (1969), through a revisitation of the introductory contribution of Terzaghi, set the basis for a reliable, repeatable, simple and relatively low cost approach. One of the big issues in the application of the observational methods is, in fact, the unjustified complexity and cost of their practical applications. For these reasons, in 1969, he formally defined all the steps that, in his opinion, are necessary for the satisfactory implementation of Observational Methods:

- a. Exploration sufficient to establish at least the general nature, pattern and properties of the deposits, but not necessarily in detail
- b. The assessment of the most probable conditions and the most unfavourable conceivable deviations from these conditions, in this assessment geology often plays a major role

- c. The establishment of the design based on a working hypothesis of behaviour anticipated under the most probably conditions
- d. The selection of quantities to be observed as construction proceeds and the calculation of their anticipated values on the basis of the working hypothesis
- e. The calculation of values of the same quantities under the most unfavourable conditions compatible with the available data concerning the subsurface conditions
- f. The selection in advance of a course of action or modification of design for every foreseeable significant deviation of the observational findings from those predicted on the basis of the working hypothesis
- g. The measurement of quantities to be observed and the evaluation of actual conditions
- h. The modification of design to suit actual conditions

In his considerations Peck emphasized the importance of the preliminary understanding of the rock mass conditions as fundament for the design project. The suggested analysis, however, is inapplicable in some cases, particularly with respect to the point (c) where the "hypothesis of behaviour anticipated under the conditions most probably" are mentioned. The knowledge of the rock mass characteristics is, instead, always affected by an unavoidable degree of uncertainty, even more so given the poor quality of the geological and geotechnical investigation techniques present in that period, which has a large impact on the usability and safety of the facilities installed. In the design phase, therefore, a moderately conservative safety factor is necessary and should be maintained, if not improved, during the whole evolution of the work, by means of technical interventions of improvement, the magnitude of which is suggested by the results of the observation.

The constantly increasing application observed in the last 30-40 years of the monitoring techniques in rock mechanics is closely linked to the development in tunneling of the "non-rigid" supports. Among these special containment systems can be listed as tunneling rods and bolts, deformable steel ribs, which allow a slow but controlled deformation of the rock mass with consequent partial dissipation of the state of stress generated in the vicinity of an excavation. In that context Rabcewicz developed the New Austrian Tunnelling method (NATM, 1964-5), which can be described as the applicative version of the approaches suggested by Terzaghi and Peck. This method has evolved considerably over the years and is, today, one of the most efficient approaches in rock mechanics. It cannot be exclusively included within the observational methods, but, due to the continued use of numerical computation for the real-time verification of the initial assumptions, can also be placed among the numerical methods.

Today, having shown great efficacy in minimization of the risk and cost reduction during the construction and maintenance of geotechnical works, the observational method has become an indispensable tool in engineering practice and research. Recently, in fact, the observational approaches have been included in the Eurocode 7 (UNI EN 1997-1:2005 and EN 1997-2:2007), the set of European rules for the geotechnical design, so their use has been officially disciplined for a consistent application in any geotechnical context.

2.6 NUMERICAL METHODS FOR UNDERGROUND OPENINGS

In rock mechanics, numerical methods are not part of the traditional methodology since they have been applied only recently. In soil and rock mechanics, unlike in mechanical and structural engineering, the use of numerical methods has long been hampered because of major difficulty in obtaining reliable constitutive relations describing the behavior of rock mass or soil. The numerical methods were not invented with the purpose of supplanting the other traditional methods, but to overcome some of their limitations. For this reason they can be only applied in combination with more traditional theories.

The extensive use of numerical methods in engineering is due to the simplicity and rapidity in solving cases that would otherwise require longer analysis. The resolution of analytical problems by numerical methods does not present any particular difficulty, only a high computational complexity, which has limited their practical application until the introduction of adequate computers and application software. Recently numerical software suites having specifically direct applications in soil and rock mechanics have been put on the market, allowing the generation and resolution of complex geo-mechanical models without particular experiences in programming and numerical analysis.

The advantages derived from the simplicity of use of the application software, as already indicated in the section of the analytical methods, can turn into significant limitations when the software is used by inexperienced users, who, in the event of erroneous results, would not be able to appreciate it. Moreover, because the rock mass is a particularly complex material, its behavior will follow many and as much complex laws. But, in the context of commercial software, it is not possible to implement such a large number of constitutive laws, whose compilation is often complex, for the resolution of specific cases. For this reason, the commercially available numerical suites incorporate only the most "traditional" constitutive laws which are widely applied in practice, giving, only in some cases, the possibility to accommodate one's own built-in constitutive models for special purposes.

The most common numerical approaches for solving geo-mechanical problems are based on the discretization of the entire domain (FEM, FDM) or on the discretization of the contour (BEM). The choice of a particular approach over another is, in a manner similar to what is seen for the different analytical approaches, usually suggested by the ratio between the size of the excavation and spacing of the rock joints of interest. These three approaches are particularly suitable when the discontinuities in the rock mass are not so frequent, such that the rock mass can be considered continuous (hard rock) or when the degree of fracturing is so high that the rock volume is comparable to a weaker equivalent continuum (weak rock). If, instead, the size of the blocks of rock observed in the volume is comparable to the size of the excavation, the determination of the possible movements of the blocks of rock are more important than the global conditions of the rock mass itself. Under these conditions, the discrete element method (DEM) is recommended.

Referring to these considerations Barton (1995) suggests choosing the most suitable numerical approach on the basis of Q value of the corresponding rock mass under examination. For values of Q smaller than 0.1 and larger than 100 FEM, FDM and BEM are preferable, while within the same range, the DEM is the more appropriate.

Here, all the different numerical approaches will not be explained in detail, as this would not be important in the development of this thesis. In Chapter 3, however, it will be explained as to how to modify the software FLAC, the two-dimensional explicit finite difference program for engineering mechanics computation, and a specific methodology for its refinement.

2.6.1 FINITE ELEMENTS METHODS (FEM)

FEM numerical method is probably the most applied method in soil and rock mechanics. The term Finite Elements, attributed to Clough (1960), but its first applications are dated back to the 50s. In principle, well in advance of the first application in rock mechanics, it was exhaustively used for the solution of practical problems in aerospace, mechanical and structural engineering.

In this approach, the continuum domain is discretized by means of reasonably small elements similar in shape (lines for one-dimensional domains, triangles and rectangles in two-dimensional domains, hexahedra and tetrahedra in those three-dimensional) with homogeneous physical characteristics, which share the corners (nodes) with the other components of the medium.

Its large development is primarily due to the simplicity of use and the ability to overcome the limits of traditional Finite Differences Methods in dealing with complex geometries and boundary singularities.

2.6.2 FINITE DIFFERENCES METHODS (FDM)

The finite differences method is one of the oldest numerical approaches. The first practical implementation is attributed to Runge (1908) that applied the finite differences to solve the partial differential equation of Saint-Venant's torsion problem (Higgins, 1943). The finite differences methods do not have a long tradition in soil and rock mechanics and only with the commercial introduction in 1996 of the software FLAC a valid alternative to the several finite elements analysis software has arrived. The software code FLAC, since the initial version introduced by Cundall and Board (1988), performs an explicit solution, which, in contrast to what happens in the FEM, does not need to allocate extra space for the stiffness matrix with great reduction in complexity and computational time.

Using the FDM, the domain is divided by ordered connected sets of discrete points (nodes). It needs of a resolving grid quite homogeneous to be properly implemented, then, there are difficulties in refining the grid just in the presence of local singularities or in representing complex boundaries. Significant improvements in this respect are observed by using irregular triangular meshes or Voronoi grid systems (Jing and Hudson, 2002).

2.6.3 BOUNDARY ELEMENTS METHODS (BEM)

In the Boundary Elements Methods, only boundaries are discretized, which imply that if the domain extends to infinity, the external artificial boundaries are not required. The presence of an artificial boundary is, instead, fundamental in FEM and FDM to control the computational complexity of a physical model. The use of the BEM is particularly advantageous when the ratio of volume / surface of the domain is very large (Katsikadelis, 2002). In addition, the model complexity increases in presence of non-homogeneous domains because at each change of material the discretization of the separation surface is required.

In BEM, unlike to what happens in FEM and FDM, the solution is approximated to the boundary of the involved domain allowing reducing the order of a problem; a three dimensional problem therefore becomes two-dimensional and two-dimensional becomes one-dimensional.

2.6.4 DISCRETE ELEMENTS METHODS (DEM)

This method was specifically developed for the determination of local and global motion of a large number of distinct elements subjected to external modification of their initial equilibrium.

The Discrete Elements Methods are often confused with the Distinct Elements Method introduced by Cundall (1971) and subsequently formalized by Cundall and Hart (1992), which is just a DEM developed for the quantification of rock blocks movements in close proximity to an excavation. The Distinct Elements Method was subsequently extended, in accordance to the studies promoted by Munjiza (2004), to many different industrial applications as pharmaceutical tableting, flow simulations and impact analysis in combination with the FEM.

2.6.5 HYBRID METHODS

The hybrid methods allow managing more complex geo-mechanical problems by combining the qualities of two different traditional numerical methods but using only one resolving code. The most common hybrid codes combine FEM or FDM, which are appropriate to manage the zones close to an excavation or a singularity, with BEM, to describe the more distant regions from them (Beer and Watson, 1992; Carter and Xiao, 1993). Phase, the commercial software distributed by Rocscience, follows this hybrid scheme.

Very common are also hybrid methods FEM / DEM (see next paragraph) or FDM / FEM (Itasca Flac that, only in specific contexts, implements the finite elements).

2.6.6 RECENT IMPROVEMENTS IN NUMERICAL METHODS IN ROCK MECHANICS

The refinement of the numerical techniques of representation and resolution has achieved accuracy absolutely unimaginable just 50 years ago. By means of specific numerical analysis, it is possible to study both local and global behavior of a fractured rock mass.

Several authors have, in fact, numerically simulated various geotechnical tests on intact and fractured rocks with the aim to investigate the origin and evolution of plasticity in order to extend the knowledge acquired in the underground real cases.

Stefanizzi (2007) by means of ELFEN (Rockfield Software, 2006) numerical finite / discrete elements software numerically simulated deformations and failure of standard homogeneous rocks in different laboratory tests (Brazilian, uniaxial and triaxial compressive tests). In their analysis, the behaviour of the intact rock is described by means of FEM until the rock fails while, at the opening of cracks, they are modeled by means of DEM. The possibility of correctly investigating formation and development of fracturing in a rock mass by means of numerical approaches is confirmed by studies of Munjiza (2004) who has positively compared the result of FEM / DEM mixed models with numerous laboratory triaxial tests on homogeneous rocks and those by Liyanapathirana et al (2005) who focused their research on the numerical behavior of anisotropic structured soils (sedimentary and residual soils).

2.7 REFERENCES

- [1] Abad J., Caleda B., Chacon E., Gutierrez V. and Hidalgo E. (1984). Application of Geomechanical Classification to Predict the Convergence of Coal Mine Galleries and to Design their Supports. 5th Int. Congr. Rock Mech., Melbourne, pp. 15-19.
- [2] A. M. Al-Ajmi and R. W. Zimmerman, (2005). Relation between the Mogi and the Coulomb failure criteria. Int. J. Rock Mech., vol. 42, pp. 431-39.
- [3] Barla, G. (1995). Squeezing rocks in tunnels. ISRM News Journal, 2(3&4), 44-49.
- [4] Barton, N.R.; Lien, R.; Lunde, J. (1974). "Engineering classification of rock masses for the design of tunnel support". Rock Mechanics and Rock Engineering (Springer) **6** (4): 189–236. doi:10.1007/BF01239496.
- [5] Barton, N.R. (1-5 November 1976). "Recent experiences with the Q-system of tunnel support design". In Bieniawski, Z.T.. Proc. Symposium on Exploration for Rock Engineering, Johannesburg. **1**. Balkema, Cape Town. pp. 107-117. ISBN 0-86961-089-9.
- [6] Barton, N.R.; Lien, R.; Lunde, J. (1977). "Estimation of support requirements for underground excavations & discussion". In Fairhurst, C.; Crouch, S.L.. Proc. of 16th Symp. on Design Methods in Rock Mechanics, University of Minnesota, Minneapolis, U. S. A, 1975. American Society of Civil Engineers (ASCE), New York. pp. 163–177, 234–241. OL19853458M.
- [7] Barton, N.R. (1988). "Rock Mass Classification and Tunnel Reinforcement Selection using the Q-system". In Kirkaldie, L.. Rock Classification Systems for Engineering Purposes: ASTM Special Technical Publication 984. 1. ASTM International. pp. 59-88. doi:10.1520/STP48464S. ISBN 978-0-8031-0988-9.
- [8] Barton, N.R.; Grimstad, E. (1993). "Updating the Q-system for NMT". In Kompen, C.; Berg, S.L.. Proc. of the International Symposium on Sprayed Concrete - Modern Use of Wet Mix Sprayed Concrete for Underground Support, Fagernes, 1993. Norwegian Concrete Association, Oslo. pp. 163–177, 234–241. OL19853458M.

- [9] Barton, N.R.; Grimstad, E. (1994). "The Q-system following twenty years of application in NMT support selection; 43rd Geomechanics Colloquy, Salzburg". Felsbau (Verlag Glückauf GmbH, Essen, Germany): 428–436. ISSN 1866-0134.
- [10] Barton, N.R. (2000). *TBM Tunnelling in Jointed and Faulted Rock*. Taylor & Francis. p. 184. ISBN 978-90-5809-341-7.
- [11] Barton, N.R. (2002). "Some new Q-value correlations to assist in site characterization and tunnel design". *International Journal of Rock Mechanics and Mining Sciences* 39 (2): 185–216. doi:10.1016/S1365-1609(02)00011-4.
- [12] Barton, N.R. (2006). *Rock Quality, Seismic Velocity, Attenuation and Anisotropy*. Taylor & Francis. p. 729. ISBN 978-0-415-39441-3.
- [13] Beer, G. and Watson, J.O. (1992), *Introduction to Finite and Boundary Element Methods for Engineers*, John Wiley & Sons, New York.
- [14] Bieniawski, Z. T. (1976). Z. T. Bieniawski. ed. "Rock mass classification in rock engineering". *Proc. Symposium on Exploration for Rock Engineering* (Balkema, Cape Town): 97–106.
- [15] Bieniawski, Z.T. "Engineering Rock Mass Classifications", John Wiley and Sons, New York, 1989.
- [16] Carranza-Torres C. and Fairhurst C. (2000) "Application of the convergence-confinement method of tunnel design to rock-masses that satisfy the Hoek-Brown failure criterion". *Tunnelling and Underground Space Technology* 15(2), 187–213.
- [17] Cameron-Clarke I. S. and Budavari S. (1981). Correlation of Rock Mass Classification Parameters Obtained from Borecore and In-Situ Observations. *Engng Geol.* 17, 19-53.
- [18] Carter, J.P. and Xiao, B. (1993) "Coupled Finite Element and Boundary Element Method for the Analysis of Anisotropic Rock Masses", *Proc. International Symposium on Application of Computer Methods in Rock Mechanics and Engineering*, Xian, China, Vol. 1, pp. 249-258.
- [19] Clough, R. W., "The Finite Element Method in Plane Stress Analysis", *Proc. 2nd ASCE Conf. On Electronic Computation*, Pittsburg, Pa. Sept. 1960.
- [20] P. A. Cundall, "A Computer Model for Simulating Progressive Large Scale Movements in Blocky Rock Systems", in *Proceedings of the Symposium of the International Society of Rock Mechanics*, Nancy, France, 1(1971), paper No. II-8.
- [21] P. A. Cundall and R. D. Hart, "Numerical Modelling of Discontinua", *Engineering Computations*, 9(1992), pp. 101–113.
- [22] Daemen, JJK, 1975, *Tunnel Support Loading Caused by Rock Failure*, Ph.D. Thesis, University of Minnesota. Detournay, E., 1982 .
- [23] Deere, D U (1964). "Technical description of rock cores", *Rock Mechanics Engineering Geology*, 1 (16-22).
- [24] Deere, D U (1989). "Rock quality designation (RQD) after twenty years", U.S. Army Corps of Engineers Contract Report GL-89-1, Waterways Experiment Station, Vicksburg, MS (67).
- [25] Deere, D U & Deere, D W (1988), "The RQD index in practice", *Proc. Symp. Rock Class. Engineering Purposes*, ASTM Special Technical Publications 984, Philadelphia, (91-101).
- [26] Deere, D U (1964). "Technical description of rock cores", *Rock Mechanics Engineering Geology*, 1 (16-22).
- [27] Deere, D U (1989). "Rock quality designation (RQD) after twenty years", U.S. Army Corps of Engineers Contract Report GL-89-1, Waterways Experiment Station, Vicksburg, MS (67).
- [28] Deere, D U & Deere, D W (1988), "The RQD index in practice", *Proc. Symp. Rock Class. Engineering Purposes*, ASTM Special Technical Publications 984, Philadelphia, (91-101).
- [29] Deere, D U, Hendron, A J, Patton, F D & Cording, E J (1967). "Design of surface and near surface constructions in rock", *Proc. 8th U.S. Symp. Rock Mechanics*, ed. Fairhurst, publ. AIME, New York, (237-302).

- [30] Drucker, D. C. and Prager, W. (1952). Soil mechanics and plastic analysis for limit design. *Quarterly of Applied Mathematics*, vol. 10, no. 2, pp. 157–165.
- [31] Dube, A. K. and Singh, B. (1986). Study of squeezing pressure phenomena in a tunnel – Part I and II. *Tunnelling and Underground Space Technology*, 1(1), 35-39 (Part I), 41-48 (Part II).
- [32] Duncan Fama, M. E. 1993. Numerical modelling of yield zones in weak rocks. In: Hudson, J. A. (ed.), *Comprehensive Rock Engineering*, Pergamon Press, Oxford, Vol 2, pp 49-75.
- [33] Goel, R. K., Jethwa, J.L. and Paithankar, A.G. (1995). Correlation between Barton's Q and Bieniawski's RMR - A New Approach, *Int. J. Rock Mech. Min. Sci. & Geomech. Abstract, Technical Note*, Vol. 33, No. 2, pp. 179-181, UK.
- [34] Goguel, *Réflexions sur l'isostasie* (1947)
- [35] Grimstad, E., Barton, N. & Løset, F. 1993. Rock mass classification and NMT support design using a new Q-system chart. *World Tunnelling*, September 1993.
- [36] Grimstad, E. & Barton, N. 1993. Updating of the Q-System for NMT. *Proceedings of the International Symposium on Sprayed Concrete - Modern Use of Wet Mix Sprayed Concrete for Underground Support*, Fagernes, 1993, (Eds Kompen, Opsahl and Berg. Norwegian Concrete Association, Oslo.
- [37] Higgins, T. J. (1943). The Approximate Mathematical Methods of Applied Physics as Exemplified by Application to Saint-Venant's Torsion Problem, *J. Appl. Phys.* 14, 469-480.
- [38] Hoek E. and Brown E.T. (1980). *Underground Excavations in Rock*. London: Institution of Mining and Metallurgy.
- [39] Hoek E. and Brown E.T. (1980). "Empirical strength criterion for rock masses". *J. Geotechnical Engineering Division ASCE*: 1013–1025.
- [40] Hoek, E. and Brown (1988). "The Hoek-Brown failure criterion - a 1988 update". *Proc. 15th Canadian Rock Mech. Symp.*: 31–38.
- [41] Hoek, E. and Marinos, P. 2000 Predicting Tunnel Squeezing. *Tunnels and Tunnelling International*. Part 1 – November 2000, Part 2 – December, 2000.
- [42] Hoek E, Carranza-Torres CT, Corkum B (2002). "Hoek-Brown failure criterion-2002 edition". *Proceedings of the fifth North American rock mechanics symposium* 1: 267–273.
- [43] L. Jing and J. A. Hudson, "Numerical Methods in Rock Mechanics", *International Journal of Rock Mechanics and Mining Sciences*, 39(2002), pp. 409–427.
- [44] John T. Katsikadelis, "Boundary Elements Theory and Applications", Elsevier, Oxford, 2002
- [45] Kirsch, 1898, *Die Theorie der Elastizität und die Bedürfnisse der Festigkeitslehre*. *Zeitschrift des Vereines deutscher Ingenieure*, 42, 797–807.
- [46] Liyanapathirana, D.S., Carter, J.P. and Airey, D.W. (2005), "Nonhomogeneous behaviour of structured soils in triaxial tests." *International Journal of Geomechanics*, ASCE, Vol. 5, No. 1, pp. 10-23.
- [47] Mogi, K., 1967. Effect of the intermediate principal stress on rock failure. *J Geophys Res*, 72, 5117-5131.
- [48] Mogi, K., 1971a. Effect of the triaxial stress system on the failure of dolomite and limestone. *Tectonophysics*, 11[11], 111-127.
- [49] Mogi, K., 1971b. Fracture and flow of rocks under high triaxial compression. *J Geophys Res*, 76[5], 1255-1269.
- [50] Moreno Tallon E. (1980). *Aplicación de las Clasificaciones Geomecánicas a los Túneles de Pajares*. II Curso de Sostenedimientos Activos en Galerías y Túneles. Fundación Gomez-Parto, Madrid.
- [51] Ante Munjiza, *The Combined Finite-Discrete Element Method* Wiley, 2004, ISBN 0-470-84199-0
- [52] Nadai, A. (1950). *Theory of flow and fracture of solids*, McGraw-Hill.
- [53] Peck, R. B. (1969). "Advantages and limitations of the observational method in applied soil mechanics." *Geotechnique*, 19, 171-187.

- [54] Rabcewicz, L. V. (1964). "The new Austrian tunneling method". *Water Power*, 16(11), 453-457.
- [55] Rabcewicz, L. V. and Golser, J. (1973). Principles of dimensioning the supporting system for the new Austrian tunneling method. *Water Power*, 25(3), 83.
- [56] Ribacchi R., 1986. *Stato di sforzo e deformazione intorno ad una galleria. "La statica delle gallerie in roccia"*. L'Ingegnere A.N.I.A.I., Numero Unico
- [57] Rutledge J. C. and Preston R. L. (1978). Experience with Engineering Classifications of Rock. *Proc. Int. Tunnelling Syrup.*, Tokyo, pp. A3.1-A3.7.
- [58] Serafim J.L., Pereira J.P. (1983) Considerations on the geomechanical classification of Bieniawski. *Proc. Int. Symp on Eng. Geol. and Underground Construction*, vol. I (II), Lisbon, Portugal, 1983, 33-44.
- [59] Singh, Bhawani, Goel, R. K., Mehrotra, V. K., Garg, S. K., and Allu, A.R. (1998). Effect of Intermediate Stress on Strength of Anisotropic Rock Mass, *Tunnelling and Underground Space Technology*, USA, Vol. 13, No. 1, pp. 71-79.
- [60] Singh, B.; Goel, R.K. (1999). *Rock Mass Classification: A Practical Approach in Civil Engineering*. Elsevier Science. p. 282. ISBN 978-0-08-043013-3.
- [61] Singh, B.; Goel, R.K. (2006). *Tunnelling in Weak Rocks. Geo-Engineering. 5*. Elsevier Science. p. 512. ISBN 978-0-08-044987-6.
- [62] Stefanizzi, S. 2007. Numerical modelling of strain-driven fractures around tunnels in layered rock masses. *Politecnico di Torino, Torino*, p. 166.
- [63] Stille, H. 1986. Experiences of design of large caverns in Sweden. *Proc. International Symposium in large rock caverns. ISRM, Helsinki, CI.20*, pp. 231-241.
- [64] Terzaghi, K., *Theoretical Soil Mechanics*, John Wiley and Sons, New York (1943) ISBN 0-471-85305-4.
- [65] Terzaghi, K., Proctor, R. V. and White, T. L., "Rock Tunneling with Steel Supports," *Commercial Shearing and Stamping Co.* (1946).
- [66] Terzaghi, K., *From theory to practice in soil mechanics;: Selections from the writings of Karl Terzaghi, with bibliography and contributions on his life and achievements* John Wiley and Sons (1967).
- [67] Terzaghi, K., Peck, R. B. and Mesri, G., *Soil Mechanics in Engineering Practice*, 3rd Ed. Wiley-Interscience (1996) ISBN 0-471-08658-4.
- [68] Terzaghi, K., *American Society of Civil Engineers, "Terzaghi Lectures, 1974-1982," American Society of Civil Engineers* (1986) ISBN 0-87262-532-X.
- [69] Wang, R and Kemeny, J. M. (1995). A new empirical failure criterion under Polyaxial compressive stresses. *Rock Mechanics: Proc. 35th U. S. Symposium*, Reprinted from: Eds: J.J.K. Daemen and R.A. Schultz, Lake Tahoe, 4-7 June 1995, 950.

Chapter 3

3 POLYAXIAL STRESS ANALYSIS OF UNDERGROUND OPENINGS USING FLAC[®]

D. Scussel^{a*}, S. Chandra^b

^a *School of Civil Engineering, Surveying and Construction, University of KwaZulu Natal, Durban, South Africa*

^b *Department of Civil Engineering, Indian Institute of Technology, Kanpur 208 016, India*

Keywords: Tunnel Excavation, Polyaxial Strength Criterion, FLAC, Strain Softening, FDM, Finite Difference Analysis.

3.1 ABSTRACT

The traditional design methodologies for tunnel and underground excavations are divided in to three categories: **Empirical approaches**, **Analytical approaches**, and **Observational approaches**, whereas in the last years the **Numerical approach** has strongly become popular both for the intrinsic simplicity of the software packages and their ability to manage problems unsolvable with the classic methods.

In this paper, the underground openings have been analyzed using constitutive models other than the Mohr-Coulomb theory. FLAC is used for the analysis and the software has been implemented to include the Polyaxial Strength Criterion. The details of the modifications made in the software are presented and the results are compared with the Singh's elasto-plastic stress distribution in squeezing grounds. This study will develop better comprehension of the behavior of the underground openings and also provide a useful tool to the designers in the planning stages.

3.2 INTRODUCTION

Many constitutive models have been developed to describe the behavior of a rock mass after modification of its equilibrium. In severe conditions none of these, however, has demonstrated sufficient correlation to the effective measured reactions. In fact, several experiences of back analysis in tunnels excavation (Jethwa, 1981), when compared to the results of the more applied designing procedures, have shown a marked tendency to overestimate the squeezing¹ of the rock masses.

To meet the needs of a more suitable theory for squeezing conditions, Wang and Kemeny (1995) performed several tests on anisotropic tuff to advance the hypothesis that the intermediate principal stress in an anisotropic rock mass under a polyaxial stress field could influences its behavior.

* Corresponding autor. Tel.: +27 (0)31 260 1077; fax: +27 (0)31 260 1411.
Email address: scussel@ukzn.ac.za (D. Scussel).

¹ According to the International Society for Rock Mechanics (ISRM), the definition of Squeezing:
"Squeezing of rock is the time dependent large deformation which occurs around the tunnel and is essentially associated with the creep cause by exceeding a limit shear stress" Barla (1995)

Rock mass in the vicinity of an underground excavation is a clear example of a medium subjected to a polyaxial stress field: σ_3 is very small or equal to zero, σ_2 is close to the in situ vertical stress (for deep tunnels) and σ_1 could be double the intermediate principal stress. Moving away in the radial direction, the difference between maximum and minimum stress is less appreciable.

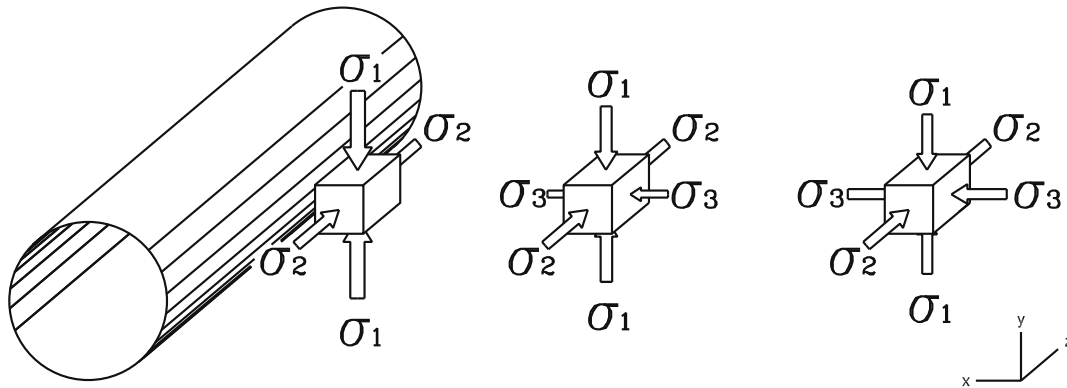


FIGURE 3-1 – TYPICAL STRESS DISTRIBUTION AROUND AN UNDERGROUND OPENING

The classical strength theory assumes that only minor and major principal stresses influence the stability of the rock surrounding the excavation. However, in practical situations, the consideration of intermediate principal stress results in enhancement of strength. This can be explained by the significant work done by the intermediate principal stress component along the tunnel direction that compresses wedges of rock, increasing their global resistance and preventing rock falls.

3.3 ELASTO-PLASTIC THEORY OF STRESS DISTRIBUTION IN BROKEN ZONE USING POLYAXIAL STRENGTH CRITERION IN SQUEEZING GROUND CONDITIONS

Singh, et. al. (1998) investigated the effects of the intermediate principal stress on the strength of anisotropic rock mass, and proposed to modify the Mohr-Coulomb criterion by replacing σ_3 with the average value of σ_2 and σ_3 . The Polyaxial Strength Criterion based on semi-empirical approach has shown better correlation between analytical results and observations. The criterion suggested by them is given below:

$$\sigma_1 - \sigma_3 = \sigma_{cr} + \left(\frac{\sigma_2 + \sigma_3}{2} \right) \frac{2 \sin \varphi}{1 - \sin \varphi} \quad (3-1)$$

Starting from Equation 3-1, they formulated an elasto-plastic theory of stress distribution in broken zone in squeezing ground.

Initial hypothesis can be summarized as follows:

- Rock mass is isotropic, homogeneous and dry;
- Rock mass follows the Polyaxial Strength Criterion in the elastic zone, whereas the Mohr-Coulomb's theory inside the broken zone
- Circular tunnel of radius r_i is uniformly supported, and circular broken zone is of radius r_p
- There is no rock burst or brittle failure.

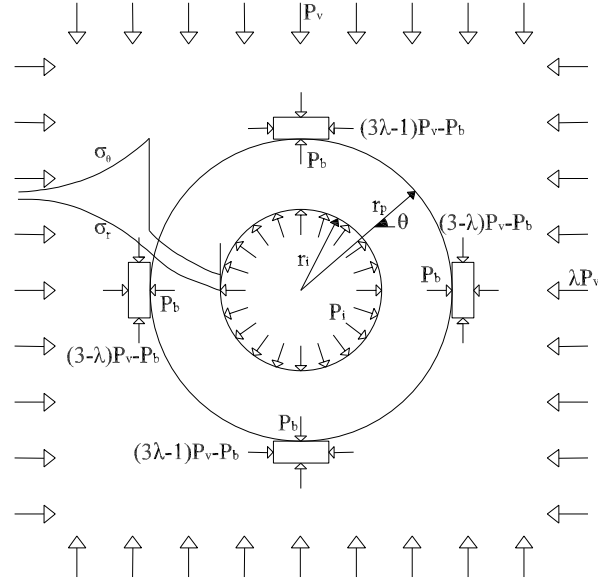


FIGURE 3-2 - SCHEMATIC BOUNDARY CONDITIONS OF THE PROBLEM

Stress distribution within the broken zone is given as:

$$\sigma_r = \left(P_b + \frac{q_{cr}}{\alpha} + \frac{\gamma}{1-\alpha} \right) \left(\frac{r}{r_p} \right)^\alpha - \frac{q_{cr}}{\alpha} \quad (3-2)$$

$$\sigma_\theta = q_{cr} + (1+\alpha)\sigma_r \quad (3-2)$$

Squeezing Pressure at the lining in the vertical direction ($\theta = 90^\circ$):

$$P_v = \left(P_b + \frac{q_{cr}}{\alpha} + \frac{\gamma}{1-\alpha} r_p \right) \left(\frac{r_i}{r_p} \right)^\alpha - \frac{q_{cr}}{\alpha} - \frac{\gamma}{1-\alpha} r_i \quad (3-4)$$

and in the horizontal direction ($\theta = 0^\circ$):

$$P_h = \left(P_b + \frac{q_{cr}}{\alpha} \right) \left(\frac{r_i}{r_p} \right)^\alpha - \frac{q_{cr}}{\alpha} \quad (3-5)$$

where
$$P_b = P_v \frac{((1+\lambda) + 2(1-\lambda)\cos 2\theta) - q_{mass} - \sigma_z A/2}{2 + A/2}$$

Squeezing pressure at the lining for hydrostatical initial stress and negligible effect of rock mass weight is:

$$P_i = \left(\frac{2P_v - q_{mass} - \sigma_z A/2}{2 + A/2} + \frac{q_{cr}}{\alpha} \right) \left(\frac{r_i}{r_p} \right)^\alpha - \frac{q_{cr}}{\alpha} \quad (3-6)$$

where $A = \frac{2 \sin \varphi_p}{1 - \sin \varphi_p}$, $\alpha = \frac{2 \sin \varphi_r}{1 - \sin \varphi_r}$, $q_{mass} = 7\gamma Q^{1/3}$, $q_{cr} = \frac{2c_r \cos \varphi_r}{1 - \sin \varphi_r}$

3.4 NUMERICAL ANALYSIS

3.4.1 STATEMENT OF THE PROBLEM

The introduction of several engineering numerical analysis suites (FEM, FDM, BEM, DEM) has changed the approach to excavation problems. Now, it is possible to carry out a more detailed analysis considering complexities such as the influence of new parameters, particular geometries and boundaries shapes, introducing new excavation technique or considering the complex rock mass-liner interaction. Many very powerful codes have been developed for different constitutive models and are available for the analysis of geo-mechanical problems, but none of them consider the effect of the intermediate principal stress in the evaluation of plasticity.

The scope of this work is to include the Polyaxial Strength Criterion among the more common constitutive model codes for FLAC and make it available for practical tunnel design. FLAC (Itasca) is a two-dimensional explicit finite difference program for solving many computational problems of geotechnical engineering and rock mechanics.

In this study FLAC has been chosen for implementing a user-defined constitutive model, which is not present in this software and also in any other standard software. The model has been compiled in FISH, the built in program language. The inclusion of this feature in this software makes it ideal software for many practical studies of underground openings.

3.4.2 MODIFICATIONS TO IMPLEMENT THE POLYAXIAL CONSTITUTIVE MODEL

To develop a FISH code to incorporate the Polyaxial Strength Criterion, it is important to redefine the constitutive model's formulation consistent with the sign convention in FLAC. Starting with this, compression is taken as negative and the ordering of the principal stresses is $\sigma_1 < \sigma_2 < \sigma_3$ as in structural engineering.

To avoid misunderstanding, when the data requested for the execution of the model are inserted by not an expert user, the variable needed are always positive in sign. This obviously affects the formulation of the constitutive model because, in such a reference system, Cohesion and Uniaxial Compressive Strength would be negatives.

Incorporating these, Mohr-Coulomb Theory and Polyaxial Strength Criterion will take the form given as:

$$\text{Mohr-Coulomb} \quad \sigma_1 - N_\varphi \sigma_3 + \sigma_{cr} = 0 \quad (3-7)$$

$$\text{Polyaxial:} \quad \sigma_1 - \sigma_3 + \sigma_{cr} - \left(\frac{\sigma_2 + \sigma_3}{2} \right) A = 0 \quad (3-8)$$

Other necessary step is to reformulate the Polyaxial Strength Criterion to make it similar to the Mohr-Coulomb formulation, as suggested below:

$$\sigma_1 - \sigma_3 N'_\phi + \sigma'_{cr} = 0 \quad (3-9)$$

Where σ_{cr} is the Compressive strength of the rock mass at the internal boundary of a tunnel

$$\sigma'_{cr} = \sigma_{cr} - \frac{\sigma_2}{2} A = 0$$

and, where
$$N_\phi = \frac{1 + \sin \phi}{1 - \sin \phi} \quad N'_\phi = \frac{1}{1 - \sin \phi}$$

The Polyaxial Strength Criterion as given by Equation 3-9 is shown in a graphical form in Figure 3-3. The similarity with the Mohr-Coulomb criterion is quite evident. However, this criterion incorporates the intermediate principal stress, which is not incorporated in Mohr-Coulomb criterion. Therefore, the parameters N'_ϕ and σ'_{cr} are different from the corresponding N_ϕ and σ_{cr} . It is appropriate to highlight that the intermediate principal stress required to be evaluated only in elastic condition and is automatically computed by FLAC.

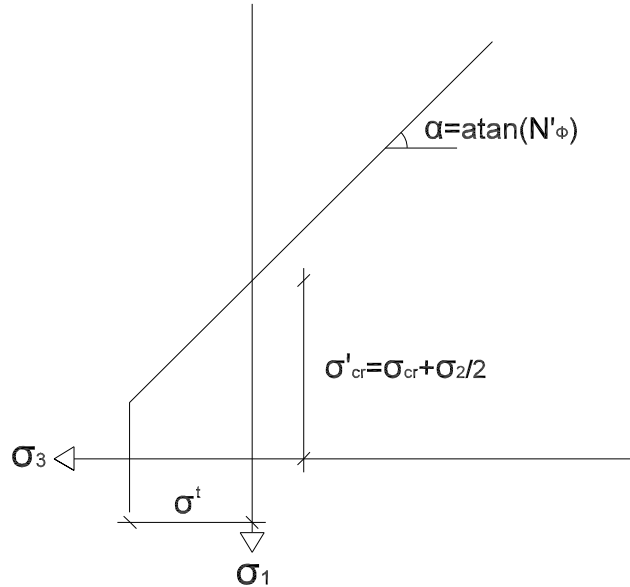


FIGURE 3-3 - GRAPHICAL POLYAXIAL STRENGTH CRITERION

In order to have a three dimensional constitutive model in elastic zone and a bi-dimensional model after it fails, in the analysis, a new approach is suggested in this paper. A new relationship based on the similarity between equations 3-7 and 3-9, is proposed below:

$$\sigma_1 - \sigma_3 \left(\frac{1 + \sin \alpha}{1 - \sin \phi} \right) + \sigma_{cr} - \sigma_2 \frac{\sin \beta}{1 - \sin \phi} = 0 \quad (3-10)$$

The advantage of the above Equation is that it can handle both elastic zone and plastic zone by appropriately choosing the parameters. The values of the parameters α , β , ϕ and σ_{cr} to be used are given in Table 3-1. Substituting the corresponding values for peak and residual state in Equation 3-10 results:

	Peak	Residual
ϕ	ϕ_p	ϕ_r
α	0	ϕ_r
β	ϕ_p	0
σ_{cr}	$7\gamma Q^{1/3}$ or $\frac{2c_p \cos \phi_p}{1 - \sin \phi_p}$	$\frac{2c_r \cos \phi_r}{1 - \sin \phi_r}$

TABLE 3-1 - VALUES PROPOSED FOR PEAK AND RESIDUAL STATE

Substituting in Equation 3-10 the peak and residuals values results in:

$$\sigma_1 - \sigma_3 \left(\frac{1}{1 - \sin \phi_p} \right) + 7\gamma Q^{1/3} - \sigma_2 \frac{\sin \phi_p}{1 - \sin \phi_p} = 0 \quad (3-11)$$

and

$$\sigma_1 - \sigma_3 \left(\frac{1 + \sin \phi_r}{1 - \sin \phi_r} \right) + \frac{2 \cos \phi_r}{1 - \sin \phi_r} = 0 \quad (3-12)$$

In this formulation the value of UCS is directly put as a parameter. The advantage of inputting the value directly is that it can be modified in the formulation without changing the FISH code every time. This way, the problem can be solved using the peak and residual parameters that could describe the behavior of an elastic rock mass and transform the formulation of the failure criteria at plasticity.

3.4.3 SOLUTION SCHEME

In each step to compute the stresses, these are evaluated, transformed in principal stresses and ordered.

FLAC chooses a guess elastic strain increment and calculates the corresponding stress increments applying the Hooke's law. The incremental stresses are given below:

$$\begin{cases} \Delta \sigma_1 = \alpha_1 \Delta e_1^e + \alpha_2 (\Delta e_2^e + \Delta e_3^e) \\ \Delta \sigma_2 = \alpha_1 \Delta e_2^e + \alpha_2 (\Delta e_1^e + \Delta e_3^e) \\ \Delta \sigma_3 = \alpha_1 \Delta e_3^e + \alpha_2 (\Delta e_1^e + \Delta e_2^e) \end{cases} \quad (3-13)$$

After this step, it is evaluated whether the new three components violate the yield criterion given by equations 3-14, representing the equation 3-11, and 3-15, representing the tension cut, for shear or tension.

$$\text{Shear Yield Function} \quad f_s = \sigma_1 - N'_\phi \sigma_3 + \sigma'_{cr} \quad (3-14)$$

$$\text{Tension Yield Function} \quad f_t = \sigma^t - \sigma_3 \quad (3-15)$$

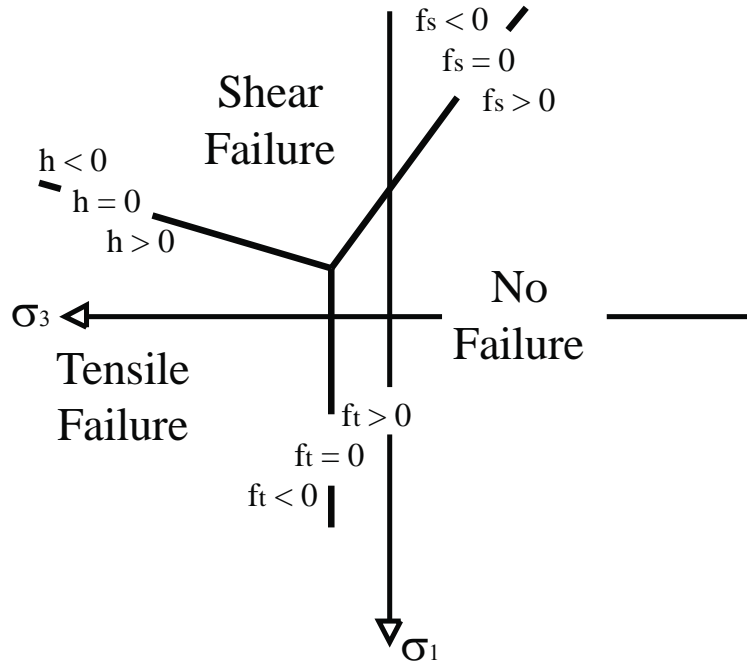


FIGURE 3-4 - DOMAINS FOR A SPECIFIC σ_2 VALUE

The equation for the bisector of the angle originated by the tension and the shear yield function is given as:

$$h(\sigma_1, \sigma_2, \sigma_3) = \sigma_3 - \sigma^t - \alpha^p (\sigma_1 - \sigma^p) \quad (3-16)$$

where

$$\sigma^p = N'_\varphi + \sqrt{1 + (N'_\varphi)^2} \quad \text{and} \quad \alpha^p = N'_\varphi \sigma^t - \sigma'_{cr}$$

Equations 3-14, 3-15 and 3-16 are shown in a graphical form in Figure 3-4 in a two dimensional plot between σ_1 and σ_3 for a particular value of σ_2 . A three dimensional plot is actually needed to represent the zones of failure or no failure but for the sake of simplicity a two dimensional plot is shown. By locating a stress point on this Figure one can make out in which zone it lies. If the sign of f_s and h are negative, shear failure takes place, when h is positive and f_t negative, tensile failure takes place and no failure when both h and f_s are positive.

The violation of the yield criterion means that FLAC calculated a point beyond the yield function and plastic deformation takes place ($e^p > 0$). A correction is needed to move it back to the yield boundary (the guess elastic strain increment was not elastic).

The treatment of the tensile failure is the same as in Mohr-Coulomb constitutive model in FLAC. Therefore only shear failure correction is applied in the present study.

Starting from the flow rule's formulation given as:

$$\Delta e_i^p = \lambda^s \frac{\partial g_s}{\partial \sigma_i} \quad (3-17)$$

$$g_s = \sigma_1 - N_\psi \sigma_3 \quad (3-18)$$

Where g_s is the Shear potential function and λ^s as unknown. In this function σ_2 is absent because, although not constant in the entire domain, it is a constant value for a particular zone. The elastic guess increments in the three directions are given as:

$$\begin{cases} \Delta e_1^p = \lambda^s \\ \Delta e_2^p = 0 \\ \Delta e_3^p = -N_\psi \lambda^s \end{cases} \quad (3-19)$$

where
$$N_\psi = \frac{1 + \sin \psi}{1 - \sin \psi}$$

The total increment applied at the beginning must be separated from its plastic part, which is calculated with the flow rule (Equation 3-17) and then substituted in Equation 3-21 that gives the value of elastic strain in the incremental expression of the Hooke's law to be used for computing the principal stresses (Equation 3-22):

$$\Delta e_i = \Delta e_i^e + \Delta e_i^p \quad i = 1,2,3 \quad (3-20)$$

$$\Delta e_i^e = \Delta e_i - \Delta e_i^p \quad (3-21)$$

$$\begin{cases} \Delta \sigma_1 = \alpha_1 \Delta e_1 + \alpha_2 (\Delta e_2 + \Delta e_3) - \lambda^s (\alpha_1 - \alpha_2 N_\psi) \\ \Delta \sigma_2 = \alpha_1 \Delta e_2 + \alpha_2 (\Delta e_1 + \Delta e_3) - \lambda^s \alpha_2 (1 - N_\psi) \\ \Delta \sigma_3 = \alpha_1 \Delta e_3 + \alpha_2 (\Delta e_1 + \Delta e_2) - \lambda^s (-\alpha_1 N_\psi + \alpha_2) \end{cases} \quad (3-22)$$

The stress increment values are used to compute the new values of stresses as given by the Equation given below:

$$\begin{cases} \sigma_1^{New} = \sigma_1^I - \lambda^s (\alpha_1 - \alpha_2 N_\psi) \\ \sigma_2^{New} = \sigma_2^I - \lambda^s \alpha_2 (1 - N_\psi) \\ \sigma_3^{New} = \sigma_3^I - \lambda^s (-\alpha_1 N_\psi + \alpha_2) \end{cases} \quad (3-23)$$

The superscript *New* means new values and *I* is used to represent the principal stresses obtained by adding the guess elastic strain to the initial principal stresses field. The second part of the expression is the stress component due to the plastic strain correction.

The value of λ^s now can be computed by using the new values of stresses using Equation 3-23 and substituted in shear yield function given by Equation 3-14. The right hand side of the Equation is equated to zero to ensure that the point lies on the shear failure yield line, since the point cannot lie above that. The value of λ^s is obtained as:

$$\lambda^s = \frac{f_s(\sigma_i^I)}{\alpha_1 - \alpha_2 N_\psi - N_\psi (-\alpha_1 N_\psi + \alpha_2)} \quad (3-24)$$

Now FLAC can compute the new stress field and repeat again until the value of the maximum unbalanced force of the system reduces to a negligible value and thus a static solution is obtained.

3.4.4 COMPARISON OF NUMERICAL AND ANALYTICAL RESULTS

In the present study an example is considered for which the geometrical configuration is shown in Figure 3-5. The numerical values of various parameters used for this problem are presented in Table 3-2. This example has been used to validate the implementation of the Polyaxial Constitutive Model in the finite difference code in FLAC.

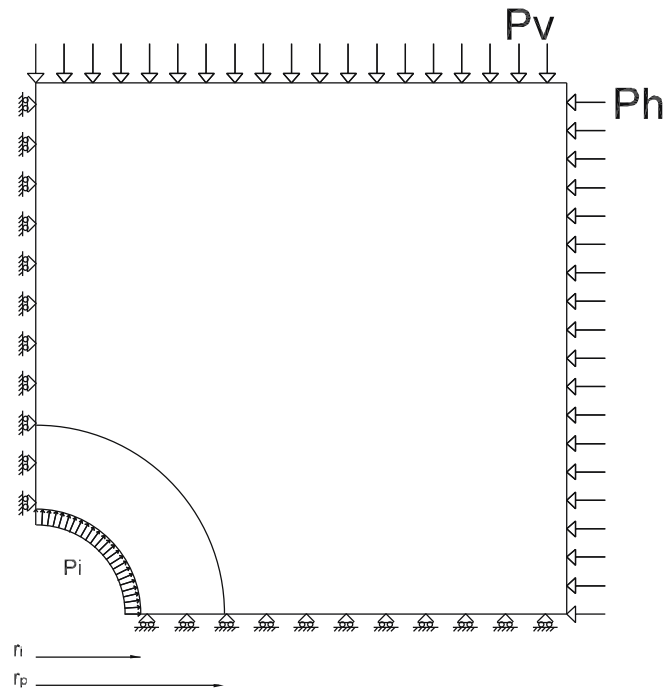


FIGURE 3-5 - GEOMETRICAL CONFIGURATION OF THE MODEL

The results of this study for this particular example are compared with the results obtained by Elasto-Plastic theory of stress distribution in broken zone in squeezing ground conditions as suggested by Singh et al.

r_i	3.2 [m]	Q	0.001
distance of boundaries	$32 * r_i$ [m]	γ	27 [kN/m ³]
ϕ_p	30 [°]	P_v	15 [MPa]
ϕ_r	20 [°]	P_i	1.52 [MPa]
c_p	2 [MPa]	P_0	15 [MPa]
c_r	0.1 [MPa]	Q_{cmass}	1.89 [MPa]
E	5 [GPa]		
ν	0.25		

TABLE 3-2 - DATA OF THE NUMERICAL PROBLEM

The analytical solution of the above problem has been obtained with the spreadsheet presented in appendix A.

Results of analytical and numerical stress distribution computation are shown in Figure 3-6.

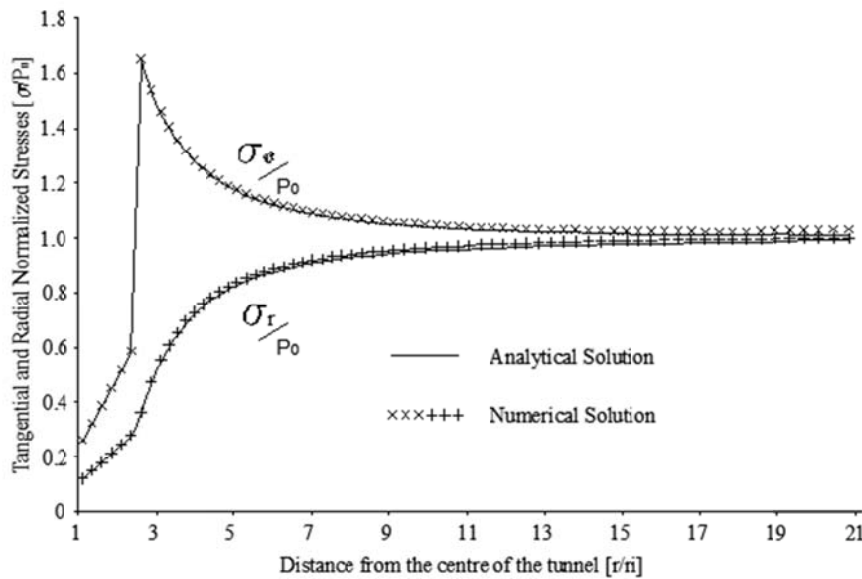


FIGURE 3-6 - COMPARISON OF ANALYTICAL AND NUMERICAL FLAC SOLUTION FOR THE TUNNEL PROBLEM IN FIGURE 3-3

The Figure shows generally good agreement between the results obtained by two methods. It can be observed that the predictions are very good up to a certain distance and beyond a certain distance. There is some problem at the boundary of the plastic zone where the predictions cannot be made at all due to the inherent drawbacks of using finite difference method and FLAC. The mesh could not be refined further in this region due to the limitation of the software. The difference in the stresses computed by two different methods at various distances in percentages is reported in appendix in Table 3-3.

3.5 CONCLUSIONS

The elasto-plastic Polyaxial Model produced in this paper introduces an alternative to design tunnels in squeezing rock masses. A new relationship between the principal stresses and uniaxial compressive strength is suggested in this work, which can handle both the elastic and plastic zone according to Singh's Theory by appropriately choosing the parameters. The proposed relationship is used to bring out the effect of intermediate principal stress as the development of principal stresses in an underground opening through an example it is shown that the effect of the intermediate principal stress contributes to the enhancement of the peak characteristics of the underground excavation.

3.6 ACKNOWLEDGMENTS

Professor Mahendra Singh, Indian Institute of Technology of Roorkee, reviewed the initial draft of the paper. The Authors are grateful for his suggestions.

3.7 LIST OF SYMBOLS:

r, r_i, r_p : Distance from the center of the tunnel, internal and plastic radius;

e^e, e^p, e : Elastic and Plastic Strain

K, G, ν, E : Bulk, Shear, Poisson's, Young's Modulus;

Q: Barton's Number;

γ : Rock Mass Unit Weight;

$\sigma_1, \sigma_2, \sigma_3$: Maximum, Intermediate, Minimum Principal Stress;

σ^t : Tension Cut;

$\sigma_r, \sigma_\theta, \tau_{\theta\rho}, P_z$: Stress distribution around a tunnel in Radial, Tangential directions and along the Tunnel direction;

P_v, P_h, λ : Overburden Pressure, Horizontal Pressure, Horizontal Ratio;

$q_{\text{mass}}, q_{\text{cr}}, \sigma_{\text{ci}}$: Peak, Residual, Uniaxial Compressive Strength;

ϕ_p, ϕ_r, ϕ : Peak, Residual, internal friction angle;

c_p, c_r, c : Peak, Residual, Cohesion;

ψ : Dilation angle;

θ : Angle between the horizontal axis of a tunnel and the line between its center and point considered.

3.8 REFERENCES

- [1] Barla, G. (1995). Squeezing rocks in tunnels. *ISRM News Journal*, 2(3&4), 44-49.
- [2] Barla, G. (2004). *Tunnelling Under Squeezing Rock Conditions*. www.polito.it/ricerca/rockmech/publcazioni/art-rivista.
- [3] Daemen, J.J.K. (1975). Tunnel Support Loading caused by Rock Failure. PhD thesis, University of Minnesota, Minneapolis, U.S.A.
- [4] Dube, A.K. (1979), Geomechanical Evaluation of Tunnel Stability Under Falling Rock Conditions in a Himalayan Tunnel; Ph.D. Thesis, Deptt. Of Civil Engg., University of Roorkee, Roorkee, India.
- [5] Itasca (2006), Reference Manual, FLAC 5.0, Itasca Consulting Group Inc, Minneapolis (2006).
- [6] Jethwa, J. L. (1981). Evaluation of Rock Pressures in Tunnels through Squeezing Ground in Lower Himalayas. PhD thesis, Department of Civil Engineering, University of Roorkee, India, 272.
- [7] Singh, M, Singh, B, Choudhari, J. Critical strain and squeezing of rock mass in tunnels, *Tunnelling and Underground Space Technology* 22 (2007) 343 - 350.
- [8] Ribacchi, R., (1986). Stato di sforzo e deformazione intorno ad una galleria, *L'ingegnere*, LXI, 135-184.
- [9] Singh, B, Goel, R. K., Mehrotra, V. K., Garg, S. K. and Allu, M. R. (1998). Effect of intermediate principal stress on strength of anisotropic rock mass. *J. Tunnelling & Underground Space Technology*, Pergamon, 13(1), 71-79.
- [10] Singh Bhawani, Jethwa J. L., Dube, A. K. and Singh, B. (1992). Correlation between observed support pressure and rock mass quality. *Tunnelling & Underground Space Technology*, Pergamon, 7(1), 59-74.
- [11] Singh, B., Goel, R.K. (2006). *Tunnelling in Weak Rocks*. *Geo-Engineering*. 5. Elsevier Science. p. 512.

- [12] Wang, R. and Kemeny, J. M. (1995). A new empirical failure criterion under polyaxial compressive stresses. *Rock Mechanics: Proc. 35th U. S. Symposium*, Reprinted from: Eds: J. J. K. Daemen and R. A. Schultz, Lake Tahoe, 4–7 June 1995, 950.

3.9 APPENDIX A: SPREADSHEET FOR THE IMPLEMENTATION OF THE TUNNEL SOLUTION

Extract from the spreadsheet for the implementation of the stress distribution around circular openings subjected to symmetrical loading:

Geometrical data and Strength Parameter

γ	27.0	kN/m ³
Q	0.001	
ϕ_D	30.0	°
ϕ_r	20.0	°
c_p	2.0	MPa
c_r	0.1	MPa

r_i	1.5	m
r_p	8.0	m
P_v	15.0	MPa
P_z	15.0	MPa
λ	1.0	

Determination of P_i

P_b	4.37	MPa
P_i	1.52	MPa

r	Flac		Theoretical		Difference	
	σ_r/P_v	σ_t/P_v	σ_r/P_v	σ_t/P_v	Radial	Tangent.
3.59	0.1186	0.2609	0.1161	0.2559	2.1162%	1.9434%
4.36	0.1497	0.3236	0.1465	0.3179	2.1755%	1.8026%
5.15	0.1807	0.3840	0.1774	0.3809	1.8515%	0.8141%
5.94	0.2125	0.4524	0.2088	0.4450	1.7605%	1.6720%
6.74	0.2453	0.5193	0.2407	0.5099	1.9201%	1.8371%
7.55	0.2813	0.5927	0.2730	0.5759	3.0231%	2.9087%
8.36	0.3586	1.6500	0.3512	1.6488	2.1048%	0.0733%
9.19	0.4706	1.5440	0.4624	1.5376	1.7746%	0.4159%
9.94	0.5497	1.4660	0.5406	1.4594	1.6849%	0.4517%
10.62	0.6071	1.4100	0.5979	1.4021	1.5448%	0.5609%
11.30	0.6546	1.3620	0.6448	1.3552	1.5188%	0.5022%
11.99	0.6946	1.3230	0.6845	1.3155	1.4738%	0.5710%
12.69	0.7284	1.2890	0.7184	1.2816	1.3980%	0.5740%
13.40	0.7572	1.2600	0.7474	1.2526	1.3096%	0.5918%
14.11	0.7821	1.2350	0.7722	1.2278	1.2830%	0.5858%
14.83	0.8036	1.2140	0.7938	1.2062	1.2377%	0.6446%
15.56	0.8224	1.1950	0.8127	1.1873	1.1970%	0.6462%
16.29	0.8389	1.1780	0.8291	1.1709	1.1838%	0.6051%
17.04	0.8535	1.1640	0.8438	1.1562	1.1496%	0.6746%
17.79	0.8664	1.1510	0.8567	1.1433	1.1332%	0.6728%
18.54	0.8778	1.1400	0.8681	1.1319	1.1230%	0.7113%
19.31	0.8882	1.1290	0.8784	1.1216	1.1197%	0.6567%
20.08	0.8973	1.1200	0.8875	1.1125	1.1025%	0.6755%
Average					1.573%	0.895%

TABLE 3-3- RESULTS OF THE DIFFERENT APPROACH

3.10 APPENDIX B: FISH CODE

```

* -----
* FISH version of Singh model with
* strain hardening/softening
* -----

set echo off

def b_singh
  constitutive_model

  f_prop m_g m_k m_fric m_dil m_ten
  f_prop m_beta m_delta m_q
  f_prop m_ftab m_ttab m_ind m_epdev m_epten
  f_prop m_btab m_dtab m_qtab
  f_prop m_e1 m_e2 m_x1 m_sh2
  f_prop m_npsi m_nphi m_csnp m_qdelta
  f_prop m_P0
;

  float $sphi $spsi $s11i $s22i $s12i $s33i $sdif $s0 $rad $s1 $s2
  $s3

  float $si $sii $psdif $fs $alams $ft $lamt $cs2 $si2 $dc2 $dss

  float $sdelta $sbeta

  float $apex $epsav $tpsav $de1ps $de3ps $depn $eps $ept $epss

  float $bisc $pdiv $anphi $tco

  int $icase $m_err $iftab $ittab

  int $ibtab $iqtab $idtab
;

  Case_of mode
; -----
; Initialisation section
; -----

  Case 1

; --- put initial table values in prop arrays ----

  if m_epdev = 0.0 then
    if m_epten = 0.0 then

```

```

$iftab = int(m_ftab)

$idtab = int(m_dtab)

$ittab = int(m_ttab)

$ibtab = int(m_btab)

$iqtab = int(m_qtab)

if $iftab # 0 then
  m_fric = table($iftab, 0.0)
end_if

if $idtab # 0 then
  m_delta = table($idtab, 0.0)
end_if

if $ittab # 0 then
  m_ten = table($ittab, 0.0)
end_if

if $ibtab # 0 then
  m_beta = table($ibtab, 0.0)
end_if

if $iqtab # 0 then
  m_q = table($iqtab, 0.0)
end_if

end_if

; --- data check ---

$m_err = 0

if m_fric > 89.0 then
  $m_err = 1
end_if

if m_ten < 0.0 then
  $m_err = 2
end_if

if m_beta < 0.0 then
  $m_err = 3
end_if

```

```

if m_delta < 0.0 then
    $m_err = 4
end_if

if $m_err # 0 then
    nerr = 126
    error = 1
end_if
;

$spphi = sin(m_fric * degrad)
$sdelta = sin(m_delta * degrad)
$sbeta = sin(m_beta * degrad)
$sppsi = sin(m_dil * degrad)
m_npsi = (1.0 + $sppsi) / (1.0 - $sppsi)
m_nphi = (1.0 + $sbeta) / (1.0 - $spphi)
m_qdelta = $sdelta / (1.0 - $spphi)
m_csnp = m_q - zs33 * m_qdelta
; m_csnp = m_q - zs33 * m_P0
;use previous for anisotropic state of stress

m_e1 = m_k + 4.0 * m_g / 3.0
m_e2 = m_k - 2.0 * m_g / 3.0
m_sh2 = 2.0 * m_g

m_x1 = m_e1 - m_e2*m_npsi + (m_e1*m_npsi -
m_e2)*m_nphi

if abs(m_x1) < 1e-6 * (abs(m_e1) + abs(m_e2)) then
    $m_err = 5
    nerr = 126
    error = 1
end_if
; --- set tension to prism apex if larger than apex ---
    $apex = m_ten

if m_fric # 0.0 then
    $apex = m_csnp / (m_nphi - 1)
end_if

m_ten = min($apex,m_ten)
;

; Case 2
; -----
; Running section
; -----
zvisc = 1.0

if m_ind # 0.0 then
    m_ind = 2.0
end_if

$anphi = m_nphi
; --- get new trial stresses from old, assuming elastic increments ---
    $s11i = zs11 + (zde22 + zde33) * m_e2 + zde11 * m_e1
    $s22i = zs22 + (zde11 + zde33) * m_e2 + zde22 * m_e1
    $s12i = zs12 + zde12 * m_sh2
    $s33i = zs33 + (zde11 + zde22) * m_e2 + zde33 * m_e1
    $sdif = $s11i - $s22i
    $s0 = 0.5 * ($s11i + $s22i)
    $rad = 0.5 * sqrt ($sdif*$sdif + 4.0 * $s12i*$s12i)
; --- principal stresses ---
    $si = $s0 - $rad
    $sii = $s0 + $rad
    $psdif = $si - $sii
; --- determine case ---
    section
        if $s33i > $sii then
; --- s33 is major p.s. ---
            $icase = 3
            $s1 = $si
            $s2 = $sii
            $s3 = $s33i
        exit section
    end_if
        if $s33i < $si then
; --- s33 is minor p.s. ---

```

```

$icase = 2
$co = $lamt * m_e2
$S1 = $s33i
$S2 = $si
$S3 = $sii
exit section
end_if
; --- s33 is intermediate ---
$icase = 1
$S1 = $si
$S2 = $s33i
$S3 = $sii
end_section
;
section
; --- shear yield criterion ---
$fs = $S1 - $S3 * $anphi + m_csnp
$alams = 0.0
; --- tensile yield criterion ---
$ft = m_ten - $S3
$lamt = 0.0
; --- tests for failure ---
if $ft < 0.0 then
$Bisc = sqrt(1.0 + $anphi * $anphi) + $anphi
$pdif = -$ft + ($S1 - $anphi * m_ten + m_csnp) * $Bisc
if $pdif < 0.0 then
; --- shear failure ---
$alams = $fs / m_x1
$S1 = $S1 - $alams * (m_e1 - m_e2 * m_npsi)
$S2 = $S2 - $alams * m_e2 * (1.0 - m_npsi)
$S3 = $S3 - $alams * (m_e2 - m_e1 * m_npsi)
m_ind = 1.0
else
; --- tension failure ---
$lamt = $ft / m_e1
$co = $lamt * m_e2
$S1 = $S1 + $co
$S2 = $S2 + $co
$S3 = m_ten
m_ind = 3.0
end_if
else
if $fs < 0.0 then
; --- shear failure ---
$alams = $fs / m_x1
$S1 = $S1 - $alams * (m_e1 - m_e2 * m_npsi)
$S2 = $S2 - $alams * m_e2 * (1.0 - m_npsi)
$S3 = $S3 - $alams * (m_e2 - m_e1 * m_npsi)
m_ind = 1.0
else
; --- no failure ---
zs11 = $s11i
zs22 = $s22i
zs33 = $s33i
zs12 = $s12i
exit section
end_if
end_if
; --- direction cosines ---
if $psdif = 0.0 then
$cs2 = 1.0
$si2 = 0.0
else
$cs2 = $sdif / $psdif
$si2 = 2.0 * $s12i / $psdif
end_if
; --- resolve back to global axes ---
case_of $icase
case 1

```



```

$dc2 = ($s1 - $s3) * $cs2
$ds2 = $s1 + $s3
zs11 = 0.5 * ($ds2 + $dc2)
zs22 = 0.5 * ($ds2 - $dc2)
zs12 = 0.5 * ($s1 - $s3) * $si2
zs33 = $s2
case 2
$dc2 = ($s2 - $s3) * $cs2
$ds2 = $s2 + $s3
zs11 = 0.5 * ($ds2 + $dc2)
zs22 = 0.5 * ($ds2 - $dc2)
zs12 = 0.5 * ($s2 - $s3) * $si2
zs33 = $s1
case 3
$dc2 = ($s1 - $s2) * $cs2
$ds2 = $s1 + $s2
zs11 = 0.5 * ($ds2 + $dc2)
zs22 = 0.5 * ($ds2 - $dc2)
zs12 = 0.5 * ($s1 - $s2) * $si2
zs33 = $s3
end_case
zvisc = 0.0
; --- accumulate hardening parameter increments ---
if m_ind = 1.0 then
$de1ps = $alams
$de3ps = -$alams * m_npsi
$depm = ($de1ps + $de3ps) / 3.0
$de1ps = $de1ps - $depm
$de3ps = $de3ps - $depm
$seps =
$seps+sqrt(0.5*($de1ps*$de1ps+$depm*$depm+$de3ps
*$de3ps))
end_if
if m_ind = 3.0 then
$sept = $sept - $alamt
end_if
end_section
$sepsav = 0.0
$stpsav = 0.0
if zsub > 0.0 then
$sepsav = $seps / zsub
$stpsav = $sept / zsub
; --- reset for the next zone ---
$seps = 0.0
$sept = 0.0
end_if
; --- softening/hardening ---
if $sepsav > 0.0 then
$seps = m_epdev + $sepsav
$stpsav = int(m_ftab)
$stpsav = int(m_dtab)
$stpsav = int(m_btab)
$stpsav = int(m_qtab)
if $stpsav # 0 then
m_fric = table($stpsav, $seps)
end_if
if $stpsav # 0 then
m_beta = table($stpsav, $seps)
end_if
if $stpsav # 0 then
m_delta = table($stpsav, $seps)
end_if
if $stpsav # 0 then
m_q = table($stpsav, $seps)
end_if
; --- data check ---
$m_err = 0
if m_fric > 89.0 then

```

```

$m_err = 1
end_if
    if m_beta < - 1.0 then
$m_err = 3
        if m_d < 0.0 then
            $m_err = 4
        end_if
    end_if
if $m_err # 0 then
    nerr = 126
    error = 1
end_if
;
m_epdev = $sepss
;
$phi = sin(m_fric * degrad)
$delta = sin(m_delta * degrad)
$beta = sin(m_beta * degrad)
$psi = sin(m_dil * degrad)
m_npsi = (1.0 + $psi) / (1.0 - $psi)
m_nphi = (1.0 + $beta) / (1.0 - $phi)
m_qdelta = $delta / (1.0 - $phi)
m_csnp = m_q - zs33 * m_qdelta
; m_csnp = m_q - zs33 * m_P0
;use previous for anisotropic state of stress
m_x1 = m_e1 - m_e2*m_npsi + (m_e1*m_npsi - m_e2)*m_nphi
;
    if abs(m_x1) < 1e-6 * (abs(m_e1) + abs(m_e2)) then
        $m_err = 5
        nerr = 126
        error = 1
    end_if
; --- reset tension to prism apex if larger than apex ---
    Sapex = m_ten

```

```

if m_fric # 0.0 then
    Sapex = m_csnp / (m_nphi - 1)
end_if
m_ten = min($apex,m_ten)
end_if
if $tpsav > 0.0 then
    $sepss = m_epten + $tpsav
    $ittab = int(m_ttab)
    if $ittab # 0 then
        m_ten = table($ittab, $sepss)
    end_if
    m_epten = $sepss
    if m_ten < 0.0 then
        $m_err = 4
        nerr = 126
        error = 1
    end_if
end_if
Case 3
; -----
; Return maximum modulus
; -----
cm_max = m_k + 4.0 * m_g / 3.0
sm_max = m_g
Case 4
; -----
; Add thermal stresses
; -----
ztsa = ztea * m_k
ztsb = zteb * m_k
ztsc = ztec * m_k
ztsd = zted * m_k
End_case

```

end

set echo=on

Chapter 4

4 A NEW APPROACH TO OBTAIN TUNNEL SUPPORT PRESSURE FOR POLYAXIAL STATE OF STRESS

D. Scussel^{a2}, S. Chandra^b

^a *School of Civil Engineering, Surveying and Construction, University of KwaZulu Natal, Durban, South Africa*

^b *Department of Civil Engineering, Indian Institute of Technology, Kanpur 208 016, India*

Keywords: Tunnel Excavation, Polyaxial Strength Criterion, FLAC, Strain Softening, FDM, Finite Difference Analysis, Finite Element Analysis.

4.1 ABSTRACT

Nowadays the numerical approaches to the tunnels designing are widely integrated to the traditional technologies (Empirical, Analytical and Observational Approaches). The numerical suites have, in fact, the advantage of an intrinsic simplicity of use and the ability to solve problems that, because of the complexity and plurality of the factors at play, cannot be easily managed through the analytical and empirical methodologies.

Unfortunately the numerical software applications, commercially available for geo-mechanical purposes, have the limitation of using only the most famous constitutive models. This study sets the target of extending the numerical applicability of a constitutive model different from the commonly used one to increment the choice of model codes available for geotechnical numerical suites.

In this paper a general methodology to extend the applicability of the Polyaxial Strength Criterion, introduced by Singh et al. (1998), to any numerical application is explained. The present procedure does not require any specific compilation of numerical constitutive model and takes advantage of the bi-dimensional Mohr-Coulomb model already present in every numerical suite.

The Polyaxial Strength Criterion is a tri-dimensional constitutive model, introduced for the analysis of severe squeezing in underground excavations. The approach explained by Singh has shown high coefficients of correlation with the observations in many cases of tunnels in high squeezing conditions in Himalayan region.

² Corresponding autor. Phone: +27 31 260 1077, Fax: +27 31 260 1411, Mail: scussel@ukzn.ac.za
University of KwaZulu-Natal
College of Agriculture, Engineering and Science, Howard College, Centenary Building
King George V Avenue, Durban 4041, South Africa

4.2 INTRODUCTION

It is in the second part of the 18th century, with the birth of the railway transport, that the construction of underground openings evolved from a nearly artisan approach to one, more scientific that combined the miners' knowledge with continuous improvements in the excavation techniques.

Terzaghi in 1946 made the first step in the direction of a new and modern designing methodology and proposed the rock mass classification, which correlated the rock mass condition to the squeezing pressure applied to the internal steel ribs of a tunnel. Subsequently, several other rock mass classification systems have been advanced, starting from Deere's RQD (1964) to the more comprehensive RMR (Bieniawski 1974, 1976, 1979, 1984) or Q system (Barton et al. 1974) classification. These analyze the characteristics of a rock mass and return both the class of quality of the material and suggestions on the best retaining system for a particular kind of work.

When the ratio between the spacing of discontinuities and the dimensions of the excavation is small, the effect of the discontinuities is shared in the whole volume, and the fractured rock mass is considered as a continuous model. In such cases, the classifications of rock masses are expected to clearly define reliable strength parameters for that particular rock mass quality and give suitable elastic/ plastic parameters for constitutive laws. This approach allowed the designers to apply elastic and elastic/plastic models to fractured rock masses, as it was already possible in soils. The first failure criterion implemented in the analytical solutions was the Mohr-Coulomb constitutive model (MC), widely utilized in soil mechanics as well, which describes the rock mass through only two parameters, Cohesion and Angle of Internal Friction. It, nowadays, is still one of the most employed models in practical applications.

In 1980, Hoek and Brown proposed an empirical nonlinear failure criterion, which combines the experience of several test on specimens of intact rock to the results of the specific rock mass classification GSI (Geological Strength Index). The model has been subjected to many updates in the years to reach its final formulation, by Hoek et al., in 2002.

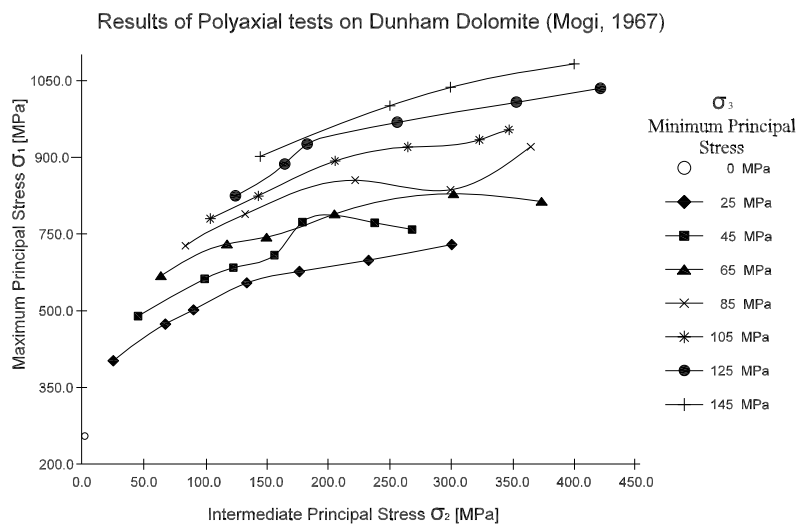


FIGURE 4-1 - RESULTS OF POLYAXIAL TESTS ON DUNHAM DOLOMITE (MOGI, 1967)

In this direction, the Polyaxial Strength Criterion (PSC) introduced by Singh et al. (1998) is another significant addition. They intuited the applicability of the large number of studies on the polyaxial constitutive models to underground applications in severe squeezing conditions, explaining the differences between what was predicted by the traditional elasto-plasticity theory and their observations.

After the careful back analysis of many data from monitored underground cavities in hard geological conditions, they observed an appreciable rock mass strength enhancement in the vicinity of the excavation that they related to a positive confining effect of the pressure in the tunnel direction (in this case intermediate principal stress σ_2).

The effect of the intermediate principal stress was not considered in the traditional theories but, now it is demonstrated from many polyaxial tests (test similar to the triaxial test, but where σ_2 and σ_3 are not equal and can be independently varied) on specimens of fractured rocks, that the intermediate principal stress holds a prominent role in the failure of rock material. In Figure 4-1, the outcomes of about 50 polyaxial tests on specimens of Dunham Dolomite (Mogi 1967) are shown. The starting point of each curve is plotted from the result of a conventional triaxial test ($\sigma_2 = \sigma_3$), and then the subsequent points correspond to the maximum principal stress at failure coming from specimens of the same material sheared keeping σ_3 constant, but increasing σ_2 .

Starting from the observation of this phenomenon, in laboratory and in field, Singh et al. (1998) suggested a semi empirical approach that incorporates the effect of the intermediate principal stress σ_2 in the conventional formulation of the Mohr-Coulomb failure criterion by replacing σ_3 with the average value of σ_2 and σ_3 in the second term of the Mohr-Coulomb formulation:

$$\text{Mohr-Coulomb} \quad \sigma_1 - \sigma_3 = \sigma_{cr} + \sigma_3 A \quad (4-1)$$

$$\text{Polyaxial (Singh et al., 1998)} \quad \sigma_1 - \sigma_3 = \sigma_{cr} + \frac{\sigma_2 + \sigma_3}{2} A \quad (4-2)$$

where $A = \frac{2 \sin \phi}{1 - \sin \phi}$

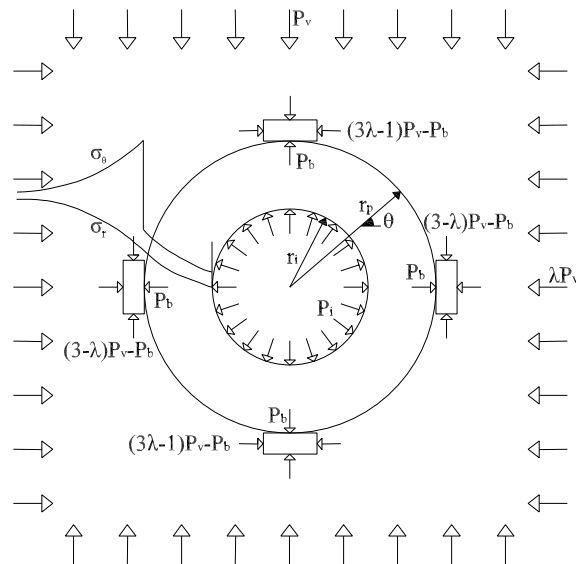


FIGURE 4-2 - PROBLEM OF A CIRCULAR TUNNEL IN ELASTO-PLASTIC ROCK MASS (SINGH AND GOEL, 2006)

Singh (2006) also produced the Elasto-Plastic Theory of Stress Distribution for tunnels in Broken Zone using the Polyaxial Strength Criterion in Squeezing Ground conditions. The stress field around an opening is shown in Figure 4-2. In this solution the plastic radius r_p (boundary between plastic and elastic zones) has a particular value for a given field problem and it is obtained by means of multipoint extensometers readings. The procedure to get the radius of broken zone from the readings of multi point extensometers is explained by Jethwa (1981). According to the Elasto-Plastic theory, the stresses are given as:

Tangential and Radial Stress in horizontal and vertical direction at the elastic zone boundary:

$$\sigma_r^+ = P_b = \frac{P_v [(1 + \lambda) + 2(1 - \lambda) \cos 2\theta] - q_{cmass} - P_0 (A/2)}{(2 + A/2)} \quad (4-3)$$

$$\sigma_\theta^+ = P_v [(1 + \lambda) + 2(1 - \lambda) \cos 2\theta] - P_b \quad (4-4)$$

where $\theta = 0^\circ$ and 90° .

In the same directions, the stress distribution inside broken zone follows the following relations:

$$\sigma_r = [P_b + c_r \cot \phi_r] \left(\frac{r}{r_p} \right)^\alpha - c_r \cot \phi_r \quad (4-5)$$

$$\sigma_\theta = N_{\phi,r} \sigma_r + q_{cr} \quad (4-6)$$

where $A = \frac{2 \sin \phi_p}{1 - \sin \phi_p}$, $\alpha = \frac{2 \sin \phi_r}{1 - \sin \phi_r}$ and $N_{\phi,r} = \frac{1 + \sin \phi_r}{1 - \sin \phi_r}$

This theory of stress distribution presupposes the use of two different constitutive models in the same solution, the Polyaxial Strength Criterion at failure that reduces to Mohr-Coulomb criterion in residual conditions. This characteristic makes its implementation in a numerical application more difficult.

Unfortunately the modern tunneling engineering theories rely less on analytical solutions and make more use of numerical models applications both for their versatility and simplicity of use. Today there are several numerical suites able to positively solve any engineering problem applying the most common failure criteria.

Scussel and Chandra (2012) have introduced one numerical constitutive model compiled in FISH code (the programming language embedded within FLAC) to include the Polyaxial Strength Criterion among the more common failure criteria codes present in the finite difference numerical suite FLAC (Itasca) with satisfactory results.

The solution scheme is based on an algorithm that, depending on the necessity, can resolve a finite difference grid in FLAC with the Polyaxial Strength Criterion or the Mohr-Coulomb theory only adequately modifying the rock mass strength parameters initially inputted in the model.

The numerical application developed in FISH does not have the simplicity of use so that it can be directly put to a commercial use. Another disadvantage of this kind of approach is the considerably slower computational velocity compared to the built in failure criteria already present in the numerical suite.

Moreover a code written exclusively for one specific software, even if probably the most common one, does not show necessary requirements of universality. In fact it does not consent the verification by

means of different numerical methodologies (FEM, BEM, etc.) of the applicability of the Polyaxial Strength Criterion to a particular case.

The present work, starting from the examination of these objections, suggests a procedure which is able to adapt the Polyaxial Strength Criterion, with the use of equivalent shear strength parameters in the Mohr-Coulomb Theory and incorporate the effects of intermediate principal stress. The application of this suggested approach in a numerical application should neutralize all the disadvantages of an application written in FISH for FLAC and would encourage the use of the Polyaxial Strength Criterion in future studies and civil works.

4.3 DEVELOPMENT OF AN EQUIVALENT MOHR-COULOMB FAILURE CRITERION

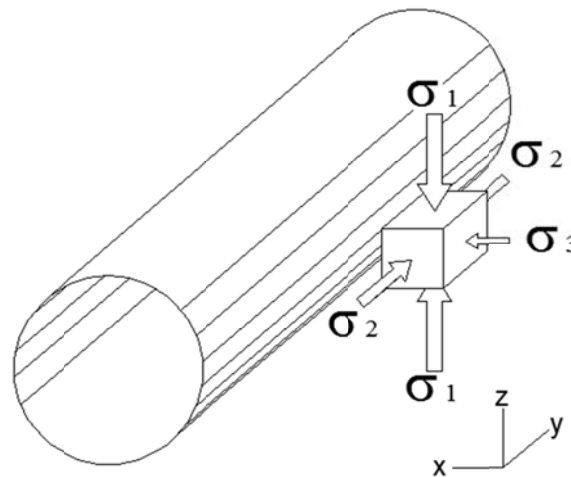


FIGURE 4-3- STRESS FIELD INDUCED IN THE VICINITY OF A CIRCULAR TUNNEL IN HYDROSTATIC STRESS CONDITIONS

The excavation of an underground opening produces a redistribution of the original stress field into the rock mass in the proximity of the excavated tunnel. As indicated in Figure 4-3, stress distribution after the modification is similar to the stress field inside a polyaxial hydraulic test cell. The in situ stress in the tunnel direction becomes intermediate principal stress σ_2 in the new configuration, and the principal stresses in the directions perpendicular to the tunnel axis are redistributed. The intermediate principal stress σ_2 compresses the joints of rocks, improving the global stability of the rock mass surrounding the excavation.

The determination of the in situ stress in direction and magnitude, therefore, is the key to apply the Polyaxial Strength Criterion to a practical underground application.

While the determination of the vertical component of the in situ stress does not pose any problem, the horizontal component is a function of many parameters not always easy to determine. It is common practice to express the horizontal stress ratio as a multiple of the vertical component through the parameter λ (sometimes K or K_0), horizontal stress ratio.

$$P_H = \lambda \cdot P_V \quad (4-7)$$

At low depths, up to 1000 m below the ground level, the gravitational effect of the rock mass is not predominant and λ is a complex combination of the effects of gravity, superficial morphology, subsidence phenomena and, for the most part, intra-crustal tectonic stresses. For this reason in the vicinity of the

ground surface λ can manifest a wide range of values. Beyond 1000 m, the difference between vertical and horizontal components of the in situ stress reduces, showing the tendency to hydrostatical conditions.

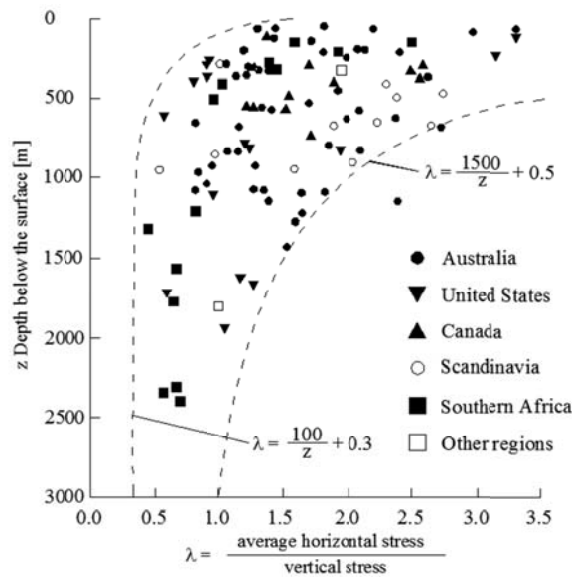


FIGURE 4-4- VARIATION OF THE RATIO OF AVERAGE HORIZONTAL STRESS TO VERTICAL STRESS WITH DEPTH BELOW SURFACE (UNDERGROUND EXCAVATION IN ROCKS, HOEK AND BROWN (1990))

The measurements of in situ stress at 116 locations, shown in Figure 4-4, collected in various parts of the world and published by Hoek (1980) confirm how, for low depths it is not possible to get an estimation of the original stress field, while the range of values for λ becomes narrow when the depth of 1000 m is exceeded.

In light of what was observed by Hoek and Brown, this paper it is assumed that for average values of the in situ stresses encountered for most of the deep underground excavations, λ may be taken as equal to 1. The methodology proposed in this paper is general enough to incorporate any other value of λ obtained by measurement of in situ stresses. The hydrostatic condition of the in situ stress allows an easy analytical determination of the state of stress induced by the opening of a circular tunnel, which will be compared with the numerical solution obtained in this study. The stress in the direction of underground excavation is then evaluated as follow:

$$\sigma_2 = P_0 \cong \gamma \cdot h \quad (4-8)$$

For specific applications of the proposed methodology, an accurate value of σ_2 should be substituted in Equations 4-2. It is, therefore, suggested that σ_2 should either be directly measured in situ or use indirect empirical relations like the one proposed by Sheorey (1994), which correlates the horizontal stress ratio λ with the deformation modulus of the upper part of the earth's crust measured in the horizontal direction E_H [GPa] at depth z [m].

$$\lambda = 0.25 + 7E_H(0.001 + 1/z) \quad (4-9)$$

For a constant value of λ , the σ_2 in the Polyaxial Strength Criterion becomes a constant and one can compare it with the Mohr-Coulomb Criterion for a specific depth in the same bi-dimensional representation. A typical plot of σ_1 and σ_3 at failure for both the criteria, for a particular value of σ_2 , is shown in Figure 4-5.

The mathematical representation of Mohr-Coulomb criterion and Polyaxial Strength Criterion in a bi-dimensional representation on the σ_1 - σ_3 plane, as presented in Figure 4-5 is expressed as:

$$\text{Polyaxial} \quad \sigma_1 = N'_\phi \sigma_3 + \sigma'_{cr} \quad (4-10)$$

$$\text{Mohr-Coulomb} \quad \sigma_1 = N_\phi \sigma_3 + \sigma_{cr} \quad (4-11)$$

where $N_\phi = \frac{1+\sin\phi}{1-\sin\phi}$, $N'_\phi = \frac{1}{1-\sin\phi}$, $\sigma_{cr} = \frac{2c \cos\phi}{1-\sin\phi}$, $\sigma'_{cr} = \left(UCS + \sigma_2 \frac{A}{2} \right)$ and $A = \frac{2 \sin\phi}{1-\sin\phi}$

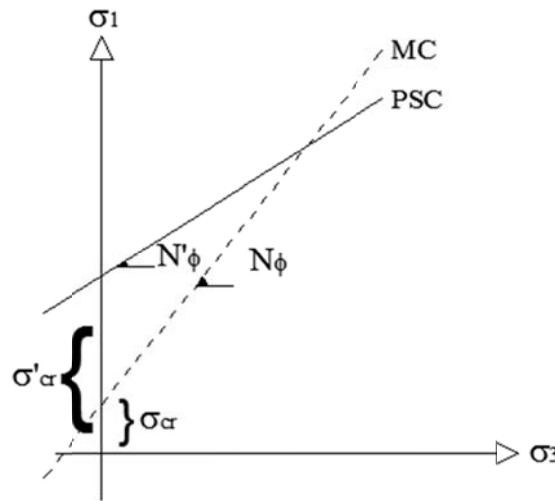


FIGURE 4-5- BI-DIMENSIONAL REPRESENTATION OF PSC AND MC IN THE σ_1 - σ_3 PLANE

The salient differences between the representations of both criteria is a smaller slope and a significantly larger value of the intercept, which correspond to a considerable increment of the rock mass strength for small values of the minimum principal stress σ_3 .

Starting with the representation shown in the σ_1 - σ_3 plane, it is possible to draw for both the failure criteria on the bi-dimensional (τ - σ) plane, as shown in Figure 4-6.

In this representation, the Polyaxial Strength Criterion keeps the same geometrical differences with respect to the Mohr-Coulomb Criterion as shown in Figure 4-5 on the σ_1 - σ_3 plane, smaller slope and bigger intercept on the shear axis.

It is, therefore, possible to describe the Polyaxial Strength Criterion by means of a modified angle of friction and cohesion as is done for the Mohr-Coulomb envelope. These modified parameters are called equivalent frictional angle (ϕ') and equivalent cohesion (c').

$$\tau = c' + \sigma \tan \phi' \quad (4-12)$$

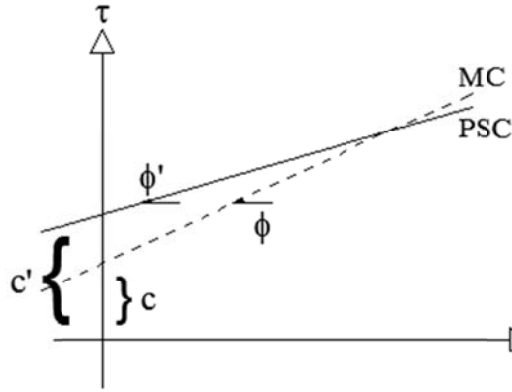


FIGURE 4-6 - BI-DIMENSIONAL REPRESENTATION OF PSC AND MC IN THE τ - σ PLANE

The positive confining effect of σ_2 is confirmed in the Mohr-Coulomb plane, the shear strength is observed to be higher using the Polyaxial Strength Criterion. The strength envelope for Polyaxial Strength Criterion shows slightly less value of the equivalent angle of friction but there is a significant increase in the value of equivalent cohesion. These two equivalent parameters of rock strength can be used to write an equivalent Mohr-Coulomb Failure Criterion in terms of maximum and minimum principal stresses. The Equation 4-10, in the modified form, is given below with the modified parameters:

$$\sigma_1 = N'_{\phi(eq)} \sigma_3 + \sigma'_{cr(eq)} \quad (4-13)$$

Where $N'_{\phi(eq)} = \frac{1 + \sin \phi'}{1 - \sin \phi'}$ and $\sigma'_{cr(eq)} = \frac{2c' \cos \phi'}{1 - \sin \phi'}$

The graphical representations of Equation 4-10 and 4-13 are completely indistinguishable from one other.

4.4 DETERMINATION OF EQUIVALENT COHESION AND ANGLE OF INTERNAL FRICTION

Equivalent cohesion c' and equivalent friction angle ϕ' can be determined taking advantage of the interchangeability of Equations 4-10 and 4-13. The values are computed firstly equating the formulation of the angular coefficients (N'_{ϕ} and $N'_{\phi(eq)}$) and, later, the intercepts (σ_{cr} and $\sigma_{cr(eq)}$) from these Equations.

The geometrical equivalence between the angular coefficient of the Equations 4-10 and 4-13 allows to determine the equivalent internal angle of friction ϕ' .

$$N'_{\phi} = N'_{\phi(eq)}$$

The above equivalence, with some easy calculation, returns the following relation between ϕ and ϕ' :

$$\phi' = \sin^{-1} \frac{\sin \phi}{2 - \sin \phi} \quad (4-14)$$

In Figure 4-7, the graphical representation of the nonlinear relation between the internal angles of friction ϕ and the corresponding equivalent angle ϕ' as expressed by Equation 4-14 is shown. Its expression involves only the Mohr-Coulomb internal angle of friction ϕ , which, as anticipated in Figure 4-6, is always higher than ϕ' . Only for ϕ equal to 0 and 90° the values are the same as that of ϕ' .

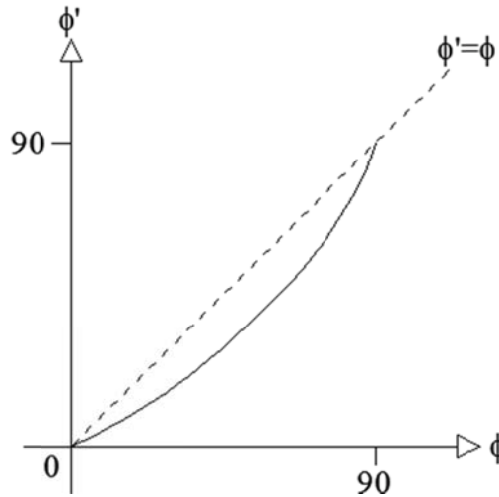


FIGURE 4-7 - GRAPHICAL RELATION BETWEEN ϕ AND ϕ'

For angles of ϕ consistent with the typical underground rock mass conditions, as shown in Table 4-1, the difference with the equivalent ϕ' varies between 9° and 11°.

ϕ [°]	20.00	22.00	24.00	26.00	28.00	30.00	32.00	34.00	36.00	38.00	40.00
ϕ' [°]	11.90	13.32	14.79	16.30	17.86	19.47	21.13	22.84	24.60	26.41	28.27

TABLE 4-1 - RELATION BETWEEN ANGLE ϕ AND EQUIVALENT ANGLE ϕ' OF INTERNAL FRICTION

If the objective of the reader is to implement a subroutine to incorporate the presented Equations in a numerical software (the subroutine in Fish ready for use for FLAC can be read in Appendix A), it should be highlighted that the function \sin^{-1} is not always present in the programming code of the numerical suites, but it can be substituted as follow by the more common function \tan^{-1} :

$$\phi' = 2 \tan^{-1} \frac{\frac{\sin \phi}{2 - \sin \phi}}{1 + \sqrt{1 + \left(\frac{\sin \phi}{2 - \sin \phi} \right)^2}} \quad (4-15)$$

Similar to the determination of the equivalent internal friction angle, the equivalent cohesion is obtained by equating the two equivalent terms of the uniaxial compressive strength of the rock mass:

$$\sigma'_{cr} = \sigma'_{cr(eq)}$$

The determination of c' is directly dependent on the knowledge of ϕ' . Substituting Equation 4-14 in σ'_{cr} (eq), the formulation of the equivalent cohesion is expressed as follow:

$$c' = \left(UCS + \sigma_2 \frac{A}{2} \right) B \quad (4-16)$$

where $A = \frac{2 \sin \phi}{1 - \sin \phi}$ and $B = \frac{1 - \sin \phi}{(2 - \sin \phi) \cos \left(\sin^{-1} \frac{\sin \phi}{2 - \sin \phi} \right)}$

The formulation of the parameters A and B is only function of the internal angle of friction and can be easily tabulated as in Table 4-2.

ϕ [°]	20.00	22.00	24.00	26.00	28.00	30.00	32.00	34.00	36.00	38.00	40.00
A	1.04	1.20	1.37	1.56	1.77	2.00	2.25	2.54	2.85	3.20	3.60
B	0.41	0.40	0.39	0.37	0.36	0.35	0.34	0.33	0.32	0.31	0.30

TABLE 4-2 - ESTIMATION OF A AND B FOR INCREASING VALUES OF INTERNAL ANGLE OF FRICTION

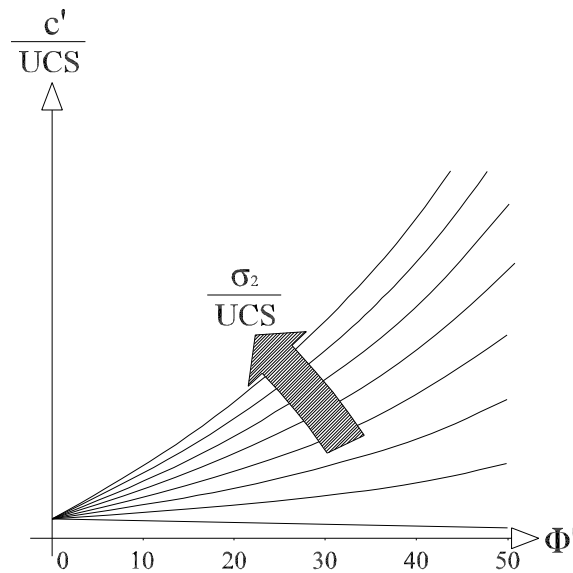


FIGURE 4-8- GRAPHICAL RELATION BETWEEN ANGLE ϕ OF INTERNAL FRICTION AND NON-DIMENSIONAL COHESION

In order to formulate a non-dimensional equivalent cohesion, both terms of Equation 4-16 must be divided by the Uniaxial Compressive Strength UCS to obtain:

$$\frac{c'}{UCS} = \left(1 + \frac{\sigma_2}{UCS} \frac{A}{2} \right) B \quad (4-17)$$

The expression of c' is more complex than that of ϕ' , it is still a function of ϕ as for the equivalent internal angle of friction but is also related to the magnitude of UCS and σ_2 , which is a function of depth. In

Figure 4-8, the effect of the variation of the internal angle of friction ϕ of the rock mass for constant increments of the σ_2 /UCS ratio is shown.

For a particular rock mass, with a given value of UCS, the increments of σ_2 correspond to a significant increment of the apparent cohesion. This behaviour is amplified for values of internal friction angles bigger than 30° .

The bottom most line in Figure 4-8, shows negative inclination, is the representation of the equivalent cohesion for the intermediate principal stress value of zero. Its decrease with increasing values of ϕ is due to total absence of any lateral confinement. This is easily explained by the Mohr's circle at failure in Figure 4-9. In fact, for a fixed combination of maximum and minimum principal stresses at failure, an enhancement of the internal angle of friction or equivalent angle of friction, (the two are directly related) correspond to a reduction in cohesion.

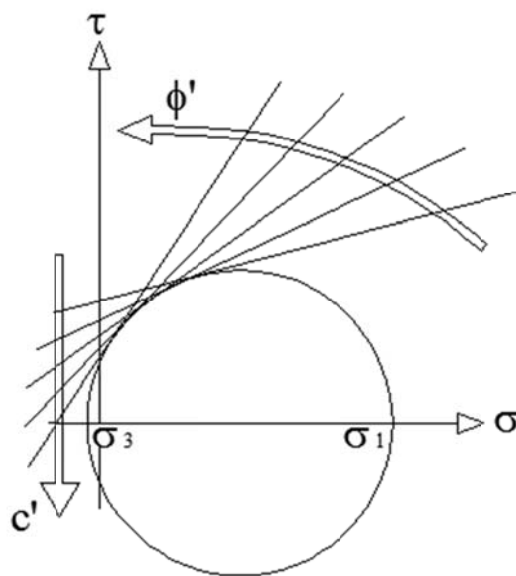


FIGURE 4-9 - RELATION BETWEEN INTERNAL FRICTION ANGLE ϕ' AND EQUIVALENT COHESION c' FOR $\sigma_2 = 0$

4.5 COMPARISON OF ANALYTICAL AND NUMERICAL RESULTS

The advantages of this methodology can be easily shown through a practical application. The following example of deep tunnel subjected to squeezing is utilised to compare the solutions making use of the Polyaxial Strength Criterion as specified in the analytical solution proposed by Singh et al. (2006) and, afterwards, substituting the equivalent parameters of resistance in the Mohr-Coulomb Theory. In another case, the proposed theory will be applied to a numerical model to illustrate the simplification in the analysis as compared to the code implemented by Scussel and Chandra (2012).

ϕ_p	ϕ_r	c_p	c_r	λ
30°	20°	0.2 MPa	0.1 MPa	1
P_v	P_0	P_i	UCS	r_i
15 MPa	15 MPa	1.52 MPa	1.89 MPa	3.2 m

TABLE 4-3 - ROCK MASS DATA OF A TYPICAL PROBLEM

A typical example of deep circular tunnel subjected to a hydrostatic in situ stress field has been selected. Stresses and rock mass quality have been dimensioned such as to observe a plastic circular zone that, under Polyaxial Strength Criterion, is 8 m long. The arbitrary rock mass and geometrical characteristics of the proposed example are summarised in Table 4-3.

The peak internal angle of friction is converted to its equivalent value for the application of Polyaxial Strength Criterion exclusively in elastic field as explained in the Singh's analytical solution. At failure the criterion adopted reduces to the Mohr-Coulomb Theory and the original residual resistance parameters are used. Substituting ϕ_p , P_0 and UCS into Equations 4-14 and 4-16 the equivalent parameters of resistance for the elastic zone are obtained as:

$$\phi'_p = \sin^{-1} \frac{\sin 30^\circ}{2 - \sin 30^\circ} = 19.47^\circ$$

$$c' = \left(1.89 + 15 \frac{\sin 30^\circ}{1 - \sin 30^\circ} \right) \left(\frac{1 - \sin 30^\circ}{(2 - \sin 30^\circ) \cos \left(\sin^{-1} \frac{\sin 30^\circ}{2 - \sin 30^\circ} \right)} \right) = 5.972 \text{ MPa}$$

The squeezing pressure applied by the rock mass to the internal lining of the tunnel, as already mentioned, is evaluated with the assumption that the broken zone surrounding the circular excavation shows a constant radius of 8 m.

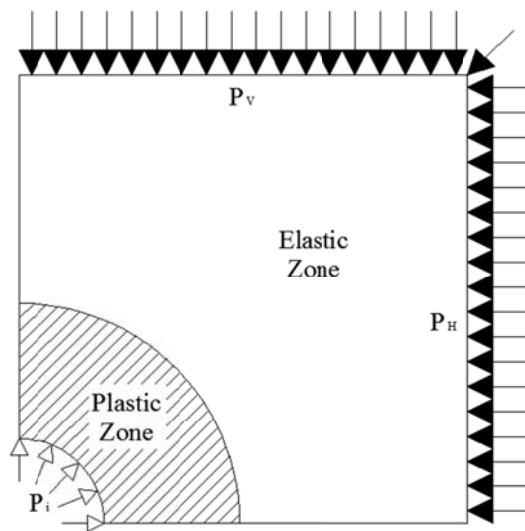


FIGURE 4-10– GEOMETRICAL CONFIGURATION OF THE APPLICATION EXAMPLE

The analytical solutions according to Singh's and Equivalent Mohr-Coulomb Theory are obtained. The formulation of squeezing pressure P_i from both the techniques is derived from the evaluation of the Equation 4-5 at a distance from the center of the tunnel r equal to its internal radius r_i .

The formulation of radial pressure at the boundary of the elastic zone P_b , instead, is direct expression of the constitutive model at peak condition, which is different for the two approaches:

$$\begin{aligned}
 P_b &= \frac{2P_v - (UCS + P_0 \sin \phi_p / (1 - \sin \phi_p))}{(2 - \sin \phi_p) / (1 - \sin \phi_p)} \\
 \text{Singh} \quad &= \frac{2 \cdot 15 - (1.89 + 15 \sin 30^\circ / (1 - \sin 30^\circ))}{(2 - \sin 30^\circ) / (1 - \sin 30^\circ)} = 4.37 \text{ MPa}
 \end{aligned}$$

$$\begin{aligned}
 P_b &= \frac{2P_v - (2c'_p \cos \phi'_p / (1 - \sin \phi'_p))}{2 / (1 - \sin \phi'_p)} \\
 \text{Equivalent Mohr} \quad &= \frac{2 \cdot 15 - (2 \cdot 5.972 \cdot \cos 19.47^\circ / (1 - \sin 19.47^\circ))}{(2 - \sin 19.47^\circ) / (1 - \sin 19.47^\circ)} = 4.37 \text{ MPa}
 \end{aligned}$$

Both the techniques, Singh's and equivalent Mohr-Coulomb Theory give the same magnitude of P_b . The direct consequence of this is that the Squeezing Pressure (calculated at $r = r_i$), as given below, is also unique:

$$\begin{aligned}
 P_i &= [P_b + c_r \cot \phi_r] \left(\frac{r_i}{r_p} \right)^{2 \sin \phi_r / (1 - \sin \phi_r)} - c_r \cot \phi_r \\
 &= [4.37 + 0.1 \cot 20^\circ] \left(3.2 / 8.0 \right)^{2 \sin 20^\circ / (1 - \sin 20^\circ)} - 0.1 \cot 20^\circ = 1.52 \text{ MPa}
 \end{aligned}$$

In appendix B, Table 4-4, it is presented a detailed analysis of the stress field induced in the rock mass at different distances from the center of the tunnel. The relative difference between the two approaches is shown in Figure 4-11, and it may be observed that there are no appreciable differences and the errors are negligible.

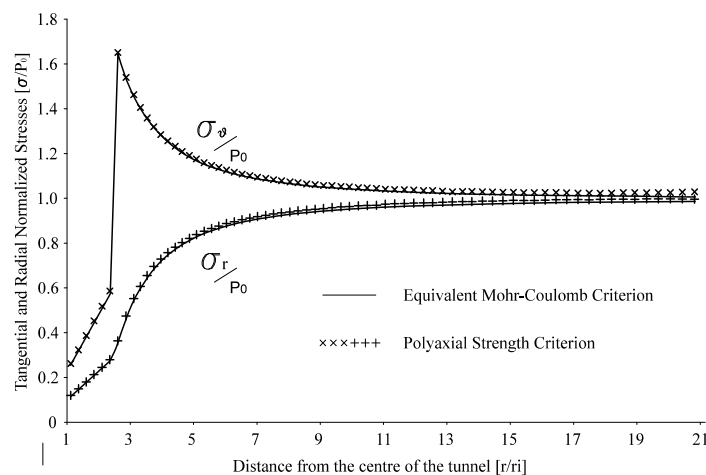


FIGURE 4-11 - COMPARISON OF THE ANALYTICAL SOLUTIONS (STRESS DISTRIBUTION)

The results obtained by the numerical application of the proposed equivalent parameters method by means of the Mohr-Coulomb model in FLAC are compared with the polyaxial numerical solutions obtained by using the modified FLAC code as suggested by Scussel & Chandra (2012). A finite

difference grid in FLAC representing the problem was developed, and the radial pressure equal to the previously determined squeezing pressure P_i has been applied to the internal surface of the tunnel to simulate the correct reaction of the support to get the same plastic radius equal to 8 m. The problem was solved, with the Polyaxial Constitutive Model composed in FISH language by Scussel and Chandra, and then with the proposed method. The results obtained by both the methods are plotted in Figure 4-12. The difference between the numerical outcomes of the two techniques is negligible, and is smaller than an average 0.1% as reported in Table 4-4.

In addition to the matching stress fields obtained from the two analyses, the time needed to solve the problem by two approaches was also determined. In both the cases a common grid was used (3500 zones). The user-defined Polyaxial Constitutive Model in FISH needed 75 s to achieve the convergence, while the modified parameters in the Mohr-Coulomb approach took only 24 s, that means that the suggested approach is more than three times faster. In more complex situations this may turn out to be more advantageous.

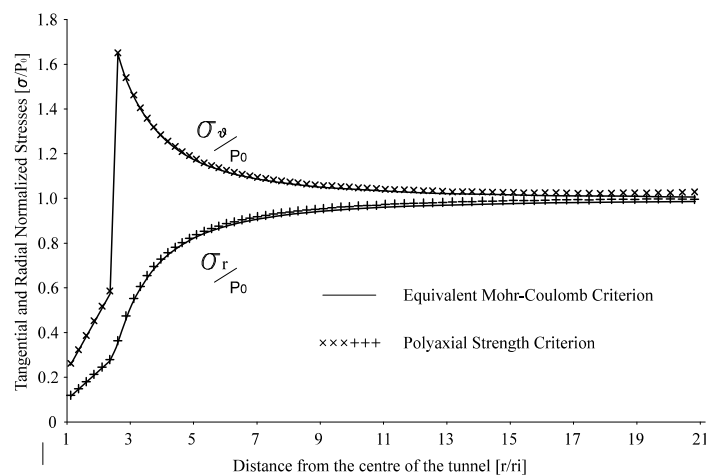


FIGURE 4-12 - COMPARISON OF THE NUMERICAL SOLUTIONS (STRESS DISTRIBUTION)

The results obtained by analytical method as proposed using equivalent parameters of Mohr-Coulomb Theory are compared with numerical solution obtained by using equivalent parameters in FLAC. The stress distribution estimated by using both the methods is presented in Figure 4-13. The results obtained are in close agreement with each other. The average difference between the results estimated by two methods is smaller than 1.0-1.2 % in the elastic zone (see again Appendix B and Table 4-4) and is slightly higher for the broken zone, due to the coarseness of the grid used in the analysis.

4.6 CONCLUSIONS

In this work a new method is proposed, where in the polyaxial state of stress can be incorporated in the analysis by a very simple approach. The proposed method incorporates the intermediate principal stress in the analysis and has the ease of applicability to many available software, This method uses modified angle of friction and cohesion values, which can be calculated by the given Equations and the analysis reduces to the same format as in Mohr-Coulomb theory. The approach is quite general and may be used for both hydrostatic and nonhydrostatic stress fields by means of any analytical or numerical method of analyzing tunnel support. The method when used in numerical scheme is easily adoptable and leads to less computational efforts.

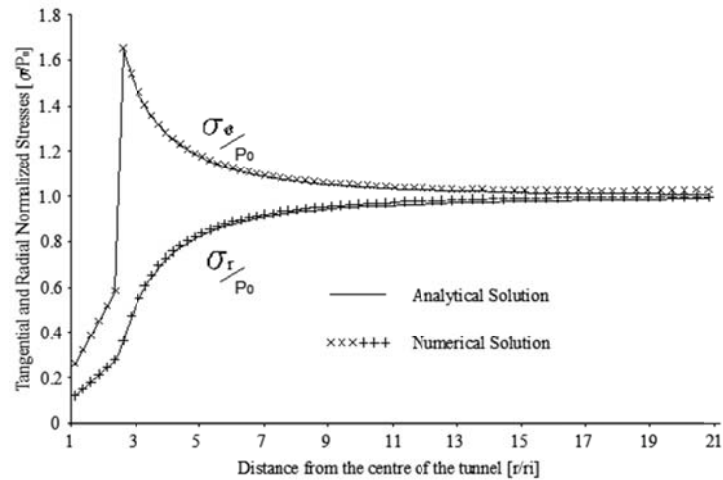


FIGURE 4-13 - COMPARISON OF THE ANALYTICAL AND NUMERICAL SOLUTIONS

The application of the Polyaxial Strength Criterion is quite important when the pressures encountered are high and the specific characteristics of rock masses produce significant squeezing phenomena in the field. In these conditions the study of the complex rock mass-support behavior cannot be simulated by means of physical models, and the use of a specific numerical model is, therefore, the only way to reproduce the response of a rock mass in accordance with the Polyaxial Theory.

Thus, the proposed methodology achieves all the objectives mentioned at the beginning of this study. The results obtained by the proposed method are compared with numerical approaches and analytical solutions and are in good agreement. It can be implemented in any geo-mechanical numerical suites with excellent results.

4.7 LIST OF SYMBOLS:

r, r_i, r_p : Distance from the center of the tunnel, internal and plastic radius;

$\sigma_1, \sigma_2, \sigma_3$: Maximum, Intermediate and Minimum Principal Stress;

$\sigma_r, \sigma_\theta, \tau_{\theta r}$: Stress distribution around a tunnel in Radial, Tangential directions;

P_0 : in situ Stress in the tunnel direction;

P_v, P_h, λ : In situ Vertical and Horizontal Pressure, Horizontal Ratio;

$q_{cmass}, q_{cr}, \sigma_{cr}$: Peak, Residual, Uniaxial Compressive Strength (UCS) of the rock mass;

ϕ_p, ϕ_r, ϕ : Peak, Residual internal angle of friction;

c_p, c_r, c : Peak, Residual Cohesion;

θ : Angle between the horizontal axis of a tunnel and the line between its center and point considered.

4.8 REFERENCES

- [1] Barton, N.R., Lien, R., Lunde, J., 1974. Engineering classification of rock masses for the design of tunnel support. *Rock Mechanics and Rock Engineering* (Springer) 6 (4), 189–236. <http://dx.doi.org/10.1007/BF01239496>.
 - [2] Bieniawski, 1974. Geomechanics classification of rock masses and its application in tunneling. In: *Proc. 3rd Cong. ISRM* (Denver), vol. 2A, pp. 27.
 - [3] Bieniawski, 1976. Rock masses classification in rock engineering. In: *Proc. of Symposium on Exploration for Rock Engineering*, vol. 1. Balkema, Rotterdam, pp. 97–106.
 - [4] Bieniawski, Z.T., 1979. The geomechanics classification in rock engineering applications. In: *Proceedings, 4th International Congress on Rock Mechanics*, vol. 2, ISRM, Montreux. A.A. Balkema, Rotterdam, pp. 41–48.
 - [5] Bieniawski, Z.T., 1984. *Rock Mechanics Design in Mining and Tunneling*. A.A. Balkema, Rotterdam, 272 p.
 - [6] Deere, D.U., 1964. Technical description of rock cores. *Rock Mechanics Engineering Geology* 1 (16–22).
 - [7] Hoek, E., Brown, E.T., 1980a. Empirical strength criterion for rock masses. *Journal of the Geotechnical Engineering Division ASCE*, 1013–1025.
 - [8] Hoek, E., Brown, E.T., 1980b. *Underground Excavations in Rock*. Institution of Mining and Metallurgy, London.
 - [9] Hoek, E., Carranza-Torres, C.T., Corkum, B., 2002. Hoek–Brown failure criterion-2002 edition. *Proceedings of the Fifth North American Rock Mechanics Symposium* 1, 267–273.
 - [10] Jethwa, J.L., 1981. *Evaluation of Rock Pressures in Tunnels through Squeezing Ground in Lower Himalayas*. PhD Thesis, Department of Civil Engineering, University of Roorkee, India, p. 272.
 - [11] Mogi, K., 1967. Effect of the intermediate principal stress on rock failure. *Journal of Geophysical Research* 72, 5117–5131.
 - [12] Scussel, D., Chandra, S., 2012. Polyaxial stress analysis of underground openings using FLAC. *Journal of Rock Mechanics and Tunnel Technologies* 18 (1), 41–54.
 - [13] Sheorey, P.R., 1994. A theory for in situ stresses in isotropic and transversely isotropic rock. *International Journal of Rock Mechanics and Mining Sciences & Geomechanics*.
 - [14] Singh, B., Goel, R.K., 2006. *Tunnelling in Weak Rocks*. *Geo-Engineering*, vol. 5. Elsevier, Science. p. 512.
 - [15] Singh, Bhawani, Goel, R.K., Mehrotra, V.K., Garg, S.K., Allu, M.R., 1998. Effect of intermediate principal stress on strength of anisotropic rock mass. *Tunnelling and Underground Space Technology*, Pergamon 13 (1), 71–79.
- Terzaghi, K., Proctor, R.V., White, T.L., 1946. *Rock Tunneling with Steel Supports*. 65 Commercial Shearing and Stamping Co.

4.9 APPENDIX A: FLAC'S CODE FOR THE AUTOMATIC DETERMINATION OF THE EQUIVALENT MOHR-COULOMB PARAMETERS

def dati

; Data entry: in situ stress in tunnel direction, uniaxial compressive strength and angle of friction as in the previously presented example:

$$P0 = 15e6$$

$$qmass = 1.89e6$$

$$fp = 30$$

; The angle of friction is now converted into radians and the rock mass resistance at the surface σ_{ci} of the tunnel is entered:

$$efp = fp * degrad$$

$$qmass1 = qmass + P0 * \sin(efp) / (1 - \sin(efp))$$

; The equivalent angle of friction ϕ' is determined accordingly to the Equation 4-15.

; The older versions of FLAC admit only a limited number of characters for each row,

; for this reason the determination of ϕ' is split in 3 rows:

$$aaa = \sin(efp) / (2 - \sin(efp))$$

$$bbb = aaa / (1 + \sqrt{1 - aaa * aaa})$$

$$efp1 = 2 * \text{atan}(bbb)$$

; Which is now converted to degrees

$$fp1 = 0.5 * efp1 * 360 / \pi$$

; Finally the equivalent cohesion c' is estimated as specified by the equation 4-16

$$coep1 = 0.5 * qmass1 * (1 - \sin(efp1)) / \cos(efp1)$$

end

dati

At this point the variable $fp1$ and $coep1$ can be implemented for the application in the numerical model. In order to evaluate the results of the subroutine, the function PRINT FISH can be used to show the magnitude of the individual variables.

Here the results of the proposed subroutine:

flac: print fish

FISH symbols ...

<i>Value</i>	<i>Name</i>
-----	----
<i>3.3333E-01</i>	<i>aaa</i>
<i>1.7157E-01</i>	<i>bbb</i>
<i>5.9715E+06</i>	<i>coep1</i>
<i>(function)</i>	<i>0 dati</i>
<i>5.2360E-01</i>	<i>efp</i>
<i>3.3984E-01</i>	<i>efp1</i>
<i>30</i>	<i>fp</i>
<i>1.9471E+01</i>	<i>fp1</i>
<i>1.5000E+07</i>	<i>P0</i>
<i>1.8900E+06</i>	<i>qmass</i>
<i>1.6890E+07</i>	<i>qmass1</i>

4.10 APPENDIX B: SPREADSHEET FOR THE COMPARISON OF THE TUNNEL SOLUTIONS

r [m]	Analytical Mohr equivalent		Analytical PSC		Relative difference analytical solutions		Flac (Mohr equiv)		Flac (PSC)		Relative difference numerical solutions		Relative difference analytical-numerical		
	σ_r/P_v	σ_θ/P_v	σ_r/P_v	σ_θ/P_v			σ_r/P_v	σ_θ/P_v	σ_r/P_v	σ_θ/P_v					
3.59	0.1161	0.2559	0.1161	0.2559	0.00%	0.00%	0.1187	0.2607	0.1187	0.2607	0.00%	0.00%	2.15%	1.84%	
4.36	0.1465	0.3178	0.1465	0.3178	0.00%	0.00%	0.1493	0.3227	0.1500	0.3233	0.45%	0.21%	2.38%	1.73%	
5.15	0.1774	0.3809	0.1774	0.3809	0.00%	0.00%	0.1807	0.3873	0.1807	0.3840	0.00%	0.86%	1.81%	0.81%	
5.94	0.2089	0.4450	0.2089	0.4450	0.00%	0.00%	0.2120	0.4507	0.2127	0.4527	0.31%	0.44%	1.81%	1.70%	
6.74	0.2408	0.5101	0.2408	0.5101	0.00%	0.00%	0.2460	0.5200	0.2453	0.5193	0.27%	0.13%	1.88%	1.79%	
7.55	0.2731	0.5761	0.2731	0.5761	0.00%	0.00%	0.2760	0.5813	0.2813	0.5927	1.91%	1.93%	2.96%	2.83%	
8.36	0.3514	1.6486	0.3514	1.6486	0.00%	0.00%	0.3653	1.6607	0.3587	1.6507	1.84%	0.60%	2.05%	0.12%	
9.19	0.4627	1.5373	0.4627	1.5373	0.00%	0.00%	0.4747	1.5453	0.4707	1.5447	0.85%	0.04%	1.72%	0.48%	
9.94	0.5410	1.4590	0.5410	1.4590	0.00%	0.00%	0.5520	1.4667	0.5500	1.4667	0.36%	0.00%	1.66%	0.52%	
10.62	0.5977	1.4023	0.5977	1.4023	0.00%	0.00%	0.6087	1.4100	0.6073	1.4100	0.22%	0.00%	1.60%	0.55%	
11.30	0.6450	1.3550	0.6450	1.3550	0.00%	0.00%	0.6560	1.3627	0.6547	1.3627	0.20%	0.00%	1.49%	0.56%	
12.00	0.6848	1.3152	0.6848	1.3152	0.00%	0.00%	0.6953	1.3227	0.6947	1.3227	0.10%	0.00%	1.43%	0.57%	
12.69	0.7185	1.2815	0.7185	1.2815	0.00%	0.00%	0.7293	1.2893	0.7287	1.2887	0.09%	0.05%	1.41%	0.56%	
13.40	0.7473	1.2527	0.7473	1.2527	0.00%	0.00%	0.7580	1.2600	0.7573	1.2600	0.09%	0.00%	1.33%	0.58%	
52.58	0.9836	1.0164	0.9836	1.0164	0.00%	0.00%	0.9953	1.0267	0.9953	1.0267	0.00%	0.00%	1.19%	1.00%	
53.69	0.9843	1.0157	0.9843	1.0157	0.00%	0.00%	0.9960	1.0267	0.9960	1.0267	0.00%	0.00%	1.19%	1.07%	
54.80	0.9849	1.0151	0.9849	1.0151	0.00%	0.00%	0.9967	1.0267	0.9967	1.0267	0.00%	0.00%	1.19%	1.13%	
55.93	0.9855	1.0145	0.9855	1.0145	0.00%	0.00%	0.9973	1.0260	0.9973	1.0260	0.00%	0.00%	1.19%	1.13%	
57.07	0.9861	1.0139	0.9861	1.0139	0.00%	0.00%	0.9980	1.0267	0.9980	1.0267	0.00%	0.00%	1.20%	1.25%	
58.22	0.9866	1.0134	0.9866	1.0134	0.00%	0.00%	0.9980	1.0260	0.9980	1.0260	0.00%	0.00%	1.15%	1.24%	
59.38	0.9871	1.0129	0.9871	1.0129	0.00%	0.00%	0.9987	1.0267	0.9987	1.0267	0.00%	0.00%	1.16%	1.35%	
60.55	0.9876	1.0124	0.9876	1.0124	0.00%	0.00%	0.9993	1.0273	0.9993	1.0273	0.00%	0.00%	1.18%	1.47%	
61.74	0.9881	1.0119	0.9881	1.0119	0.00%	0.00%	0.9993	1.0273	0.9993	1.0273	0.00%	0.00%	1.13%	1.51%	
62.94	0.9885	1.0115	0.9885	1.0115	0.00%	0.00%	0.9993	1.0273	0.9993	1.0273	0.00%	0.00%	1.08%	1.56%	
64.14	0.9890	1.0110	0.9890	1.0110	0.00%	0.00%	1.0000	1.0280	1.0000	1.0280	0.00%	0.00%	1.11%	1.67%	
65.36	0.9894	1.0106	0.9894	1.0106	0.00%	0.00%	1.0000	1.0293	1.0000	1.0293	0.00%	0.00%	1.07%	1.84%	
66.60	0.9898	1.0102	0.9898	1.0102	0.00%	0.00%	1.0000	1.0300	1.0000	1.0300	0.00%	0.00%	1.03%	1.94%	
Average					0.00%	0.00%	Average					0.11%	0.07%	1.27%	0.93%
A	B	C	D	E	F	G	H	I	J	K	L	M	N		

TABLE 4-4 - COMPARISON OF THE TUNNEL SOLUTIONS

Column A: Plastic Zone $\sigma_r/P_v = \left((P'_b + c_r \tan^{-1} \phi_r) \left(\frac{r}{r_i} \right) - c_r \tan^{-1} \phi_r \right)$

Elastic Zone $\sigma_r/P_v = \left(P_v - (P_v - P'_b) \left(\frac{r_p}{r} \right)^2 \right)$

Column B: Plastic Zone $\sigma_{\theta}/P_V = (N_{\phi,r}\sigma_r + q_{cr})$

Elastic Zone $\sigma_{\theta}/P_V = (2P_V - \sigma_r)$

Column C: Plastic Zone $\sigma_r/P_V = \left((P_b + c_r \tan^{-1} \phi_r) \left(\frac{r}{r_i} \right) - c_r \tan^{-1} \phi_r \right)$

Elastic Zone $\sigma_r/P_V = \left(P_V - (P_V - P_b) \left(\frac{r_p}{r} \right)^2 \right)$

Column D: Plastic Zone $\sigma_{\theta}/P_V = (N_{\phi,r}\sigma_r + q_{cr})$

Elastic Zone $\sigma_{\theta}/P_V = (2P_V - \sigma_r)$

Column E and F: $|A-B|/avg(A,B)$ and $|C-D|/avg(C,D)$

Column G and H: Numerical solution (Mohr Equivalent)

Column I and J: Numerical solution (Singh's Theory)

Column K and L: $|G-H|/avg(G,BH)$ and $|I-J|/avg(I,J)$

Column M and N: $|A-G|/avg(A,G)$ and $|B-H|/avg(B,H)$

where $P'_b = \frac{2P_V - (2c'_p \cos \phi'_p / (1 - \sin \phi'_p))}{2/(1 - \sin \phi'_p)}$ and $P_b = \frac{2P_V - (UCS + P_0 \sin \phi_p / (1 - \sin \phi_p))}{(2 - \sin \phi_p)/(1 - \sin \phi_p)}$

Chapter 5

5 A NEW APPROACH TO DESIGN OF TUNNELS IN SQUEEZING GROUND

D. Scussel^{a3}, S. Chandra^b

^a *School of Civil Engineering, Surveying and Construction, University of KwaZulu Natal, Durban, South Africa*

^b *Department of Civil Engineering, Indian Institute of Technology, Kanpur 208 016, India*

Keywords: Tunnel Support Pressure, Polyaxial Strength Criterion, FLAC, Strain Softening, FDM, Finite Difference Analysis, Finite Element Analysis.

5.1 ABSTRACT

The study of the mechanical behavior of discontinuous rock masses is a rapidly growing subject. Many researches are reported in literature concerning the estimation of the tunnel support pressures incorporating the real behavior of a rock mass using different types of constitutive models and rock parameters. These studies have favored the introduction of various analytical solutions for the easier geo-mechanical cases but have not been converted into numerical models suited for commercially available software and, therefore could not be used in real and more complex engineering applications.

The notable constitutive models used in common practice in rock mechanics are Mohr-Coulomb and Hoek-Brown failure criteria. Most of the commonly available software supports only these two failure criteria. The difficulties faced in possibly implementing new constitutive model into the numerical suites already available, are so large that the studies using innovative constitutive models result in a mere academic exercise.

In this paper a new methodology is described for the application of the Polyaxial Strength Criterion suggested by Singh et al. (1998), which is characterized by the direct influence of all the principal stresses in the resistance of a rock mass. The methodology applied in this research, uses the format of the Mohr-Coulomb model using equivalent angle of friction and cohesion of the rock mass surrounding the underground opening as introduced by Scussel and Chandra (2012). The equivalent parameters of rock mass resistance, which are directly derived from the common Mohr-Coulomb parameters, are also influenced by the intermediate principal stress σ_2 , in accordance with what was suggested in the Polyaxial Strength Criterion, and by the approach chosen for quantifying the uniaxial compressive strength σ_{cr} of the rock mass. In demonstration of the practical applicability of this constitutive model, it has been used

³Corresponding author

Phone: +27 31 260 1077, Fax: +27 31 260 1411, Mail: scussel@ukzn.ac.za
University of KwaZulu-Natal
College of Agriculture, Engineering and Science, Howard College, Centenary Building
King George V Avenue, Durban 4041, South Africa

to predict the squeezing of rock observed and measured at three different instrumented sections of a tunnel from an Indian squeezing rock conditions.

5.2 INTRODUCTION

One of the biggest challenges of the Rock Mechanics, and specifically of Underground Engineering, is to develop a reliable theory for predicting support pressures for the Squeezing ground conditions in order to prevent any adverse situations. It is observed that squeezing of rock results in extreme deformations at the internal surfaces of a deep underground opening.

The squeezing of rock is a phenomenon that may sometimes continue for long periods of time. The present study is focused with particular emphasis to the short-term analysis of squeezing in tunneling, which represents the immediate reaction of the rock mass surrounding a tunnel section moving away from the excavated face and that is the base from which the time dependent deformations will develop.

The Squeezing of Rock is the result of a complex overstress field applied to the rock mass due to the transformation in the original state of tension subsequent to the opening of an underground excavation. When the induced stress exceeds the resistance of the affected material, the rock fails and the radial deformations at the lining become unacceptable. The squeezing condition defines, therefore, the boundary between stable and unstable excavations. A late identification of the unsafe stress conditions result in slow and hazardous excavation, use of faulty construction techniques and tunnel misalignments, which directly increase the overall costs of the work.

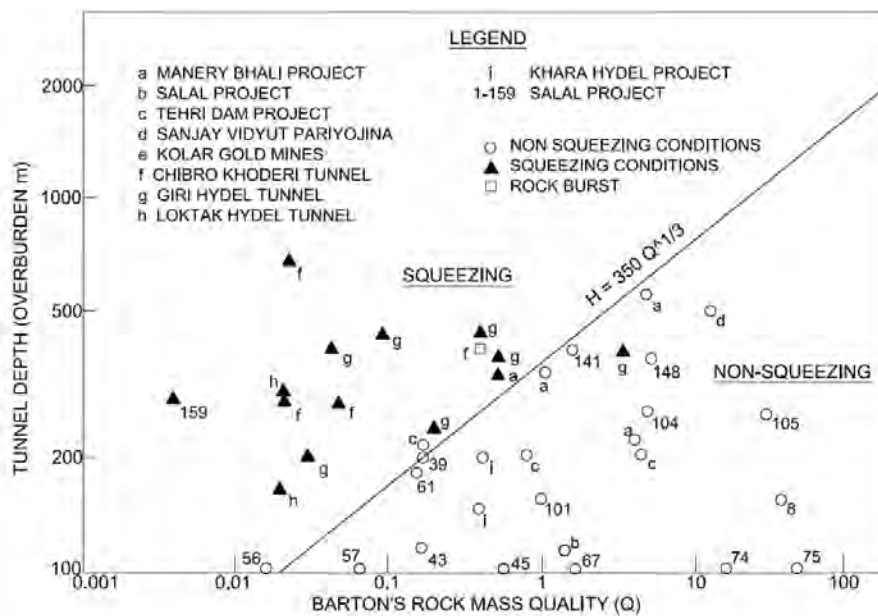


FIGURE 5-1 - SINGH ET AL. (1992)
APPROACH FOR PREDICTING SQUEEZING CONDITIONS

The modern worldwide sharing of information coming from different case studies has increased the amount of observational data available and encouraged several attempts of predicting the Squeezing potential of a rock mass. Singh et. al. (1992) defined a clear boundary between safe and unsafe excavation conditions in underground openings. A relevant set of 39 case histories, subdivided among stable, squeezing and rock busting conditions, was represented in a semi-log plot as function of depth and Barton's Number Q as given in Figure 5-1.

The entire region is sub divided in two regions, one region showing Squeezing and the other region showing Non-Squeezing conditions. The relation below gives the boundary between these two regions:

$$H = 350Q^{1/3} \quad [\text{m}] \quad (5-1)$$

In accordance to the classical Theory of Elasticity, in hydrostatic conditions of stress, the maximum tangential stress σ_θ induced at the surface of an unconfined circular tunnel is equal to two times the overburden pressure P, which is equal to $\gamma \cdot h$. At failure, the maximum value of the tangential stress is equal to the uniaxial resistance of the rock mass σ_{cr} and the depth of the excavation h is equal or bigger than the limit depth of Squeezing H. Substituting in equation σ_θ , then, the value of H in h, Singh produced the following formulation of Uniaxial Compressive Strength of a rock mass:

$$\sigma_{cr} = 0.7\gamma Q^{1/3} \quad [\text{MPa}] \quad (5-2)$$

where the unit weight of the rock mass γ is expressed in kN/m^3 . The present formulation is fitted for weak rock mass condition, Barton's number Q smaller than 10, in absence of water (J_w equal to 0).

In case of excavations in weak rocks, when squeezing conditions are expected, it would be better to rely only on empirical relations derived from the results of the rock mass observations according to the Barton's classification. This classification, in fact, has the highest number of case studies that prove efficacy of the classification system shown particularly for weak rock conditions.

The choice of the right σ_{cr} is important for the correct application of any constitutive model since it can vary considerably their behavior. In 2002 Barton proposed a formulation conceptually analogous to that suggested by Singh et. al., but, as given in Equation 5-2, it presents a further margin of safety:

$$\sigma_{cr} = 0.5\gamma Q_c^{1/3} \quad [\text{MPa}] \quad (5-3)$$

where Q_c is the modified Barton's Number, which can be expressed as follow.

$$Q_c = Q \frac{\sigma_{ci}}{100}$$

Expressed in Equation 5-4 is the Mohr-Coulomb classical formulation of the Uniaxial Compressive Strength, as a function of the internal angle of friction ϕ and cohesion c. Initially introduced for hard rocks, it is widely used for any rock mass and is given as:

$$\sigma_{cr} = \frac{2c \cos \phi}{1 - \sin \phi} \quad (5-4)$$

Further, Singh et al. (1998), emphasizing the relevance of the intermediate principal stress σ_2 in the resistance of the rock mass in the vicinity of tunnel, suggested a modified Mohr-Coulomb constitutive model in order to incorporate it and introduced the Polyaxial Strength Criterion. According to the Singh's approach, the confining effect of the minimum principal stress in the right part of the Mohr-Coulomb Theory, equation 5, is substituted in the new criterion by the average of the intermediate and minimum principal stress in order to consider the real confining stress configuration in field. The revised expression is given in Equation 5-6:

$$\text{Mohr-Coulomb Failure Criterion} \quad \sigma_1 - \sigma_3 = \sigma_{cr} + \sigma_3 A \quad (5-6)$$

$$\text{Polyaxial Strength Criterion} \quad \sigma_1 - \sigma_3 = \sigma_{cr} + \frac{\sigma_2 + \sigma_3}{2} A \quad (5-6)$$

$$\text{where } A = \frac{2 \cdot \sin \phi}{1 - \sin \phi}$$

The important confining effect developed due to the intermediate principal stress, and its role in predicting a more realistic behavior at failure of a rock mass has been shown by many authors in recent past (Mogi 2006, Al-Ajimi 2007, Haimson 2009 and M. Singh 2011). The laboratory studies of Mogi (1969-74, 1977, 1979, 1981 and 2006) have shown, instead, that the effect of the intermediate principal stress is strongly affected by the ratio σ_2/σ_3 . When this ratio increases, as it is observed on the internal boundary of an underground excavation, the effect of the intermediate principal stress consequently increases. According to several observations made in the field, the tension distribution at the internal surface of an underground opening cannot be treated as a truly uniaxial stress field because the stress along the direction of a tunnel, generally the intermediate principal stress, has a dominant role in the definition of the start of squeezing.

The rock mass surrounding the internal surface of an underground void, in absence of radial confinement ($\sigma_3 = 0$), satisfies the conditions needed to apply Equation 5-6. In these conditions, for a particular case of hydrostatic original stress, substituting the uniaxial rock mass resistance given by Equation 5-3 as suggested by Singh, the Polyaxial Strength Criterion given by Equation 5-6 reduces to the formulation of the ultimate compressive strength of the rock mass at the tunnel surface, $\sigma_{\theta \text{ lim}}$, given as:

$$\sigma_{\theta \text{ lim}} = 0.7 \gamma Q^{1/3} + \sigma_2 \frac{A}{2} \quad (5-7)$$

At the surface of the tunnel, therefore, a truly uniaxial stress is not applied but a biaxial combination of tangential σ_{θ} and longitudinal P_0 stress exists. The magnitude and the orientation of the original stress field is a function of many parameters of not easy definition, and it cannot be expressed as only function of the excavation depth. For this reason it is also not possible to quantify the intermediate principal stress and to give a clear definition of the depth of potential squeezing making use of the Equation 5-7 as shown for determining Equation 5-1 without a specific investigation of the original stress conditions.

Scussel and Chandra (2012), on the basis of an accurate analysis of the state of stress in the region of rock mass surrounding an underground opening, using the similarity between Polyaxial Strength Criterion and Mohr-Coulomb model, suggested the Equivalent Mohr-Coulomb constitutive model. The Equivalent Mohr-Coulomb Constitutive Model (M-C) maintains the Mohr's structure and can simulate the effect of the intermediate principal stress σ_2 by only modifying the parameters of shear resistance. It allows and simplifies the analytical and numerical applications of the Polyaxial Strength Criterion (PSC). Attempts of this kind have been already made to express the Hoek and Brown criterion through the Mohr-Coulomb constitutive law. Hoek et al. (2002), Carranza-Torres (2004), Priest (2005), Sofianos and Nomikos (2006), Yang and Yin (2010) and Shen et al. (2011) have simulated its behavior in several different numerical and analytical soil and rock mechanics applications. These approaches, however, have shown results more or less approximated for the objective analytical difficulties of describing, through one linear, a non-linear model (Brown, 2008).

The present method is applicable when one of the principal stresses is constant, which is generally the case for long underground excavations, where the stress along the length is fixed and equal to the component of the original stress in that direction. For this particular condition the Polyaxial Strength Criterion is fully comparable with a bi-dimensional linear failure criterion, which presents intercept and

slope different to the original shear resistance parameters. According to this hypothesis, the Polyaxial Strength Criterion can be easily rewritten in the form of a Mohr-Coulomb failure model making use of the new equivalent Internal Angle of Friction ϕ' and the equivalent Cohesion c' and may be expressed as given in the Equation 5-8.

$$\sigma_1 - \sigma_3 N_{\phi'(eq)} = \sigma'_{cr} \quad (5-8)$$

where $\sigma'_{cr} = \frac{2c' \cos \phi'}{1 + \sin \phi'}$ and $N_{\phi'(eq)} = \frac{1 + \sin \phi'}{1 - \sin \phi'}$

The two equivalent parameters of resistance can be easily determined by means of the Equations 5-9 and 5-10:

$$\phi' = \sin^{-1} \frac{\sin \phi}{2 - \sin \phi} \quad (5-9)$$

$$c' = \left(\sigma_{cr} + \sigma_2 \frac{A}{2} \right) B \quad (5-10)$$

where $A = \frac{2 \sin \phi}{1 - \sin \phi}$ and $B = \frac{1 - \sin \phi}{(2 - \sin \phi) \cos \left(\sin^{-1} \frac{\sin \phi}{2 - \sin \phi} \right)}$

The formulation of the equivalent internal angle of friction ϕ' , as well as the parameters A and B, which are only functions of the angle of internal friction and can be easily tabulated substituting a realistic range of values for rock masses into the expressions given above and are tabulated as shown in Table 5-1 and Table 5-2.

ϕ [°]	20.00	22.00	24.00	26.00	28.00	30.00	32.00	34.00	36.00	38.00	40.00
ϕ' [°]	11.90	13.32	14.79	16.30	17.86	19.47	21.13	22.84	24.60	26.41	28.27

TABLE 5-1 - RELATION BETWEEN ANGLE ϕ AND EQUIVALENT ANGLE ϕ' OF INTERNAL FRICTION

ϕ [°]	20.00	22.00	24.00	26.00	28.00	30.00	32.00	34.00	36.00	38.00	40.00
A	1.04	1.20	1.37	1.56	1.77	2.00	2.25	2.54	2.85	3.20	3.60
B	0.41	0.40	0.39	0.37	0.36	0.35	0.34	0.33	0.32	0.31	0.30

TABLE 5-2 - ESTIMATION OF A AND B FOR INCREASING VALUES OF INTERNAL ANGLE OF FRICTION

The ultimate rock mass strength at the tunnel surface in the absence of radial confinement can be, therefore, expressed in the following way as equivalent uniaxial compressive strength σ'_{cr} :

$$\sigma'_{cr} = \frac{2c' \cos \phi'}{1 + \sin \phi'} \quad (5-11)$$

A rational choice of the three parameters characterizing σ'_{cr} , (σ_2 , ϕ , and σ_{cr}) is essential for the correct application of the method. A preliminary investigation of the site characteristics is recommended for the evaluation of the in situ intermediate principal stress, while the internal angle of friction can be determined directly by means of Equation 5-12 suggested by Barton (2002) which Singh and Goel (2006)

modified to incorporate the effect of the rock blocks interlocking. This relation is directly related to the factors J_r , J_a and J_w as defined in his classification system.

$$\tan \phi = \left(J_r \frac{J_w}{J_a} \right) + 0.1 \quad (5-12)$$

In this paper for the determination of uniaxial compressive strength the use of the Equation 5-3 is strongly recommended. Its feasibility in a real underground application will be investigated in the following sections of this work.

Singh (2006), proposed an analytical elasto-plastic solution of stress distribution in broken zone as an application of his Polyaxial Strength Criterion in tunnel engineering, which can be used to determine the Squeezing Pressure P_i . The solution given by Singh as presented in Figure 5-2 is similar to the Daemen's approach (1975) and applicable in the direction of the principal in situ stress to any initial state of stress, given the initial hypothesis of radial broken zone. This assumption, based on his in situ observations, made in several Himalayan tunnels, does not entail a constant reaction of the lining when a non-hydrostatic original stress field is considered.

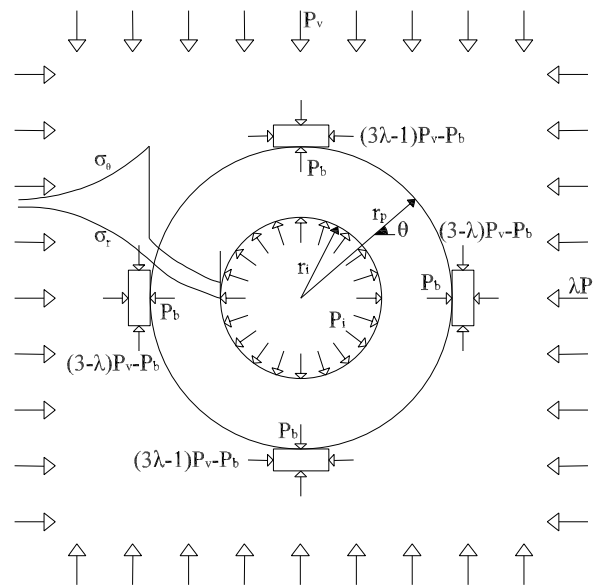


**FIGURE 5-2 - PROBLEM OF A CIRCULAR TUNNEL
IN AN ELASTO-PLASTIC ROCK MASS**

According to Singh's solution, given the circular shape of the broken zone and the in situ principal stresses coincident with horizontal and vertical directions, the radial σ_r and tangential σ_θ stresses in horizontal, $\theta = 0^\circ$ in Figure 5-2, and vertical direction, $\theta = 90^\circ$ in the same figure, correspond to the minimum σ_3 and maximum σ_1 principal stresses and, in elastic region, can be evaluated by means of the Kirch's equations.

If the radial pressure σ_r at the plastic radius r_p is P_b , the tangential stress at the elastic boundary in vertical directions can be expressed as follows:

$$\sigma_\theta = (3-\lambda)P - P_b \quad (5-13)$$

Since, at the plastic radius, the peak failure conditions are reached, the values of the principal stresses can be substituted in the Polyaxial Strength Criterion as expressed in equation 5-6 to determine the magnitude of P_b .

$$P_b = \frac{(3-\lambda)P - \sigma_{cr} - P_0(A/2)}{(2 + A/2)} \quad (5-14)$$

where P_0 , the component of the original in situ stress in the tunnel direction, is substituted in σ_2 .

Inside the broken zone the residual failure criterion is valid but, it must be highlighted that, in accord to the Singh's approach the Polyaxial Strength Criterion reduces to the Mohr-Coulomb theory, as expressed by equation 5-16, after failure. In the plastic zone, therefore, the state of stress is governed by the equation of equilibrium and by the Mohr-Coulomb failure criterion in terms of residual parameters:

$$\frac{\partial \sigma_r}{\partial r} = \frac{\sigma_\theta - \sigma_r}{r} \quad (5-15)$$

$$\sigma_\theta = \frac{1 + \sin \phi_r}{1 - \sin \phi_r} \sigma_r + \frac{2c_r \cos \phi_r}{1 - \sin \phi_r} = 0 \quad (5-16)$$

Substituting the tangential stress as maximum principal stress from Equation 5-16 in the equation of equilibrium 5-15, it can be integrated with the following boundary condition, $\sigma_r = P_b$ $r = r_p$, to determine the evolution of radial stress in vertical direction:

$$\sigma_r = [P_b + c_r \cot \phi_r] \left(\frac{r}{r_p} \right)^\alpha - c_r \cot \phi_r \quad (5-17)$$

$$\text{where } \alpha = \frac{2 \sin \phi_r}{1 - \sin \phi_r}$$

The same procedure can be reproduced in the horizontal direction to determine the relative squeezing at the wall.

If needed, by means of an analytical solution, the increment of squeezing pressure due to the gravitational effect of the fractured rock mass in crown can be quantified by just introducing the self-weight of the rock mass in the equation of equilibrium.

The application of two different constitutive criteria in the same solution, easy to be solved in an analytical treatment, has limited applicability when the real conditions of excavation do not satisfy the initial hypotheses of the original solution. The use of the approach proposed by Scussel and Chandra permits the application of the same criterion both in peak and residual condition and the resolution with any commercial numerical suite.

Making use of the equivalent Mohr-Coulomb resistance parameters, P_b can be expressed as in equation 18 and substituted in Equation 5-17 to determine the distribution of the radial stress in vertical direction.

$$P_b = \frac{(3-\lambda)P - \sigma'_{cr}}{(N_{\phi(eq)} - 1)} \quad (5-18)$$

5.3 CASE STUDY – THE CHHIBRO KHODRI TUNNEL

In this research the case study analyzed is the Indian project of the Chhibro-Khodri Tunnel, which is famous for large magnitude of the observed squeezing phenomenon and excessive delays suffered during its excavation. This project has been chosen for the amount and quality of the information coming from the work of characterization and back analysis carried out by Jethwa (1979) in the sections of larger geo-mechanical weaknesses.

The Chhibro-Khodri Tunnel is an important part of the Yamuna (River) Hydroelectric Project. The whole scheme was subdivided into 4 main stages. It started with the 516 m long barrage built at Dakpathar on Yamuna River to provide water to the power houses of Dhakrani and Dhalipur and completed in 1965.

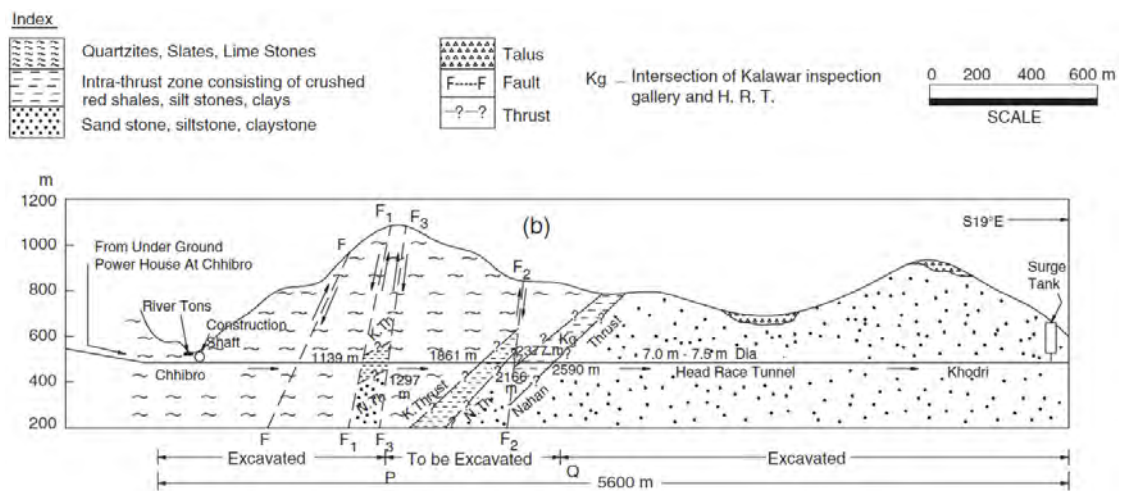


FIGURE 5-3 - GEOLOGICAL SECTION ALONG THE CHHIBRO KHODRI TUNNEL (JAIN ET AL., 1975)

The following parts of the project extended the hydroelectric activities to the entire area and realized a dense and complex net of dams and tunnels in order to take advantage of the favorable morphology and the infinite water reserve.

The tunnel between Chhibro and Khodri was excavated in the second part of the second stage of the works. It receives the water discharged from the Chhibro Power station and directs it to the 120 MW (4*30MW) capacity Khodri power house. The tunnel is 5.6 km long and has 7.5 m diameter circular cross section.

The main inconveniences in the excavation were expected through the Krol and Nohan intra-thrust regions. A small inclined tunnel, the Kalawar Inspection Gallery, was excavated to observe the reaction of the Red Shales and Black Clays in those formations at the installation of the proposed linings.

Jethwa instrumented this tunnel and determined the radial horizontal Squeezing Pressures P_1 , deformations u_a at the surface of the tunnel as well as the radii of the plastic region r_p around the excavations. The final geological mapping, shown in Figures 5-6 and 5-7, was carried out by Jain et al (1975) while the determination of the Physical, mineralogical and shear resistance characteristics of the rock masses went through once again by Jethwa (1979).

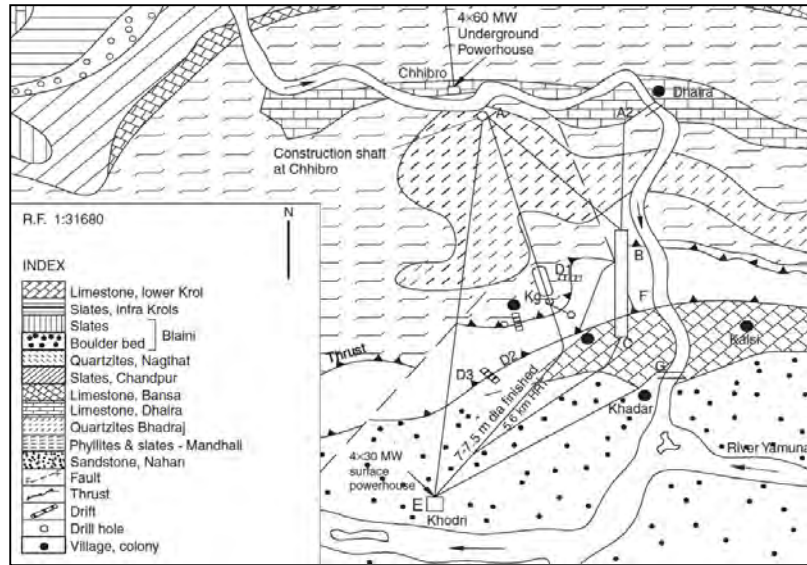


FIGURE 5-4 - REGIONAL GEOLOGY OF THE CHHIBRO KHODRI TUNNEL

A reasonably acceptable range of values for the shear resistance parameters, describing the behavior at failure of the weaker rock masses was assumed on the basis of the surveys conducted by Dube (1979). Three relevant tunnel sections are considered in this analysis; two were excavated in Red Shales and one in Black Clays and a concise summary of the essential geometrical and geotechnical characteristics of the instrumented sections is contained in Table 5-3.

Sect #	Soil/Rock Type	r_i [m]	r_p [m]	Depth [m]	γ [kN/m ³]	Q	σ_{ci} [kPa]	ϕ_p	ϕ_r	c_p	c_r	u_p/r_i [%]	Degree of Squeezing	P_i [kPa]
								[°]		[kN/m ²]				
1	Red Shales	1.5	6.0	280	27.3	.025-.10	≈ 75	30-35	25-32	0.1-0.15	0	2.8	Severe	0.17
2	Red Shales	4.5	31.1	680	27.3	.012-.05	≈ 75	30-35	25-32	0.1-0.15	0	6.0	Very Severe	0.30
3	Black Clays	4.5	14.4	280	26.4	.016-.03	≈ 25	25-30	20-25	0.1-0.15	0	4.5	Severe	1.22

TABLE 5-3 - GEOMETRICAL DIMENSIONS AND ROCK MASS CHARACTERISTICS

Without any specific analysis by the author of the uniaxial strength of the matrix σ_{ci} of the two rock masses, the use of data in the literature is, therefore, necessary. According to Terzaghi and Peck (1967) very weak clays show σ_{ci} between 5 and 25 MPa, while a weak clay between 25 and 50 MPa. For this reason, in this analysis an intermediate value between these two classes, 25 MPa, has been taken as reference for the uniaxial strength the black clays. The observation of a different behavior by the red shales surrounding the other two instrumented sections allows to assume better conditions for the rock matrix. This hypothesis is confirmed by Hoek (2000), which suggests an σ_{ci} for the shales between 50 and 100 MPa, and Koncagul and Santi (1999), which, in turn, observed values between 60 and 100 MPa in their laboratory tests. Even in this case, in the absence of specific information, an intermediate value equal to 75 MPa was chosen. The geometrical extensions and the suggested values of the rock mass quality and resistance can be used for the numerical or analytical determination of the Squeezing Pressure. In this paper, the analytical solutions according to the classical Mohr-Coulomb and suggested Equivalent Mohr-Coulomb Theories are compared to the measured Squeezing pressures as shown in Table 5-3.

5.4 METHOD OF ANALYSIS

If the hypothesis, presented in the introductory part of this paper, that the influence of the stress in the tunnel direction on the rock mass resistance is accepted, the results of the observation of the rock mass behavior in the tunnel proximity may be also influenced by the effect of the lateral confinement. In support to this hypothesis, a simple comparison of the Equation 5-2 with the other proposed relations shows that the Singh's approach returns always considerably higher values as compared to the other methods.

In this research, to avoid doubling the effect of the intermediate principal stress on the rock mass resistance, the major principal stress at the tunnel surface is obtained using Equation 5-7, but substituting for σ_{cr} as given in Equation 5-3. To determine the ultimate compressive strength at the tunnel surface, therefore, the following relation may be used:

$$\sigma_{\theta\text{lim}} = 0.5 \gamma Q_c^{1/3} + \sigma_2 A/2 \quad (5-19)$$

In the absence of a detailed estimation of the original state of stress, and for the rock mass characterization as suggested by Jethwa (1979), a hydrostatic original stress field is assumed in this analysis. Such simplification is often used in the designing stage of underground excavation and, when pronounced stress anisotropy is not prefigured, it does not entail results too dissimilar from the real rock mass-support behavior.

Given the simple geometry of the excavation, a circular and uniformly lined tunnel, surrounded by a substantially homogeneous and isotropic fractured rock mass, the state of stress induced around the gallery can be determined by means of analytical approaches. In this paper, four different approaches are used to obtain the results for the above-mentioned case study. The first approach uses Mohr-Coulomb Theory and the other three approaches use the Equivalent Mohr-Coulomb Theory but are different in the sense that the uniaxial strength σ_{ci} has been obtained differently. The details of the four approaches used in the present research are described below:

Approach 1: In this, the Mohr-Coulomb Failure Criterion has been used.

Approach 2: The Equivalent Mohr-Coulomb Failure Criterion is applied and the uniaxial compressive strength as given by Equation 5-4 is used.

Approach 3: Equivalent Mohr-Coulomb Failure Criterion has been applied and the uniaxial compressive strength is used as suggested by Barton and given in Equation 5-3.

Approach 4: Equivalent Mohr-Coulomb Failure Criterion has been used and the uniaxial compressive strength is used as suggested by Singh and given in Equation 5-2.

Sect #	Approach 1			Q	Approach 2			Approach 3			Approach 4		
	ϕ	c	$q_{c\text{mass}}$		ϕ'	c'	$q'_{c\text{mass}}$	ϕ'	c'	$q'_{c\text{mass}}$	ϕ'	c'	$q'_{c\text{mass}}$
	[°]	[MPa]	[MPa]		-	[°]	[kPa]	[MPa]	[°]	[MPa]	[MPa]	[°]	[MPa]
1	30	0.1	0.346	0.025	19.47	2.83	0.346	19.47	3.98	3.626	19.47	4.68	5.588
2	30	0.1	0.346	0.012	19.47	6.69	0.346	19.47	7.56	2.839	19.47	8.11	4.375
3	25	0.1	0.314	0.016	15.54	2.17	0.314	15.54	2.85	2.095	15.54	3.82	4.657

TABLE 5-4 - PEAK RESISTANCE PARAMETERS FOR THE DIFFERENT APPROACHES

In the present analysis, the measured radii of the plastic zone are used for the determination of the radial component of the squeezing pressure and, then, compared to the results of the real squeezing pressures

monitored by Jethwa (1979) in the field. This study uses lowest among the parameters of resistance as suggested by Dube (1977), since when they carried out the study, there was a consolidated predisposition in the engineering rock mass classifications to overestimate the resistance of the weak rocks. This approach was subsequently corrected in the following classifications.

In Table 5-4 are presented the equivalent shear peak resistance parameters corresponding to each suggested approach and calculated by means of the Equations 5-9 and 5-10. The equivalent parameters are derived from the Mohr-Coulomb peak shear parameters suggested by Jethwa, as shown in Table 5-1 - configuration 1. From these results it is confirmed that the modified approaches show increasing values of equivalent cohesion; this behavior is consistent with the relation expressed in Equation 5-10, which is directly influenced by the magnitudes of the uniaxial compressive strength computed for each approach.

Sect #	observations		Approach 1			Approach 2		Approach 3		Approach 4	
	P ₀	ΔP _v	P _i	P _i	Avg Err	P _i	Avg Err	P _i	Avg Err	P _i	Avg Err
	[MPa]	[MPa]	[MPa]	[MPa]	[%]	[MPa]	[%]	[MPa]	[%]	[MPa]	[%]
1	7.64	0.04	0.17	0.49	-189%	0.32	-88%	0.18	-4%	0.09	47%
2	18.56	0.16	0.30	0.54	-81%	0.36	-19%	0.31	-3%	0.28	7%
3	7.39	0.14	1.22	1.25	-2%	0.99	19%	0.80	35%	0.52	58%
			AVG	90.6%		AVG	42.1%	AVG	13.8%	AVG	37.2%

TABLE 5-5 - COMPUTED SQUEEZING PRESSURES

The Squeezing Pressure analytically computed using all the four approaches for the three different monitored sections described in Table 5-3 are summarized in Table 5-5. The presented values are obtained by substituting the relative combination of equivalent cohesion and internal angle of friction in the Equation 5-17 when $r = r_1$.

The results presented in the table are then compared with the measured Squeezing Pressures and the relative percent variance are alongside listed. It is observed that the squeezing pressures computed using approach 3 give the smallest error as compared to the observed values and on an average for all the three sections it is obtained as 13.8 %. In approach 4, the pressures calculated are consistently smaller than the observed values in the field. The underestimation of the Squeezing Pressure, which is about 37% on an average, can be explained as a direct consequence of overestimation of the confining stress due to the use of Polyaxial Strength Criterion along with the Singh's formulation of the Uniaxial Compressive Strength. The major reason for this could be the value of uniaxial compressive strength which has been computed using equation given by Singh's, which itself is dependent on intermediate principal stress. Thus implying that the effect of intermediate principal stress is incorporated two times. This approach resulted in underestimation of the expected squeezing pressure, which may turn out to be dangerous in some cases.

The Singh's and Barton's formulations of the uniaxial compressive strength are modified in more general relations, as shown in Equations 5-20 and 5-21, where the initial constant factor which characterizes the two approaches is substituted by the variables f_1 and f_2 .

$$\sigma_{cr} = f_1 \gamma Q^{1/3} \quad (5-20)$$

$$\sigma_{cr} = f_2 \gamma Q_c^{1/3} \quad (5-21)$$

The entity of the uniaxial compressive strength in accordance to the Equations 5-20 and 5-21 was calculated for a reasonable range of values of the parameters f_i . The resulting σ_{cr} were applied, as in the

approaches 3 and 4, to the Polyaxial Strength Criterion and corresponding Squeezing pressures calculated. The outcomes of these are summarized in Tables 5-6 and 5-7 respectively.

		factor f_1											
Observ.		0.45	0.465	0.48	0.495	0.51	0.525	0.54	0.555	0.58	0.595	0.61	0.625
Sect #	P_i												
	[MPa]	[MPa]	[MPa]	[MPa]	[MPa]	[MPa]	[MPa]	[MPa]	[MPa]	[MPa]	[MPa]	[MPa]	[MPa]
1	0.17	0.177	0.172	0.167	0.162	0.157	0.151	0.146	0.141	0.132	0.127	0.122	0.116
2	0.30	0.310	0.308	0.306	0.304	0.302	0.301	0.299	0.297	0.294	0.292	0.290	0.288
3	1.22	0.697	0.686	0.675	0.664	0.653	0.642	0.632	0.621	0.602	0.592	0.581	0.570
Error [%]		16.9	15.9	16.2	17.3	18.4	19.5	20.9	22.4	25.0	26.5	28.1	29.6

TABLE 5-6 - VARIATION OF THE INTERNAL PRESSURE P_i FOR DIFFERENT VALUES OF THE FACTOR f_1

When the factor f_1 is equal to 0.471, corresponding to an average error of 15.5 %, and f_2 equal to 0.519, corresponding to an average error of 12.66%, the differences between the observed pressure and the analytical predictions are minimum. The optimum values of f_i obtained are in the proximity of 0.5, as suggested by Barton, in confirmation with the initial hypotheses of this research.

		factor f_2											
Observ.		0.45	0.465	0.48	0.495	0.51	0.525	0.54	0.555	0.58	0.595	0.61	0.625
Sect #	P_i												
	[MPa]	[MPa]	[MPa]	[MPa]	[MPa]	[MPa]	[MPa]	[MPa]	[MPa]	[MPa]	[MPa]	[MPa]	[MPa]
1	0.17	0.192	0.187	0.182	0.178	0.173	0.168	0.163	0.159	0.151	0.146	0.141	0.136
2	0.30	0.315	0.313	0.312	0.310	0.308	0.307	0.305	0.303	0.300	0.299	0.297	0.295
3	1.22	0.818	0.811	0.804	0.797	0.790	0.784	0.777	0.770	0.758	0.752	0.745	0.738
Error [%]		16.9	16.0	15.1	14.1	13.2	13.0	14.0	14.9	16.5	17.7	19.0	20.3

TABLE 5-7 - VARIATION OF THE INTERNAL PRESSURE P_i FOR DIFFERENT VALUES OF THE FACTOR f_2

The errors determined for the different values of f_i are also shown in Figure 5-7.

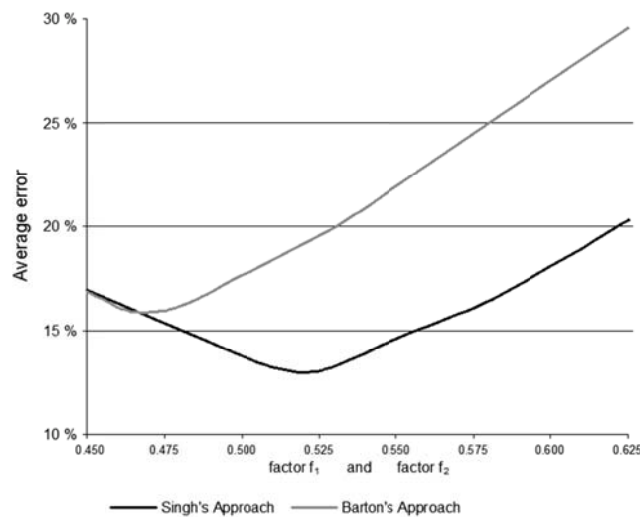


FIGURE 5-5 - AVERAGE ERRORS IN THE DETERMINATION OF THE SQUEEZING PRESSURE P_i FOR DIFFERENT VALUES OF f_i

To be precise, for the f_i equal to 0.471 and 0.519, the Squeezing pressures determined in the two test section surrounded by Red Shales are almost coincident with the observations, but the same cannot be said for the instrumented tunnel section in Black Clays.

In the end, the results obtained using the approach 2 in general overestimate the Squeezing Pressures observed in field by an average of 42 % because of the low entity of the chosen Uniaxial Strength formulation. The high errors registered in approach 1, 91% using Mohr-Coulomb theory, are due to the fact that the intermediate principal stress is not included in the analysis at all.

5.5 CONCLUSIONS

The methodology suggested in this paper, if wisely used, gives more realistic results for Squeezing conditions than the other traditional theories prevalent in tunnel engineering. The combined use of Polyaxial Strength Criterion and Mohr-Coulomb uniaxial compressive strength demonstrated high correlation in the Squeezing Pressure determination in conditions of severe squeezing due to the weakness of the rock mass affected by an excavation.

The proposed Equivalent Mohr-Coulomb failure criterion, which is a modified form of Polyaxial Strength Criterion, has been applied to three instrumented test sections, simulated the behavior of the rock mass in squeezing conditions, and demonstrated its concrete applicability and simplicity of being embedded into analytical solution as well as into numerical models. The present methodology uses the Barton's engineering rock mass classification and by considering improved resistance parameters incorporates the effect of a tridimensional state of stress in rock mass.

Out of the four approaches adopted in this research to evaluate the support pressures for the three sections of the tunnel chosen for this study, it has been observed that using the equivalent Mohr-Coulomb failure criterion with the uniaxial compressive strength obtained by the Barton's relationship using γ and Q and σ_{ci} only gives the minimum error as compared to the actual observations which is of the order of 14 percent. If the uniaxial compressive strength is obtained as suggested by Singh, the results differ on average by about 37 percent. If the uniaxial compressive strength is obtained using Mohr-Coulomb correlation, the difference in the observed and the predicted results on an average are lower by about 42 percent. If the Mohr-Coulomb criterion was used instead of the Polyaxial Strength Criterion, the pressures predicted are higher by about 91 percent on an average. It is therefore recommended to use the equivalent Mohr-Coulomb failure criterion for polyaxial state of stress with the uniaxial compressive strength evaluated by using the Barton's Theory.

5.6 ACKNOWLEDGMENTS

I am grateful to Dr. J.L. Jethwa for having granted the use of the essential data use in the present the publication. Also, I would like to thank Dr. R.K. Goel for having shared with me his copy of the data coming from the Chhibro-Khodri gallery monitoring, without which this research would not have been accomplished.

5.7 LIST OF SYMBOLS:

H_p : Terzaghi's Rock Load Factor;

γ : Rock Mass Unit Weight;

h, H : Depth and Limit Depth of Squeezing;

P : Overburden Pressure;

r, r_i, r_p : Distance from the center of the tunnel, internal and plastic radius;

$\sigma_1, \sigma_2, \sigma_3$: Maximum, Intermediate and Minimum Principal Stress;
 $\sigma_r, \sigma_\theta, \tau_{\theta r}$: Stress distribution around a tunnel in Radial, Tangential directions;
 P_0 : Hydrostatic in situ Stress;
 λ : Horizontal Stress Ratio;
 P_i, P_v, P_h : Squeezing Pressure, Squeezing Pressure in vertical and horizontal directions;
 $q_{\text{mass}}, q_{\text{cr}}, \sigma_{\text{cr}}$: Peak, Residual, Uniaxial Compressive Strength (UCS) of the rock mass;
 σ_{ci} : Uniaxial Compressive Strength (UCS) of the rock matrix;
 $\sigma_{\theta \text{lim}}$: Ultimate Compressive Strength of the rock mass at the tunnel surface;
 ϕ_p, ϕ_r, ϕ : Internal Friction Angle, Peak Internal Friction Angle, and Residual Internal Angle of Friction;
 c_p, c_r, c : Peak, Residual, Cohesion;
 $\phi', c', \sigma'_{\text{cr}}$: Equivalent Internal Friction Angle, Cohesion and Uniaxial Compressive Strength (UCS) of the rock mass;
 θ : Angle between the horizontal axis of a tunnel and the line between its center and point considered;
 Q, Q_c : Barton's Number and Modified Barton's Number;
 J_r, J_w, J_a : Joint Roughness, Seepage, Alteration Numbers.

5.8 REFERENCES

- [1] Barton, N. (2002). Some new Q-value correlations to assist in site characterization and tunnel design. *Int. J. Rock Mech., Min. Sci. Geomech. Abstr.*, 39:2:185-216
- [2] Barton, N.R.; Lien, R.; Lunde, J. (1974). "Engineering classification of rock masses for the design of tunnel support". *Rock Mechanics and Rock Engineering* (Springer) 6 (4): 189–236. doi:10.1007/BF01239496
- [3] Bieniawski, Z. T. (1974): geomechanics classification of rock masses and its application in tunneling. Proc. 3rd Cong. ISRM (Denver). Vol. 2A p.27
- [4] Bieniawski, Z. T. (1976): Rock masses classification in rock engineering. Proc. of Symposium on Exploration for rock engineering. Balkema, Rotterdam. Vol. 1, pp. 97-106
- [5] Bieniawski, Z. T. (1979). "The Geomechanics Classification in Rock Engineering Applications," Proceedings, 4th International Congress on Rock Mechanics, ISRM, Montreux. A. A. Balkema, Rotterdam, Vol. 2: 41-48.
- [6] Bieniawski, Z. T. (1984). "Rock Mechanics Design in Mining and Tunneling. A.A. Balkema, Rotterdam, 272 p.
- [7] Daemen, J.J.K. (1975). Tunnel Support Loading caused by Rock Failure. PhD thesis, University of Minnesota, Minneapolis, U.S.A.
- [8] Dube, A.K. (1979), Geomechanical Evaluation of Tunnel Stability Under Falling Rock Conditions in a Himalayan Tunnel; Ph.D. Thesis, Deptt. Of Civil Engg., University of Roorkee, Roorkee, India.
- [9] Haimson, B., Rudnicki, J.W., The effect of the intermediate principal stress on fault creation and angle in siltstone, *Struct. Geol.*, doi:10.1016/j.jsg.,2009

- [10] Hoek E. and Brown E.T. (1980). "Empirical strength criterion for rock masses". *J. Geotechnical Engineering Division ASCE*: 1013–1025.
- [11] Hoek E. and Brown E.T. (1980). *Underground Excavations in Rock*. London: Institution of Mining and Metallurgy.
- [12] Hoek, E. and Brown E.T. (1988). "The Hoek-Brown failure criterion - a 1988 update". *Proc. 15th Canadian Rock Mech. Symp.*: 31–38.
- [13] Hoek, E., Big tunnels in bad rock, *ASCE Journal of Geotechnical and Geoenvironmental Engineering*, 127 (9) (2001), pp. 726–740
- [14] Hoek E, Carranza-Torres CT, Corkum B (2002). "Hoek-Brown failure criterion-2002 edition". *Proceedings of the fifth North American rock mechanics symposium 1*: 267–273.
- [15] Hoek, E., Kaiser, P.K., and Bawden, W.F.. (2000) Support of Underground Excavations in Hard Rock
- [16] Jain, M.S., Andotra, B.S. and Sondhi, S.N. (1975). Note on Geological Features of the Chhbroad Khodri Tunnel and Occurrences of Sub Shales, Unpubl. Re. of Geol. Surv. Of India.
- [17] Jethwa, J. L. (1981). Evaluation of Rock Pressures in Tunnels through Squeezing Ground in Lower Himalayas. PhD thesis, Department of Civil Engineering, University of Roorkee, India, 272.
- [18] Koncagu, E.C., Santi, P.M. / *International Journal of Rock Mechanics and Mining Sciences* 36 (1999) 139±153.
- [19] Al-Ajmi, A.M., Zimmerman, R.W. (2007). The Mogi-Coulomb True-Triaxial Failure Criterion and Some Implications for Rock Engineering; 11th ISRM Congress, July 9 - 13, 2007, Lisbon, Portugal.
- [20] Scussel D. and Chandra S. (2012). Polyaxial Stress Analysis of Underground Openings using FLAC; *Journal of Rock Mechanics and Tunnel Technologies*, Volume 18, Number 1, 41 – 54.
- [21] Scussel, D., Chandra, S. A new approach to obtain tunnel support pressure for polyaxial state of stress. *Tunnel. Underg. Space Technol.* (2013), <http://dx.doi.org/10.1016/j.tust.2013.01.006>
- [22] Singh, Bhawani, Jethwa, J. L., Dube, A. K. and Singh, B. (1992). Correlation between observed support pressure and rock mass quality. *Tunnelling & Underground Space Technology*, Pergamon, 7(1), 59-74.
- [23] Singh, B, Goel, R. K., Mehrotra, V. K., Garg, S. K. and Allu, M. R. (1998). Effect of intermediate principal stress on strength of anisotropic rock mass. *J. Tunnelling & Underground Space Technology*, Pergamon, 13(1), 71-79.
- [24] Singh, B.; Goel, R.K. (2006). *Tunnelling in Weak Rocks. Geo-Engineering. 5. Elsevier Science.* p. 512.
- [25] Singh M. Raj A. Singh B. (2011) Modified Mohr-Coulomb Criterion for Non-linear Triaxial and Polyaxial Strength of Intact Rocks, *International Journal of Rock Mechanics & Mining Sciences* 48 (2011) 546–555
- [26] Mahendra Singh, Bhawani Singh, Jaysing Choudhari. Critical strain and squeezing of rock mass in tunnels, *Tunnelling and Underground Space Technology* 22 (2007) 343 - 350.
- [27] Terzaghi, K., Proctor, R. V. and White, T. L., "Rock Tunneling with Steel Supports," *Commercial Shearing and Stamping Co.* (1946).
- [28] Terzaghi, K., and Peck, R.B., 1967, *Soil Mechanics in Engineering Practice*, Second Edition: John Wiley & Sons, New York, 729 p.

Chapter 6

6 CONCLUSIONS

6.1 SUMMARY

In the present research the following goals have been achieved.

- Firstly, a detailed bibliographic review of the traditional and innovative design techniques of underground excavation was produced. The interest was particularly directed to the empirical and the analytical approaches and how the experience and the results of the rock mass observation can be translated into realistic constitutive laws used for engineering purposes.
- It was carried out a careful analysis of the similarities and differences between the Polyaxial Strength Criterion and the Mohr-Coulomb Failure Criterion. Based on the results obtained, different formulations of the Polyaxial Strength Criterion were proposed and validated. Their application allows the implementation of the Polyaxial Strength Criterion in personalized numerical applications.
- The first attempt, as presented in the Equation 3-10 of Chapter 3, permits to have an adaptable Polyaxial Criterion that, depending on the necessities, can easily change into the Mohr-Coulomb Theory only conveniently modifying two specific parameters. On the base of this Equation, an appropriate code in FISH for the famous geo-mechanical finite differences numerical suite FLAC (FDM) was produced.
- In the same Chapter, the proposed user defined constitutive model for FLAC was applied to a simple numerical model of circular tunnel excavated in weak rocks and plasticized by an adequate choice of the original state of stress. The numerical resolution of the stress field induced by the excavation was successfully compared to the analytical polyaxial elasto-plastic theory of stress distribution in broken zone in squeezing ground as proposed by Sing et al (2006).
- The suggested formulation of the Polyaxial Strength Criterion was furthermore evolved in the subsequent Chapter. The analytical expression of the Equivalent Mohr-Coulomb Failure Criterion, as already suggested by its name, is totally undistinguishable from the more common Mohr-Coulomb Theory. It relies on clear analytical relation for the determination of the equivalent parameters of resistance ϕ' and c' , which, differently from the Mohr-Coulomb parameters ϕ and c , incorporate the positive confining effect of the intermediate principal stress σ_2 . The present approach was, on turn, applied to the same typical case of plasticized tunnel and the results compared to those already generated by the previous numerical technique.
- Analytical analyses by means of the Equivalent Mohr-Coulomb Theory were performed on three representative sections of the Chhibro-Khodri instrumented inspection gallery. The determination of the parameters of the Equivalent Mohr-Coulomb Theory is described steps by steps for the correct application of the methodology in cases of severe squeezing conditions.

6.2 CONCLUSIONS

The elasto-plastic Polyaxial model produced in Chapter 3 introduces an alternative to numerically design tunnels in squeezing rock masses. A new relationship between the principal stresses and uniaxial compressive strength is suggested in this work, which can handle both the elastic and plastic zone according to Singh's Theory by appropriately choosing the parameters.

The application of the Polyaxial Strength Criterion, as explained in Singh's Theory, is fairly important when the pressures encountered are high and the weakness of rock masses produce significant squeezing phenomena in the field. In these conditions the study of the complex rock mass-support behavior cannot be simulated by means of physical models and the use of a specific numerical model is, therefore, the only way to reproduce the response of a rock mass in accordance with the Polyaxial Theory.

The proposed relationship is used to bring out the effect of intermediate principal stress as the development of principal stresses in an underground opening. Through an example it is shown that the effect of the intermediate principal stress contributes to the enhancement of the peak characteristics of the underground excavation but it can easily overestimated.

In Chapter 4 is proposed a new constitutive model where the polyaxial state of stress can be incorporated in the analysis by a very simple approach. The analytical formulation of the Polyaxial Strength Criterion is converted to Mohr-Coulomb theory with modified angle of friction and cohesion values. The approach is quite general and may be used for any analytical or numerical method of analyzing tunnel support.

The methodology suggested in this thesis, if wisely used, gives more realistic results for Squeezing conditions than the other traditional theories prevalent in tunnel engineering.

The proposed Equivalent Mohr-Coulomb failure criterion, in Chapter 5, has been applied to three instrumented test sections to simulate the behavior of the rock mass in squeezing conditions, demonstrating its concrete applicability and simplicity of being embedded into analytical solution as well as into numerical models. The present methodology suggests the use of the Barton's engineering rock mass classification Q and uniaxial rock mass resistance formulation and by considering improved resistance parameters incorporates the effect of a tridimensional state of stress in rock mass.

Out of the four approaches adopted in this research to evaluate the support pressures for the three sections of the tunnel chosen for this study, it has been observed that using the equivalent Mohr-Coulomb failure criterion with the uniaxial compressive strength obtained by the Barton's relationship using γ and Q_c only gives the minimum error as compared to the actual observations which is of the order of 14 percent. If the uniaxial compressive strength is obtained as suggested by Mohr-Coulomb, the results differ on average by about 42 percent. If the uniaxial compressive strength is obtained using Singh's correlation, the difference in the observed and the predicted results on an average are lower by about 37 percent. If the Mohr-Coulomb criterion was used instead of the Polyaxial Strength Criterion, the pressures predicted are higher by about 91 percent on an average. It is therefore recommended to use the equivalent Mohr-Coulomb failure criterion for polyaxial state of stress with the uniaxial compressive strength evaluated by using γ and Q_c .

The method can be implemented in any analytical solution or geo-mechanical numerical suite with excellent results. It, when used in numerical schemes, is easily adoptable and leads to less computational efforts. The results obtained by the proposed method are in good agreement with the available analytical solutions and, if applied to real cases of squeezing conditions, it predicts the Squeezing. Thus, the proposed methodology achieves all the objectives mentioned at the beginning of this study.

6.3 RECOMMENDATIONS FOR FURTHER DEVELOPMENTS

In view of the limitations of the present study future work might be undertaken with attention on the following subjects.

- i. A better computational capacity and integration in the numerical suite of the constitutive model in FISH proposed for FLAC in the Chapter 3 can be achieved by converting the shown code to C++, the natural programming language of the embedded numerical constitutive models in FLAC.

- ii. There are real cases in which the stress acting in the direction parallel to a tunnel axis is not intermediate between the major and minor principal stresses existing in the perpendicular direction but, just, the biggest. This combination of the involved stresses is typical of tunnel excavated in the perpendicular direction to the axes of a recent mountain chain (i.e. Himalaya). In these conditions, failure is generated in the tunnel direction and the stresses acting in the perpendicular plane became the intermediate confining pressure. A failure mechanism like that can be efficiently modeled by reformulating the algorithm presented in Chapter 3 as explained in Chapter 4.
- iii. On the base of the assumption expressed in Chapter 5, the Polyaxial Strength Criterion formulation expressed in Equation 5.14 can be positively extended to cases of rock masses subjected to evident anisotropy.
- iv. The choice of the correct theory for the uniaxial compressive stress σ_{cr} determination when it is associated to the Polyaxial Strength Criterion is a complex problem. An intensive work of back analysis would allow not overestimating its magnitude and, therefore, avoiding a possibly dangerous underestimation of the squeezing pressure ascertained.